University of Urbino "Carlo Bo"

Department of Biomolecular Sciences

Ph.D. Course on

LIFE SCIENCES, HEALTH AND BIOTECHNOLOGIES

Curriculum in Biochemical, Pharmacological e Biotechnology Sciences

XXXIII Cycle

ERYTHROCYTES LOADED WITH RECOMBINANT PROTEINS AS ENZYME REPLACEMENT THERAPY FOR THE TREATMENT OF RARE DISEASES

SSD: BIO/10

Supervisor

Prof. MAURO MAGNANI

Ph.D Candidate

Dott. MATTIA PAOLO ALIANO

ACADEMIC YEAR 2019/2020

Summary

Abbreviations

AGAT: Arginine:Glycine Amidinotransferase deficiency
BH4: Tetrahydrobiopterin
CCDS: Cerebral creatine deficiency syndromes
CNS: Central Nervous System
Cr: Creatine
ERT: Enzyme Repalcement Therapy
GAA: Guanidinoacetate
GABA: γ-aminobutyric acid
GAMT: Guanidinoacetate*N*-methyltransferase
His: Histidines
IMAC: Ion Affinity Chromatography
MAT: Methionine adenosyltransferase
PAH: Phenylalanine Hydroxylase
PHE: Phenylalanine
PKU: Phenylketonuria
RBC: Red Blood Cell
rGAMT: recombinant Guanidinoacetate*N*-methyltransferase
rHis-USP2: His-tagged deubiquitinating enzyme
rMAT: Recombinant Methionine adenosyltransferase
SAH: S-adenosylhomocysteine
SAM: S-adenosylmethionine
Ub: Ubiquitin

THESIS RATIONALE

Enzyme replacement therapy (ERT) is based on the periodic intravenous administration of specific enzymes produced with recombinant DNA technology. ERT consists in restoring a lacking or non-functioning enzyme with its native counterpart or with an enzyme able to degrade toxic metabolites or secondary compounds of the reaction catalyzed by the deficient enzyme (1).
In 1964, Christian de Duve first proposed replacing the defective enzymes with a recombinant human enzyme by applying this strategy in lysosomal storage diseases (LSDs).
Up to now, several ERT strategies have been approved for the clinical applications in Gaucher, Fabry, Krabbe, and Pompe diseases, as well as in different mucopolysaccharidoses (MPSs, e.g., MPS I, II, and IV) as lysosomal storage disorders (2).
This method provides excellent efficacy for those metabolic diseases for which there are recombinant enzymes that can be replaced. But there are many limitations in the use of the ERT, the following paragraph lists some of them:
Safety: Adverse Infusion Reactions (AIR), such as rash, urticaria, angioedema, bronchoconstriction, rhinitis, anaphylaxis for approved drugs (Based on clinical trials);
Immunogenicity: immune response and the IgG antibodies generation against the foreign infused enzymes is another considerable issue of the ERT, which plays a pivotal role in the patients' safety as well as efficacy and success of the treatment;
Delivery: in some pathologies it is difficult to deliver the enzyme to the target sites involved by the pathology. An additional problem is related to the overcoming of some biological barriers;
Frequency of administrations: the half-life of free enzymes can be very short and therefore close doses are required;
Identification of appropriate biomarkers that reflect the therapeutic effectiveness.
The main limitations are also summarized in Figure (1).

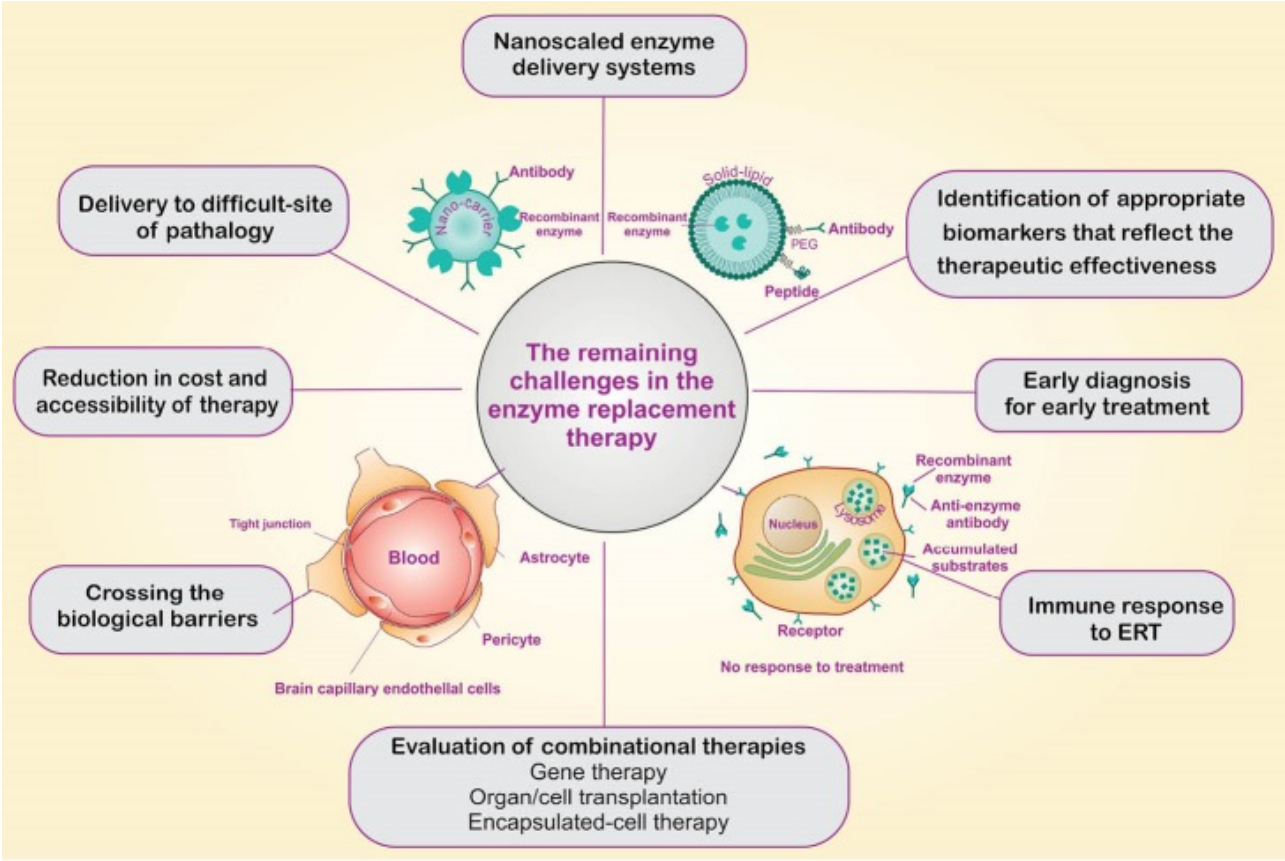

Figure 1 Schematic representation for the remaining challenges in the enzyme replacement therapy (2).

On the light of the above, this thesis will focus on the use of engineered Red Blood Cells (RBCs) in drug delivery and in particular in Enzyme Replacement Therapy and then will display two applications of engineered RBCs in the treatment of two metabolic diseases that are phenylketonuria (PKU) and Guanidinoacetate-*N*-methyltransferase (GAMT) deficiencies.

ONGOING DEVELOPMENTS AND CLINICAL PROGRESS IN DRUG LOADED RED BLOOD CELL TECHNOLOGIES

Running heading: Clinical Development of Drug-Loaded Red Blood Cells

Luigia Rossi[1,2], Francesca Pierigè[1], Mattia Paolo Aliano[1], Mauro Magnani[1,2*]

[1]Department of Biomolecular Sciences, Università degli Studi di Urbino Carlo Bo, 61029 Urbino (PU), Italy
[2]EryDel SpA, 20091 Bresso (MI), Italy

[*]Corresponding Author: mauro.magnani@uniurb.it

ORCID: 0000-0001-6456-6626

Abstract

Engineered red blood cells (RBCs) appear to be a promising method for therapeutic drug and protein delivery. With a number of agents in clinical trials (e.g. dexamethasone 21-phosphate in Ataxia Telangiectasia, asparaginase in pancreatic cancer/acute lymphoblastic leukemia, thymidine phosphorylase in mitochondrial neurogastrointestinal encephalomyopathy, RTX-134 in phenylketonuria, etc.), this leading article summarizes the ongoing efforts in developing these agents, focuses on the clinical progress, and provides a brief background into engineered RBCs and the different ways in which they can be exploited for therapeutic/diagnostic purposes. References to available data on safety, efficacy and tolerability are reported. Due to the continuous progress in this field, the information is updated as of January 2020 from databases, web sites and press release of the involved companies and information that are in the public domain.

Key points:

- Engineered RBCs have now reached clinical development with some products already in Phase 3
- Leading companies in Phase III include EryDel SpA and Erytech Pharma, others have received FDA and/or EMA clearance for patient recruitment (Rubius Therapeutics and St George's, University of London with Orphan Technologies)
- Orphan Drug designation have been obtained by FDA and EMA for several drug products; several regulatory paths to approval have been defined with main regulatory agencies

Published: Luigia Rossi, Francesca Pierigè, Mattia Paolo Aliano, Mauro Magnani Ongoing Developments and Clinical Progress in Drug Loaded Red Blood Cell Technologies. Bio Drugs 2020, 34, 265–272 Doi:10.1007/s40259-020-00415-0

1. Engineered erythrocytes

RBCs are the most numerous cells present in the blood. In a human being, 4-5 millions of RBCs are present in each microliter of blood. By a simple estimate of 5 liters of blood in a 70 Kg adult, a total of approx. 20-25 x 10^{12} RBCs can be calculated. In transfusion medicine, it is common practice to collect blood from healthy donors to be transfused in compatible patients in need. This operation, that usually accounts for a 400-450 ml of blood, can be safely repeated many times, every year, having our hematopoietic system the ability to replace the removed RBCs with new erythrocytes with an output of 2.5 million of cells per second. Of interest, when mature human RBCs enter into circulation, they can survive for more than 110-120 days and are removed from circulation only when they are senescent. Thus, the removal of the RBCs from the blood is a very sophisticated process capable of distinguishing, among all circulating RBCs, only those that have reached their programmed life span. Human RBCs possess additional advantageous characteristics. Due to an extreme differentiation process, they have lost the nucleus and other organelles, thus they are to be considered a not-viable container of about 90fl with a biconcave shape and a diameter of 7-8 µm. This apparently simple cell is able to squeeze through our capillaries (that are less than 2 µm in diameter) without being damaged, and to travel all our circulatory system in about 20 seconds. Because of these special properties, years ago several investigators thought that erythrocytes can possibly be used not only to replace blood lost for trauma or other reasons, but could represent an invaluable cell source easily available for the delivery of therapeutic and contrasting agents in the circulatory system.

Human erythrocytes have been suggested as carriers and bioreactors since 1973 [1]. The bases for these potential applications derived from the seminal work of Joe Hoffman [2, 3] who demonstrated that pores opened on the erythrocyte membrane in hypotonic conditions can be resealed restoring the main properties of the native cell membrane. Since then, many groups have documented the feasibility of this approach in different animal species [4] for the encapsulation of therapeutic proteins, antigens, contrasting agents, small chemical entities [5,6] as well as for the delivery of agents coupled to the external surface of the RBC membrane [7, 9]. Thus, in addition to the osmotic based procedures, RBC engineering can be obtained by multiple strategies as reviewed in [10,11]. It is worth noting that RBCs can serve both as a delivery system for the release of drugs in circulation or to keep the therapeutic agent inside the cell when the metabolite to be degraded can cross the RBC membrane. Both approaches are already in clinical studies today.

2. Clinical progress

The clinical developments reported in this section have received approval by international regulatory agencies, many have also received the designation of “orphan drug”, and the most advanced are based on solid preclinical and/or Phase I/II clinical investigations. Table 1 summarize the therapeutic goals and the drugs discussed in this paper.

TABLE 1. Therapeutic goals and drugs considered in this leading article related to the use of drug-loaded RBCs as therapeutic agents

Condition treated	Drug	Company
Ataxia Telangiectasia	Dexamethasone 21-Phosphate	EryDel Italy & USA www.erydel.com
Acute Lymphoblastic Leukemia /Pancreatic Cancer	Asparaginase	ERYtech Pharma France & USA www.erytech.com
Mitochondrial Neurogastrointestinal Encephalomyopathy	Thymidine Phosphorylase	St George's, University of London UK The Clinical Trial Company UK Orphan Technologies Ltd CH
Phenylketonuria	RTX-134	Rubius USA www.rubiustx.com

2.1. RBCs for the delivery of dexamethasone

Dexamethasone is a glucocorticoid analogue without mineralocorticoid activity and with the highest potency with respect to hydrocortisone. Because of its chemistry, it can easily cross cell membranes (including the RBC membrane) by simple diffusion. As a consequence, it is not retained within the RBCs upon encapsulation. This problem was solved by Magnani et al [12] by encapsulating the corticosteroid derivative dexamethasone 21-phosphate (Dexa 21-P). A specific equipment to perform the encapsulation procedure was also developed [13]. The idea of using a non-diffusible prodrug of dexamethasone using autologous erythrocytes was also very beneficial in terms of pharmacokinetics (PK). In fact, Dexa 21-P is slowly converted to the diffusible dexamethasone by RBC resident enzymes and detected in circulation for > 1 month in human volunteers receiving a single infusion of Dexa 21-P-loaded RBCs [14]. In the same study, sponsored by EryDel SpA, it was also shown that the processed RBCs have a normal in vivo survival and fully compliant with the rules for FDA defined transfusion products. Mambrini et al [13] were also able to document that the human RBCs can be efficiently loaded with a large range of Dexa 21-P concentrations while maintaining the RBCs' fundamental properties. Dexa 21-P-loaded RBCs have been used in several investigators' initiated clinical studies in COPD patients [15], cystic fibrosis [16], steroid-dependent IBD [17], Crohn's disease [18, 19], and ulcerative colitis [20, 21], documenting safety and clinical effect in hundreds of patients. Most recently, EryDel SpA started a registration program in Ataxia Telangiectasia patients. The treatment received Orphan Drug designation both by FDA and EMA. The Phase 2 trial enrolled 22 patients receiving a monthly administration of autologous RBCs loaded ex vivo with Dexa 21-P for six months and was very successful reaching both primary and secondary endpoints [18], namely improvement of the neurological conditions measured by a validated International Cooperative Ataxia Rating Scale (ICARS) and adaptive behavior measured by the Vineland adaptive behavior scale (VABS), and an acceptable safety profile. Based on these results, EryDel started a Phase 3 registration study. This is an international, multi-center, one-year, randomized, prospective, double-blind, placebo-controlled, phase III study, designed to assess the effect of two non-overlapping dose ranges of Dexa 21-P, administered by IV infusion once per month, on neurological symptoms of patients with Ataxia Telangiectasia. This study is being conducted in 22 centers located in the US, Europe, Israel, Asia, Africa & Australia (for more details visit: www.attest-trial.com). A total of 180 patients will be enrolled equally into three groups of two Dexa 21-P doses and a placebo. Patients completing this study will be allowed to continue treatment in an open-label extension study.

2.2. RBCs for the delivery of asparaginase

The idea of using RBCs for the delivery of asparaginase was proposed by Ihler et al [1] but without any experimental evidence for its feasibility. Preclinical investigations in baboons were reported in 1976 [23], and in monkeys 1983 [24]. In the years 1990-1996, Ropars et al. [25-29] proved the feasibility and provided evidence that asparaginase-loaded homologous RBCs are safe, well tolerated and effective in reducing plasma asparagine in humans. Results from a Phase 1/2 clinical trial of asparaginase-loaded RBCs (named GRASPA ®, property of Erytech Pharma) in the treatment of refractory or relapsed lymphoblastic leukemia were published in 2011 [30]. In 2015, GRASPA was

evaluated for the treatment of acute lymphoblastic leukemia in elderly patients in a Phase 2 study [31]. The dose of 100 IU/kg was found to show the best safety and efficacy profile for these elderly patients. However, median overall survival was disappointing in this treatment regime being 15.8 and 9.7 months, in the 100 and 150 IU/kg cohorts. Asparaginase-loaded RBCs were also evaluated in a Phase I study in patients with pancreatic adenocarcinoma [32] with a reasonable safety profile. Results of a Phase 2b study with erythrocyte-containing asparaginase (now named eryaspase) in combination with chemotherapy in second line treatment of advanced pancreatic cancer, were recently published [33]. The study, funded by Erytech Pharma, was conducted using the ERYCAPS® technology. For the entire population, median overall survival in the eryaspase arm was 6.0 months versus 4.4 months in the control arm receiving chemotherapy. Median progression-free survival was 2.0 months in the eryaspase arm and 1.6 months in the control arm. Overall, the incidence of adverse events was similar in the two arms. Actually, an open-label, randomized Phase 3 study of eryaspase in combination with chemotherapy compared with chemotherapy alone as second line treatment in patient with pancreatic cancer is ongoing and recruiting (NCT03665441). The company Erytech Pharma has also planned a Phase 2 in triple negative breast cancer (NCT03674242) and in other solid tumors and a Phase 2 in lymphoblastic leukemia.

2.3 RBCs for the delivery of thymidine phosphorylase

Accumulation of thymidine and deoxyuridine in human tissues and body fluids, including blood, is a consequence of a complete or partial absence of the enzyme thymidine phosphorylase and results in a fatal autosomal recessive disorder best described as mitochondrial neurogastrointestinal encephalomyopathy or MNGIE (Online Mendelian inheritance in Man #603041, Genome Database accession #9835128). The biochemical consequences of a high deoxyribonucleosides concentration cause an increased concentration of the corresponding triphosphates within mitochondria leading to multiple deletions, point mutations and depletion in mitochondrial DNA. Moran et al. [34] reported the first treatment of a MNGIE patient with autologous erythrocyte-encapsulated recombinant thymidine phosphorylase from *Escherichiacoli*. A detailed description of the clinical and biochemical improvements with this treatment was reported by Bax et al. [35] confirming a successful enzyme replacement therapy for the treatment of MNGIE. These conclusions were confirmed in three patients receiving increasing doses of the encapsulated enzyme [36], and a full Phase 2, multi-centre, multiple dose, uncontrolled, open-label trial will investigate the application of erythrocyte-encapsulated thymidine phosphorylase (EE-TP) as an enzyme replacement therapy for MNGIE. Three EE-TP dose levels are planned with patients eventually receiving the dose level that achieves metabolic correction. The study has a 3-month run-in period followed by a 24-month treatment phase [37, 38]. The treatment has received the designation of Orphan Drug both by EMA and FDA. At the date of writing (January 2020) this study is not recruiting yet.

4.3 RBCs for the delivery of phenylalanine ammonia lyase

Phenylketonuria (PKU, OMIM 261600) is an inborn error of metabolism caused by inherited mutations in the enzyme phenylalanine hydroxylase converting phenylalanine (Phe) into L-Tyr. This deficiency leads to systemic accumulation of Phe leading to intellectual disabilities and

neurocognitive impairments also in early and continuous treated patients on a Phe-restricted diet [39, 40]. An enzyme replacement therapy based on pegvaliase administration (enzyme produced by BioMarin Pharmaceutical Inc.) has recently been approved by the FDA (May 2018) and EMA (April 2019) for adults with Phe ≥ 600 µM. The administered enzyme is a pegylated recombinant *Anabaema variabilis* phenylalanine ammonia lyase (PAL) to be administered daily. About 60% of treated patients in a Phase III clinical trial achieved blood Phe ≤ 360 µM, but adverse reactions and anaphylaxis were associated with this therapy [41]. To overcome these limitations, a RBC-mediated delivery of PAL was investigated in a validated murine model of PKU [42, 43]. These experiments provided evidence that pegylation is not necessary when the recombinant enzyme is administered encapsulated within autologous RBCs. Furthermore, the selected dose was equally effective at all time-points investigated proving that anti-drug-antibodies do not inactivate the recombinant PAL once encapsulated into autologous RBCs. Recently, Rubius announced that their first product to be developed would be based on the delivery of PAL expressed into RBCs (RTX-134) (Link 1). It is worth noting that Rubius' technology, as described on the company web site, is based on CD34+ hematopoietic precursor cells collected by apheresis from a healthy O negative donor and purified. These precursor cell populations are genetically engineered with a lentiviral vector, or gene cassette, to express PAL within the cells. The cells are then exposed to media in a bioreactor to promote further expansion and differentiation until the nucleus is ejected, resulting in mature reticulocytes to be administered to patients in need. The company announced FDA clearance (Link 2). The primary objective of this study is to evaluate the safety and tolerability of RTX-134 following intravenous administration of a single dose. RTX-134 consists of allogeneic human red cells expressing the AvPAL (*Anabaena variabilis* phenylalanine ammonia lyase). The trial is designed to determine a preliminary dose and inform a dosing schedule that is deemed safe, tolerable, and potentially effective. Four dose levels are planned and additional dose levels may be explored. Following administration, subjects will be monitored until 28 days after last detection of RTX-134. Detection of RTX-134 will be evaluated using multiple pharmacokinetic and pharmacodynamic assessments including measurement of trans-cinnamic acid (tCA). The number of participants was originally planned to be 12 and the study start date September 2019. However, as of today, based on company disclosure, only the first patient has been treated thus delays are expected in the reading of the clinical data.

3. Preclinical pipeline

The two companies with the most advanced clinical programs (EryDel and Erytech) have a robust pipeline with leading products and developments in additional conditions and new therapeutics. Rubius has also announced a strong pipeline with some preclinical data published. Of interest, due to space limitation, we will address readers to several reviews that have summarized the potential clinical developments of several different candidates already tested in suitable animal models [44-48]. The envisaged applications cover many different areas including delivery of small chemical entities, therapeutic proteins, enzymes, immune-modulators and contrasting agents for diagnostic applications.

4. Concluding remarks

The technology based on the use of RBCs for the delivery of therapeutic and/or diagnostic agents has strongly evolved from a research field to advanced clinical development programs. Some companies are leading the clinical applications with products currently in Phase 3 and robust pipelines. The modalities selected by each company for the production of the modified RBCs are different. While Rubius' technology is mainly based on the genetic engineering of precursor erythroid cells to be modified by viral vectors, expanded ex vivo and differentiated in cell bioreactors before infusion in patients in need, Erytech Pharma is producing the modified RBCs in dedicated cell facilities starting from blood donations obtained by immune-compatible donors. In contrast, EryDel processes autologous blood at the bedside of the patient. In other words, the patient provides a small amount of blood (i.e. about 50 ml in most studies) which is processed in a dedicated automated system (composed by a drug and medical devices) by a patented technology and re-infused into the original donor within 1.5-2 hours from the time of blood collection. Thus, each patient receives his own blood once it is processed by the encapsulation of drugs or other therapeutic agents. This approach is repeated monthly and does not require a centralized cell factory and a distribution logistic.

The regulatory authorities in the US and Europe have been involved in several steps of EryDel process development. In addition, clearance of all Investigational New Drug Applications (see Table 2) has greatly contributed in defining the main regulatory requirements in terms of safety and efficacy for the benefit of patients in need. EryDel has shown that transformed RBCs have a 24-hour survival and a half-life in circulation that conform to the FDA criteria for the approval of blood transfusion products [10]. Erytech, based on asparaginase activity [26], has shown that the entrapped asparaginase is detectable in circulation for about 1 month. Procedure-related adverse events of RBC-mediated delivery have not been observed in hundreds of administrations in adults and children. In conclusion, the enormous efforts that a large number of researchers have made in advancing our knowledge in the biology, physiology, immunology and biochemistry of RBCs, is finally contributing to develop new therapeutics for unmet medical needs, frequently in the area of rare diseases. This great effort is now in the last phase of clinical development for a few products, and this is also thanks to a number of investors and patient's associations that have joined their efforts to push this fascinating technology up to new therapeutic breakthroughs.

TABLE 2. Clinical Trials considered in this leading article related to the use of RBCs loaded with therapeutic agents

Study title	Posted	Link and ClinicalTrials.gov Identifier	Status
Intra-Erythrocyte Dexamethasone Sodium Phosphate in Ataxia Telangiectasia Patients (IEDAT01)	2010	https://clinicaltrials.gov/ct2/show/NCT01255358?term=erydel&draw=2&rank=7 NCT01255358	completed
EryDex Pharmacokinetics in Healthy Volunteers (EryDex)	2013	https://clinicaltrials.gov/ct2/show/NCT01925859?term=erydel&draw=2&rank=5 NCT01925859	completed
Recovery and Survival of EryDex in Non-patient Volunteers	2015	https://clinicaltrials.gov/ct2/show/NCT02380924?term=erydel&draw=2&rank=4 NCT02380924	completed
EDS in Ataxia Telangiectasia Patients (ATTeST)	2016	https://clinicaltrials.gov/ct2/show/NCT02770807?term=red+blood+cells+and+delivery&draw=12&rank=214 NCT02770807	completed
Open-label, Long-term, Extension Treatment Using Intra-Erythrocyte Dexamethasone Sodium Phosphate in Patients With Ataxia Telangiectasia Who Participated in the IEDAT-02-2015 Study (OLE-IEDAT)	2018	https://clinicaltrials.gov/ct2/show/NCT03563053?term=erythrocytes&cond=Ataxia+Telangiectasia&draw=2&rank=1 NCT03563053	recruiting
Administration of Allogenic Red Blood Cells Loaded L-asparaginase in Cases of Relapse of Acute Lymphoblastic Leukaemia (GRASPALL)	2008	https://clinicaltrials.gov/ct2/show/NCT00723346?term=erytech+pharma&draw=2&rank=10 NCT00723346	completed
GRASPA (Erythrocytes Encapsulating L-asparaginase) in Patients With Relapse of Acute Lymphoblastic Leukemia (GRASPIVOTALL)	2012	https://clinicaltrials.gov/ct2/show/NCT01518517?term=erytech+pharma&draw=2&rank=9 NCT01518517	completed
Administration of GRASPA (Suspension of Erythrocytes Encapsulating L-asparaginase) in Elderly Patients With First Line Acute Lymphoblastic Leukemia	2012	https://clinicaltrials.gov/ct2/show/NCT01523782?term=erytech+pharma&draw=2&rank=8 NCT01523782	completed
Administration of GRASPA (Suspension of Erythrocytes Encapsulating L-asparaginase)in Patients With Pancreatic Cancer	2012	https://clinicaltrials.gov/ct2/show/NCT01523808?term=erytech+pharma&draw=2&rank=7 NCT01523808	completed
GRASPA Treatment for Patients With Acute Myeloblastic Leukemia (ENFORCE)	2013	https://clinicaltrials.gov/ct2/show/NCT01810705?term=erytech+pharma&draw=2&rank=6 NCT01810705	completed
Efficacy and Safety of L-asparaginase Encapsulated in RBC Combined With Gemcitabine or FOLFOX in 2nd Line for Progressive Metastatic Pancreatic Carcinoma	2014	https://clinicaltrials.gov/ct2/show/NCT02195180?term=erytech+pharma&draw=2&rank=4 NCT02195180	completed
Study of Eryaspase in Combination With Chemotherapy Versus Chemotherapy Alone as 2nd-Line Treatment in PDAC (Trybeca-1)	2018	https://clinicaltrials.gov/ct2/show/NCT03665441?term=erytech+pharma&draw=2&rank=2 NCT03665441	recruiting
Study of Eryaspase in Combination With Chemotherapy Versus Chemotherapy Alone as 1st Line Treatment of TNBC (TRYbeCA-2)	2018	https://clinicaltrials.gov/ct2/show/NCT03674242?term=erytech+pharma&draw=2&rank=1 NCT03674242	recruiting
Trial of Erythrocyte Encapsulated Thymidine Phosphorylase In Mitochondrial Neurogastrointestinal Encephalomyopathy (TEETPIM)	2019	https://clinicaltrials.gov/ct2/show/NCT03866954?term=MNGIE&draw=2&rank=3 NCT03866954	not yet recruiting
Safety and Tolerability of RTX-134 in Adults With Phenylketonuria	2019	https://clinicaltrials.gov/ct2/show/NCT04110496?term=Rubius&cond=PKU&draw=2&rank=1 NCT04110496	recruiting

5. References

1. Ihler GM, Glew RH, Schnure FW. Enzyme loading of erythrocytes. Proc Natl Acad Sci USA. 1973; 70:2663–6.
2. Hoffman JF. Physiological characteristics of human red blood cell ghosts. J Gen Physiol. 1958; 42:9–28.
3. Hoffman JF. On red blood cells, hemolysis and resealed ghosts. Adv Exp Med Biol. 1992; 326:1–15.

4. DeLoach JR. Hypotonic dialysis encapsulation in erythrocytes of mammalian species. Bibl Haematol. 1985; 51:1–6.

5. Pierige F, Bigini N, Rossi L, Magnani M. Reengineering red blood cells for cellular therapeutics and diagnostics. WIREs Nanomed Nanobiotechnol. 2017. https://doi.org/10.1002/wnan.1454.

6. Villa CH, Anselmo AC, Mitragotri S, Muzykantov V. Red blood cells: supercarriers for drugs, biologicals, and nanoparticles and inspiration for advanced delivery systems. Adv Drug Deliv Rev. 2016; 106:88–103.

7. Rossi L, Fraternale A, Bianchi M, Magnani M. Red blood cell membrane processing for biomedical applications. Front Physiol. 2019. https://doi.org/10.3389/fphys.2019.01070.

8. Ji W, Smith PN, Koepsel RR, Andersen JD, Baker SL, Zhang L, Carmali S, Myerson JW, Muzykantov S, Russell AJ. Erythrocytes as carriers of immunoglobulin-based therapeutics. Acta Biomater. 2020; 101:422–35. https://doi.org/10.1016/j.actbio.2019.10.027.

9. Villa CH, Pan DC, Johnston IH, Greineder CF, Walsh LR, Hood ED, Cines DB, Poncz M, Siegel DL, Muzykantov VR. Biocompatible coupling of therapeutic fusion proteins to human erythrocytes. Blood Adv. 2018;2(3):165–76. https://doi.org/10.1182/bloodadvances.2017011734.

10. Han X, Wang C, Liu Z. Red blood cells as smart delivery systems. Bioconjug Chem. 2018;29(4):852–60. https://doi.org/10.1021/acs.bioconjchem.7b00758.

11. Brenner JS, Pan DC, Myerson JW, Marcos-Contreras OA, Villa CH, Patel P, Hekierski H, Chatterjee S, Tao JQ, Parhiz H, Bhamidipati K, Uhler TG, Hood ED, Kiseleva RY, Shuvaev VS, Shuvaeva T, Khoshnejad M, Johnston I, Gregory JV, Lahann J, Wang T, Cantu E, Armstead WM, Mitragotri S, Muzykantov V. Red blood cell-hitchhiking boosts delivery of nanocarriers to chosen organs by orders of magnitude. Nat Commun. 2018;9(1):2684. https://doi.org/10.1038/s41467-018-05079-7.

12. Magnani M, Rossi L, D'ascenzo M, Panzani I, Bigi L, Zanella A. Erythrocyte engineering for drug delivery and targeting. Biotechnol Appl Biochem. 1998;28(1):1–6.

13. Mambrini G, Mandolini M, Rossi L, Pierigè F, Capogrossi G, Salvati P, Serafini S, Benatti L, Magnani M. Ex vivo encapsulation of dexamethasone sodium phosphate into human autologous erythrocytes using fully automated biomedical equipment. Int J Pharm. 2017;517(1–2):175–84.

14. Coker SA, Szczepiorkowski ZM, Siegel AH, Ferrari A, Mambrini G, Anand R, Hartman RD, Benatti L, Dumont LJ. A study of the pharmacokinetic properties and the in vivo kinetics of erythrocytes loaded with dexamethasone sodium phosphate in healthy volunteers. Transfus Med Rev. 2018;32(2):102–10.

15. Rossi L, Serafini S, Cenerini L, Picardi F, Bigi L, Panzani I, Magnani M. Erythrocyte-mediated delivery of dexamethasone in patients with chronic obstructive pulmonary disease. Biotechnol Appl Biochem. 2001;33(2):85–9.

16. Rossi L, Castro M, D'Orio F, Damonte G, Serafini S, Bigi L, Panzani I, Novelli G, Dallapiccola B, Panunzi S, Di Carlo P, Bella S, Magnani M. Low doses of dexamethasone constantly delivered by autologous erythrocytes slow the progression of lung disease in cystic fibrosis patients. Blood Cells Mol Dis. 2004;33(1):57–63.

17. Annese V, Latiano A, Rossi L, Lombardi G, Dallapiccola B, Serafini S, Damonte G, Andriulli A, Magnani M. Erythrocytes-mediated delivery of dexamethasone in steroid-dependent IBD patients—a pilot uncontrolled study. Am J Gastroenterol. 2005;100(6):1370–5.

18. Castro M, Knafelz D, Rossi L, Ambrosini MI, Papadatou B, Mambrini G, Magnani M. Periodic treatment with autologous erythrocytes loaded with dexamethasone 21-phosphate for fistulizing pediatric Crohn's disease: case report. J Pediatr Gastroenterol Nutr. 2006;42(3):313–5.

19. Castro M, Rossi L, Papadatou B, Bracci F, Knafelz D, Ambrosini MI, Calce A, Serafini S, Isacchi G, D'Orio F, Mambrini G, Magnani M. Long-term treatment with autologous red blood cells loaded with dexamethasone 21-phosphate in pediatric patients affected by steroid-dependent Crohn disease. J Pediatr Gastroenterol Nutr. 2007;44(4):423–6.

20. Bossa F, Latiano A, Rossi L, Magnani M, Palmieri O, Dallapiccola B, Serafini S, Damonte G, De Santo E, Andriulli A, Annese V. Erythrocyte-mediated delivery of dexamethasone in patients with mild-to-moderate ulcerative colitis, refractory to mesalamine: a randomized, controlled study. Am J Gastroenterol. 2008;103(10):2509–16.

21. Bossa F, Annese V, Valvano MR, Latiano A, Martino G, Rossi L, Magnani M, Palmieri O, Serafini S, Damonte G, De Santo E, Andriulli A. Erythrocytes-mediated delivery of dexamethasone 21-phosphate in steroid-dependent ulcerative colitis: a randomized, double-blind Sham-controlled study. Inflamm Bowel Dis. 2013;19(9):1872–9.

22. Chessa L, Leuzzi V, Plebani A, Soresina A, Micheli R, D'Agnano D, Venturi T, Molinaro A, Fazzi E, Marini M, Ferremi Leali P, Quinti I, Cavaliere FM, Girelli G, Pietrogrande MC, Finocchi A, Tabolli S, Abeni D, Magnani M. Intra-erythrocyte infusion of dexamethasone reduces neurological symptoms in ataxia teleangiectasia patients: results of a phase 2 trial. Orphanet J Rare Dis. 2014. https://doi.org/10.1186/1750-1172-9-5.

23. Updike SJ, Wakamiya RT, Lightfoot EN Jr. Asparaginase entrapped in red blood cells: action and survival. Science. 1976;193(4254):681–3.

24. Updike SJ, Wakamiya RT. Infusion of red blood cell-loaded asparaginase in monkey. Immunologic, metabolic, and toxicologic consequences. J Lab Clin Med. 1983;101(5):679–91.

25. Kravtzoff R, Colombat PH, Desbois I, Linassier C, Muh JP, Philip T, Blay JY, Gardenbas M, Poumier-Gaschard P, Lamagnere JP, Chassaigne M, Ropars C. Tolerance evaluation of L-asparaginase loaded in red blood cells. Eur J Clin Pharmacol. 1996;51(3–4):221–5.

26. Kravtzoff R, Desbois I, Lamagnere JP, Muh JP, Valat C, Chassaigne M, Colombat P, Ropars C. Improved pharmacodynamics of L-asparaginase loaded in human red blood cells. Eur J Clin Pharmacol. 1996;49(6):465–70.

27. Garín MI, Kravtzoff R, Chestier N, Sanz S, Pinilla M, Luque J, Ropars C. Density gradient separation of L-asparaginase-loaded human erythrocytes. Biochem Mol Biol Int. 1994;33(4):807–14.

28. Ktavtzoff R, Desbois I, Doinel C, Colombat P, Lamagnere JP, Chassaigne M, Ropars C. Immunological response to L-asparaginase loaded into red blood cells. Adv Exp Med Biol. 1992;326:175–82.

29. Kravtzoff R, Ropars C, Laguerre M, Muh JP, Chassaigne M. Erythrocytes as carriers for L-asparaginase. Methodological and mouse in vivo studies. J Pharm Pharmacol. 1990;42(7):473–6.

30. Domenech C, Thomas X, Chabaud S, Baruchel A, Gueyffier F, Mazingue F, Auvrignon A, Corm S, Dombret H, Chevallier P, Galambrun C, Huguet F, Legrand F, Mechinaud F, Vey N, Philip I, Liens D, Godfrin Y, Rigal D, Bertrand Y. L-Asparaginase loaded red blood cells in refractory or relapsing acute lymphoblastic leukaemia in children and adults: results of the GRASPALL 2005-01 randomized trial. Br J Haematol. 2011;153(1):58–65.

31. Hunault-Berger M, Leguay T, Huguet F, Leprêtre S, Deconinck E, Ojeda-Uribe M, Bonmati C, Escoffre-Barbe M, Bories P, Himberlin C, Chevallier P, Rousselot P, Reman O, Boulland ML, Lissandre S, Turlure P, Bouscary D, Sanhes L, Legrand O, Lafage-Pochitaloff M, Béné MC, Liens D, Godfrin Y, Ifrah N, Dombret H, Group for Research on Adult Acute Lymphoblastic Leukemia (GRAALL). A phase 2 study of L-asparaginase encapsulated in erythrocytes in elderly patients with Philadelphia chromosome negative acute lymphoblastic leukemia: the GRASPALL/GRAALL-SA2-2008 study. Am J Hematol. 2015;90(9):811–8.

32. Bachet JB, Gay F, Maréchal R, Galais MP, Adenis A, MsC DS, Cros J, Demetter P, Svrcek M, Bardier-Dupas A, Emile JF, Hammel P, Ebenezer C, Berlier W, Godfrin Y, André T. Asparagine synthetase expression and phase I study with L-asparaginase encapsulated in red blood cells in patients with pancreatic adenocarcinoma. Pancreas. 2015;44(7):1141–7.

33. Hammel P, Fabienne P, Mineur L, Metges JP, Andre T, De La Fouchardiere C, Louvet C, El Hajbi F, Faroux R, Guimbaud R, Tougeron D, Bouche O, Lecomte T, Rebischung C, Tournigand C, Cros J, Kay R, Hamm A, Gupta A, Bachet JB, El Hariry I. Erythrocyte-encapsulated asparaginase (eryaspase) combined with chemotherapy in second-line treatment of advanced pancreatic cancer: an open-label, randomized Phase IIb trial. Eur J Cancer. 2019; 124:91–101.

34. Moran NF, Bain MD, Muqit MM, Bax BE. Carrier erythrocyte entrapped thymidine phosphorylase therapy for MNGIE. Neurology. 2008;71(9):686–8.

35. Bax BE, Bain MD, Scarpelli M, Filosto M, Tonin P, Moran N. Clinical and biochemical improvements in a patient with MNGIE following enzyme replacement. Neurology. 2013;81(14):1269–71.

36. Levene M, Bain MD, Moran NF, Nirmalananthan N, Poulton J, Scarpelli M, Filosto M, Mandel H, MacKinnon AD, Fairbanks L, Pacitti D, Bax BE. Safety and efficacy of erythrocyte encapsulated thymidine phosphorylase in

mitochondrial neurogastrointestinal encephalomyopathy. J Clin Med. 2019. https://doi.org/10.3390/jcm8040457.

37. Bax BE, Levene M, Bain MD, Fairbanks LD, Filosto M, Kalkan Uçar S, Klopstock T, Kornblum C, Mandel H, Rahman S, Roubertie A, Scarpelli M, Sedgwick PM, Baru M, Sellos-Moura M, Price J, Horn P, Nirmalananthan N. Erythrocyte encapsulated thymidine phosphorylase for the treatment of patients with mitochondrial neurogastrointestinal encephalomyopathy: study protocol for a multi-centre, multiple dose, open label trial. J Clin Med. 2019. https://doi.org/10.3390/jcm8081096.

38. Pacitti D, Levene M, Garone C, Nirmalananthan N, Bax BE. Mitochondrial neurogastrointestinal encephalomyopathy: into the fourth decade, what we have learned so far. Front Genet. 2018. https://doi.org/10.3389/fgene.2018.00669.

39. Bilder DA, Noel JK, Baker ER, Irish W, Chen Y, Merilainen MJ, Prasad S, Winslow BJ. Systematic review and meta-analysis of neuropsychiatric symptoms and executive functioning in adults with phenylketonuria. Dev Neuropsychol. 2016;41(4):245–60.

40. Leuzzi V, Chiarotti F, Nardecchia F, van Vliet D, van Spronsen FJ. Predictability and inconsistencies of cognitive outcome in patients with phenylketonuria and personalised therapy: the challenge for the future guidelines. J Med Genet. 2019. https://doi.org/10.1136/jmedgenet-2019-106278.

41. Gupta S, Lau K, Harding CO, Shepherd G, Boyer R, Atkinson JP, Knight V, Olbertz J, Larimore K, Gu Z, Li M, Rosen O, Zoog SJ, Weng HH, Schweighardt B. Association of immune response with efficacy and safety outcomes in adults with phenylketonuria administered pegvaliase in phase 3 clinical trials. EBioMedicine. 2018;37:366–73.

42. Rossi L, Pierigè F, Carducci C, Gabucci C, Pascucci T, Canonico B, Bell SM, Fitzpatrick PA, Leuzzi V, Magnani M. Erythrocyte-mediated delivery of phenylalanine ammonia lyase for the treatment of phenylketonuria in BTBR-Pah(enu2) mice. J Control Release. 2014;194:37–44.

43. Pascucci T, Rossi L, Colamartino M, Gabucci C, Carducci C, Valzania A, Sasso V, Bigini N, Pierigè F, Viscomi MT, Ventura R, Cabib S, Magnani M, Puglisi-Allegra S, Leuzzi V. A new therapy prevents intellectual disability in mouse with phenylketonuria. Mol Genet Metab. 2018;124(1):39–49.

44. Pierigè F, Bigini N, Rossi L, Magnani M. Reengineering red blood cells for cellular therapeutics and diagnostics. Wiley Interdiscip Rev Nanomed Nanobiotechnol. 2017. https://doi.org/10.1002/wnan.1454.

45. Rossi L, Pierigè F, Antonelli A, Bigini N, Gabucci C, Peiretti E, Magnani M. Engineering erythrocytes for the modulation of drugs' and contrasting agents' pharmacokinetics and biodistribution. Adv Drug Deliv Rev. 2016;106(Pt A):73–87.

46. Leuzzi V, Rossi L, Gabucci C, Nardecchia F, Magnani M. Erythrocyte-mediated delivery of recombinant enzymes. J Inherit Metab Dis. 2016;39(4):519–30.

47. Sprandel U. Erythrocytes as carrier for therapeutic enzymes—an approach towards enzyme therapy of inborn errors of metabolism. Bibl Haematol. 1985;51:7–14.

48. Magnani M, Serafini S, Fraternale A, Antonelli A, Biagiotti S, Pierigè F, Sfara C, Rossi L. Red blood cell-based delivery of drugs and nanomaterials for therapeutic and diagnostic applications. In: Nalwa HS, editor. Encyclopedia of nanoscience and nanotechnology. New York: American Scientific Publishers; 2011. p. 309–54.

49. A new era in cellular medicine. Rubius Therapeutics, Inc. 2019. https://ir.rubiustx.com/static-files/d5ef2cfc-3c34-4950-ac6f-b03ca9ff11e4. Accessed 3 Mar 2020.

50. Rubius Therapeutics Announces FDA Clearance of Investigational New Drug Application for First-Ever Red Cell Therapeutic, RTX-134, for Treatment of Phenylketonuria (press release). Rubius Therapeutics, Inc., 11 Mar 2019. https://www.globenewswire.com/news-release/2019/03/11/1751139/0/en/Rubius-Therapeutics-Announces-FDA-Clearance-of-Investigational-New-Drug-Application-for-First-Ever-Red-Cell-Therapeutic-RTX-134-for-Treatment-of-Phenylketonuria.html. Accessed 3 Mar 2020.

Links

1. Link 1 https://ir.rubiustx.com/static-files/d5ef2cfc-3c34-4950-ac6f-b03ca9ff11e4.
2. Link 2 https://www.globenewswire.com/news-release/2019/03/11/1751139/0/en/Rubius-Therapeutics-Announces-FDA-Clearance-of-Investigational-New-Drug-Application-for-First-Ever-Red-Cell-Therapeutic-RTX-

134-for-Treatment-of-Phenylketonuria.html) of a Phase 1b trial in March 2019 (https://clinicaltrials.gov/ct2/show/NCT04110496

6. Compliance with ethical standards

Funding: This work was partially supported by Horizon 2020 IEDAT grant n. 667946.

Conflicts of interest: Mauro Magnani and Luigia Rossi hold shares in EryDel SpA a company with interests in the technology of RBC-based drug delivery. The other authors declare that the research was conducted in the absence of any commercial or financial relationships that could be construed as a potential conflict of interest.

APPLICATION OF PAL-LOADED RBCs IN THE TREATMENT OF PKU

1. Introduction

1.1. L-Tyrosine

L-Tyrosine (L-Tyr) is one of the 20 standard amino acids that are used by cells to synthesize proteins. It is a non-essential amino acid with a polar side group.

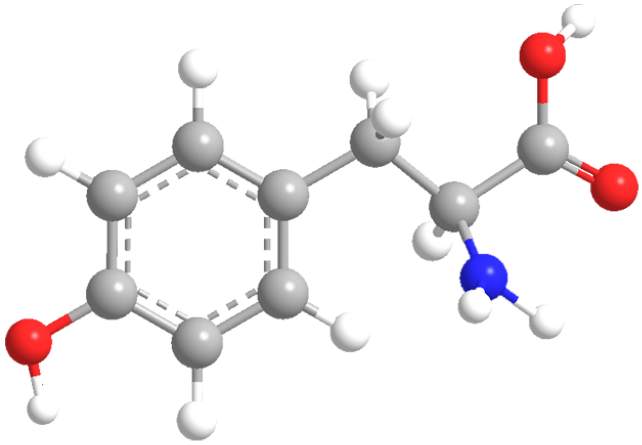

Figure 2 Structure of L-Tyrosine

Aside from being a proteinogenic amino acid, L-Tyr has a special role by virtue of the phenol functionality. It occurs in proteins that are part of signal transduction processes and functions as a receiver of phosphate groups that are transferred by way of protein kinases.
In dopaminergic cells in the brain, L-Tyr is converted to L-DOPA by the enzyme tyrosine hydroxylase (TH).
Mammals synthesize L-Tyr from the essential amino acid phenylalanine (L-Phe), which is derived from food. The conversion of L-Phe to L-Tyr is catalyzed by the enzyme phenylalanine hydroxylase (PAH). This enzyme catalyzes the reaction causing the addition of a hydroxyl group to the end of the 6-carbon aromatic ring of phenylalanine, such that it becomes L-Tyr.

1.2. Phenylalanine hydroxylase

Phenylalanine hydroxylase (PAH) (EC 1.14.16.1) catalyzes the hydroxylation of the aromatic side-chain of phenylalanine to generate L-Tyr. PAH is one of three members of the biopterin-dependent aromatic amino acid hydroxylases, a class of monooxygenase that uses tetrahydrobiopterin (BH4, a pteridine cofactor).
The gene encoding PAH it is located on the long arm of chromosome 12 (12q22-12q23.2), has a size of 79.28 kb (NT_029419.13) and is composed of 13 exons and related introns (3).

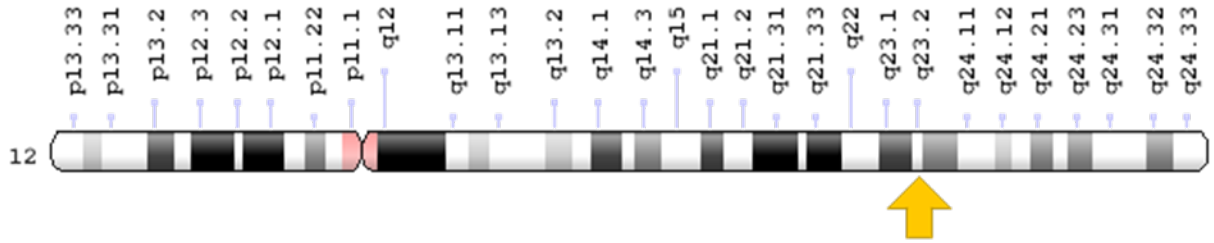

Figure 3 Basic structure and localization of the human PAH gene. Located on the long arm of chromosome 12, the human PAH gene contains 13 exons that encode a polypeptide of 452 amino acid

The mammalian PAH protein is a homotetrameric enzyme consisting of 50 kDa subunits (200 kD as a tetramer). Each subunit consists of an N-terminal regulatory domain (residues 1-110), a central catalytic domain (residues 111-410) and a C-terminal oligomerization domain (411-452) Figure 4 (4) (5).

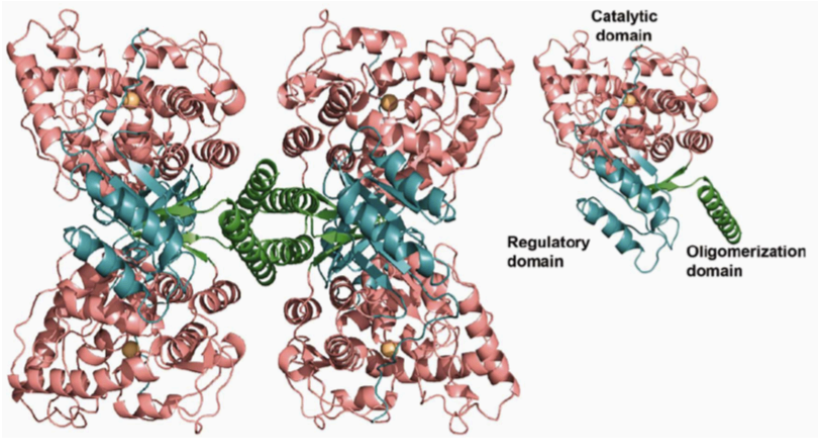

Figure 4 Structure and organization of phenylalanine hydroxylase domains

The tetramer formed by PAH is asymmetrical because it is a “dimer of dimers” (6), where secondary elements switch their mutual position in order to promote a stable oligomerization, together with the formation of an antiparallel coiled-coil structure with the other monomers.

The N-terminal regulatory domain is classified as an ACT domain, this flexibly binds the central catalytic domain of its subunit but interacts, for an extended area, with the central catalytic domain of the adjacent subunit (7). The regulatory domain is necessary for the purpose of regulating the activity of the enzyme, for example, activation by L-Phe.

The catalytic domain contains a binding site for iron, the BH4 cofactor and the substrate of the enzyme. Phenylalanine hydroxylase catalyzes the hydroxylation of its substrate by incorporating an oxygen atom within the aromatic ring, while the other oxygen atom is reduced to water, using two electrons supplied by BH4. BH4 also functions as a co-substrate, which is in turn oxidized to pterin-4α-carbinolamine (4 α-OH- BH4) and therefore dissociates from the enzyme (8). The mechanism is displayed in Figure 5.

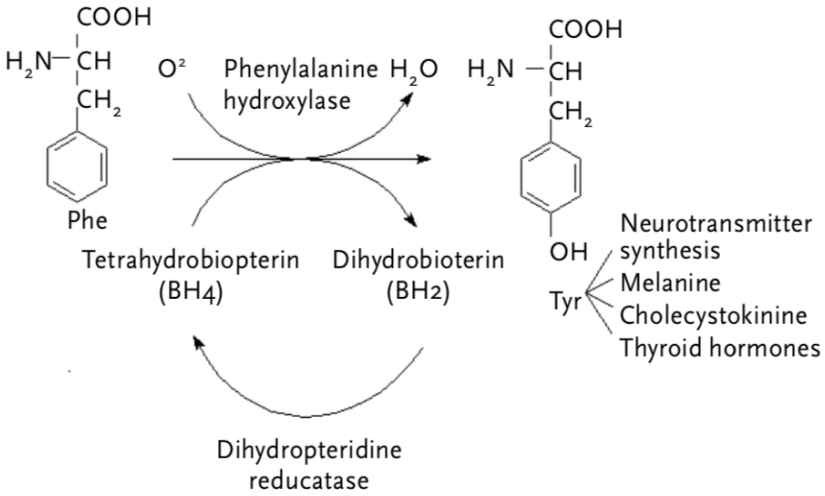

Figure 5 PAH mechanism of action

1.3. PAH gene mutations and phenylketonuria

851 gene variants, 61.5% missense mutations, 15% splice variants, 12.8% deletions, 5.8% nonsense mutations, 1.9% insertions and 3% indel, deletions and silent mutations were found. Mutations are distributed throughout the gene but mainly present on exons 6, 7 and 11 (9).

Mutations in both alleles of the PAH gene cause a disease called phenylketonuria (PKU). PKU is a result of an inborn error of amino acid metabolism caused by a deficiency of the enzyme phenylalanine hydroxylase which catalyze the irreversible conversion, via para-hydroxylation, of the amino acid L-phenylalanine (L-Phe) into L-Tyr, a limiting step for the complete oxidation of L-Phe to CO_2 and H_2O (10).

PKU is an autosomal recessive metabolic disease characterized by severe intellectual impairment, motor problems and skin abnormalities and occupies a unique place in the history of the study of metabolic diseases, not only for its role as the main inborn error of amino acid metabolism but also because it was the first cause of mental retardation to be discovered.

1.4. Characteristics of the disease

Untreated phenylketonuria is associated with progressive cognitive retardation accompanied by secondary symptoms such as autism, seizures, eczema and motor deficits that drastically reduce the person's quality of life. Furthermore, possible problems during the development of the subject, anomalous behaviors and psychiatric problems are not excluded (10). Almost all subjects with untreated PKU show aggression, anxiety, hyperactivity, lack of control of movements and problems in integrating into society. Physical aspects are slowed growth, microcephaly, reduced pigmentation of hair, skin and iris, eczema, and finally, urine with a typical moldy smell. In some cases, abnormal electroencephalograms, seizures, tics and alterations of the gait cycle, hypereflexia, tremors and other symptoms have also been found.

The toxic effects of high concentrations of L-Phe mainly occur in the brain, where L-Phe arrives by crossing the blood brain barrier via the neutral amino acid transporter LAT1. High levels of L-Phe in the circulation cause an increase in the uptake of L-Phe from the systemic to the cerebral circulation, reduce the uptake of other neutral amino acids and favor their expulsion. Specifically, the amino acids that undergo an important decrease are L-Tyr and tryptophan (11).

The high concentration of L-Phe in the circulation can inhibit the passage of L-Tyr and tryptophan to the brain via LAT1, causing a deficiency of the latter in the brain, which results in neurotransmitter deficiency and slowing down of protein synthesis (12).
Furthermore, the transporter LAT1 implements an antiport: for each neutral amino acid transported across the blood brain barrier, another neutral amino acid is transported out into the systemic circulation. This also happens for the F-dihydroxyphenylalanine (F-DOPA) molecule, which in turn uses the LAT1 transporter to cross the blood-brain barrier and which, therefore, is deficient in the brain in patients with PKU (13).
In addition, the decrease of LNAA in the brain, in subjects with PKU, could be the cause of the cognitive and neurological deficits found in untreated patients (14).
The potential mechanisms of neurological damage caused by high levels of phenylalanine can be summarized in Figure. 6

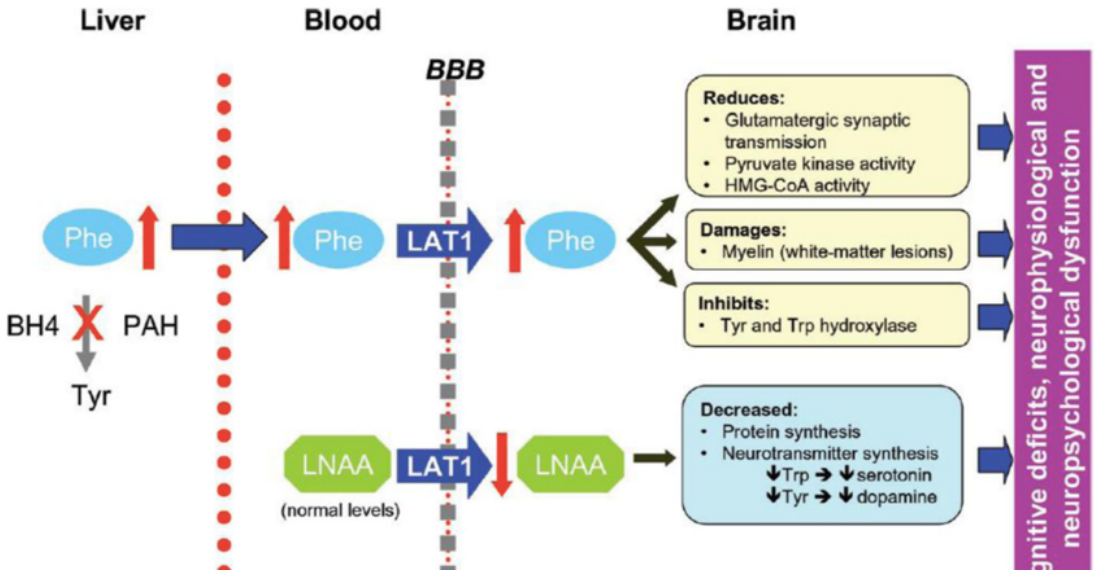

Figure 6 mechanisms of neurological damage caused by high levels of phenylalanine

1.5. Diagnosis

PKU was the first congenital disorder of metabolism for which neonatal screening was instituted. The diagnosis on a biochemical basis is carried out by identifying high concentrations of L-Phe in the circulation. This analysis is performed by mass spectrometry, thanks to which the concentrations of various analytes, such as L-Phe and L-Tyr, can be identified in a single drop of blood.

Finally, PKU must be diagnosed through molecular analysis and encompasses the identification of the mutation carried by the subject (10). Next generation sequencing (NGS) is the technique of choice for identifying causative mutations.
In October 2016, in Italy was issued the D.L. 13.10.2016: "Provisions for the initiation of newborn screening for the early diagnosis of hereditary metabolic diseases". The decree of the President of the Council of Ministers extended the obligation to carry out tests useful for the early diagnosis and timely treatment of congenital hypothyroidism, phenylketonuria and cystic fibrosis to all Italian regions and to the autonomous provinces of Trento and Bolzano. These screening generally use the method of "tandem mass spectrometry", but in some cases ELISA and immunofluorimetric tests are used.

1.6. Therapeutic Approaches for PKU

PKU is the first genetic disease that has effective treatments, even if it is not a cure.

The main aim of all available therapeutic approaches is to restore at least near-physiological levels of circulating L-Phe and L-Tyr. Optimal blood L-Phe levels should be ranged between 120-360 µmol/l in all patients. This could be achieved by low-Phe diet.

1. Low-Phe diet therapy:

   To date, the main treatment strategy of phenylketonuria appears to be diet therapy with a low content of L-Phe. Dietary treatment must be adopted as soon as possible after birth, following the diagnosis on a newborn. The strategy is to introduce adequate doses of L-Phe, assessed on the basis of individual response, so as to support cell growth and repair and, at the same time, keep plasma L-Phe concentrations within the range (15). The diet consists of reducing the introduction of foods rich in L-Phe such as meat, fish, eggs, etc. Generally, as summarized in table 1, in Europe diet therapy provides 2/3 g/kg/day of total protein in children from 0 to 1 year (16).

   To obtain an adequate metabolic regime it is necessary to calculate the tolerance to L-Phe defined as milligrams of L-Phe per kilogram of body weight, per day. A parameter that changes during the life cycle of the individual and also according to one's susceptibility.

   In the first 3 months of life, higher levels of Phe will be tolerated (55 mg/kg/day), while upon reaching 12 months, these levels will be halved (27 mg/kg/day) (17). After the first year of life, children with classic PKU tolerate 200-500 mg/day of L-Phe, while milder forms of this pathology allow the introduction of quantities greater than 500 mg/day of this amino acid.

   The protein requirement will be covered by the introduction of free L-amino acids in the form of supplements, with the exception of L-Phe.

   L-amino acid supplementation should be scheduled throughout the day to minimize amino acid losses and fluctuations of L-Phe plasmatic levels (18). Particular attention must be paid on the intake of L-Tyr, an amino acid normally synthesized from L-Phe. In fact, as already mentioned, L-Tyr is essential for the synthesis of neurotransmitters such as adrenaline, noradrenaline and dopamine, of melanin and hormones such as thyroxine (19).

   Usually, L-Tyr represents the 9-11% of total amino acids present in the synthetic preparation, so as to provide the subject with about 100 mg of L-Tyr per gram of protein equivalent.

   As an alternative to synthetic L-amino acid supplements, a protein preparation derived from whey has been developed; this takes the name of glycomacropeptide (GMP). However, GMP does not completely cover the L-amino acid needs of the subject who thus requires additional L-Tyr, tryptophan, histidine and leucine supplementation. Moreover, GMP contains small doses of L-Phe (20).

2. Innovative therapies

   2.1. Administration of tetrahydrobiopterin (BH4)

   In some cases of hyperphenylalaninemia, exogenous BH4, is able to stabilize the PAH tetramer and prevents its misfolding, aggregation, proteolytic degradation and thermal inactivation. In these case we will talk about BH4-reactive phenylketonuria (21). It has been shown that a single dose of 10-20 mg/kg per day is sufficient to maintain L-Phe concentrations stable for 24 hours in BH4-reactive subjects (22). The formulation approved by the Food and Drug Administration (FDA) and European Medicines Agency (EMA) is the sapropterin dihydrochloride developed by BioMarin Pharmaceutical Inc. Nevertheless, it must be pointed out that BH4 is especially effective in cases of hyperphenylalaninemia, rather than phenylketonuria.

2.2. Gene therapy and Cell therapy

Gene therapy for PKU consists in restoring the function of the PAH enzyme with a gene approach. The gene approach in question is based on the delivery of the PAH cDNA, through different vectors within organs or tissues such as the liver (23). The Adeno-associated recombinant virus (rAAV) has attracted great attention because of its advantages of being poorly immunogenic, its ability to infect cells that do not divide, its low tissues specificity and the absence of liver damage (24). When targeted to the liver, as in the case for PKU, the main drawback is that a little cell turnover exists, and the acquired gene copies are lost when hepatocytes divide.

Cell therapy has been also proposed for the treatment of inborn errors of metabolism. The transplantation of hepatocytes with functioning PAH would be a definitive approach to restore liver repopulation with donor-derived wild-type hepatocytes. Nevertheless, liver transplantations would require the long-lasting treatment with immunosuppressant to contrast the host rejection.

2.3. Enzyme replacement therapy

Enzyme Replacement Therapy (ERT), as already discussed, is a medical treatment that replaces an enzyme that is deficient or absent in the body. This technique is not feasible by replacing the PAH enzyme, owing to the instability of the enzyme and to the need for the BH4 cofactor to act, as well as the enzymes that regenerates the cofactor itself. All these issues make PHA administration difficult (25).

However, it is possible to exploit ERT technique by introducing the enzyme phenylalanine ammonium lyase (PAL) as a substitute for the PAH enzyme, which is deficient in PKU subjects. This enzyme catalyzes the conversion of L-Phe into ammonia and trans-cinnamic acid.

1.7. Phenylalanine Ammonium Lyase

PAL (EC 1.3.1.5) is a bacterial enzyme that catalyzes the conversion of L-Phe into ammonia and trans-cinnamic acid (Figure 7).

The catalyzed reaction is completely harmless, as ammonia will be metabolized in the liver and trans-cinnamic acid will be excreted with the urine in the form of hippurate, cinnamate and benzoic acid (small amounts) (26).

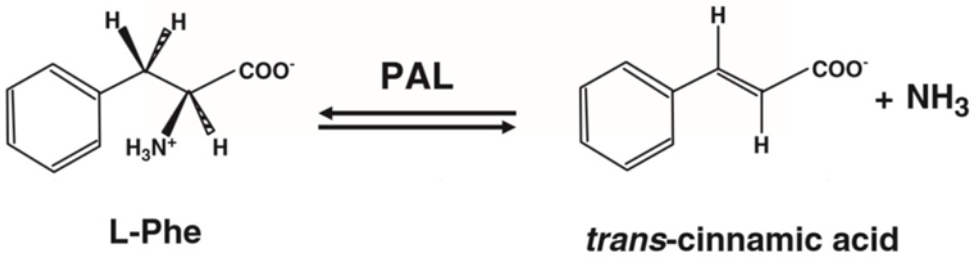

Figure 7 Phenylalanine Ammonia Lyase reaction

PAL is a protein belonging to the superfamily of ammonium lyases, deaminases that catalyze the removal of an amino group from L-amino acids (27).

PAL protein (homonymous to the gene) is a homotetramer containing four active sites formed by four distinct monomer units. Among the prokaryotic organisms in which PAL has been identified, we find some

cyanobacteria including Anabaena variabilis ATCC 29413. The PAL identified in Anabaena variabilis ATCC 29413 (Ava_3988, AvPAL) consists of 567 residues (Fig.8) encoded by the AvPAL gene that generates a transcript of 1710bp.

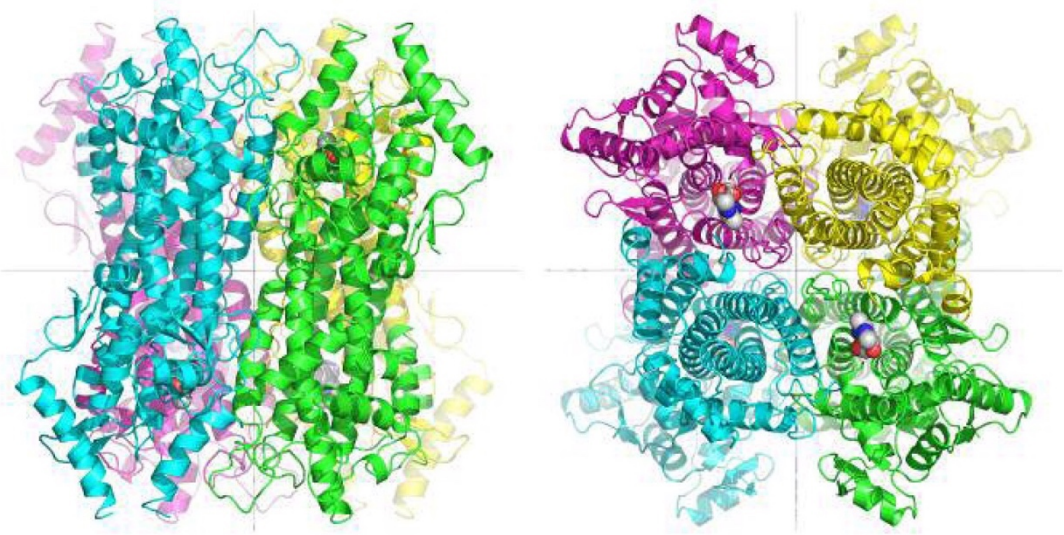

Figure 8 AvPA homotetramer: The related polypeptide chains represent the different colors: A (green), B (blue), C (magenta) and D (yellow). The atoms of the four MIO prosthetic groups are represented by spheres. The image on the left depicts the side of the helix bundle of the four monomers, the image on the right depicts a top view of the homotetramer in which it is possible to identify the active sites of two monomers.

Within the active site, there is a prosthetic group that is required for the catalytic activity: 4-methyldene-imdizaol-5-one (MIO). MIO is formed with a cyclization and dehydration process starting from an active site represented by a tripeptide Ala-Ser-Gly (28) (29). The imidazolone ring is fixed to the side chain of 363Phe with an interplanar distance of 4 Å. The 168N atom of MIO forms a hydrogen bond with the OH of 314Tyr (residue numbering refers to the polypeptide chain of a single monomer (A)). The other MIO atom available for polar interactions, 168O, forms a hydrogen bond with the side chain of Asn 223, and is also sourrounded by a small pocket lined out by the backbone amide-nitrogens of Leu 171 and Gly 224.
In the AvPAL structure, two disordered polypeptide-chain segments (residues 75–91 and 301–309) are located near to the entrance of the active-site cleft (30). In 2001, BioMarin Pharmaceutical began developing a free PAL enzyme formulation. A polyethylene glycol (PEG) molecule was then added to the enzyme and a series of mutations and combinations of the same were evaluated to obtain an enzyme suitable for enzyme replacement therapy in PKU (31). Various PEG-PALs derived from multiple species were tested, including Anabaena variabilis, and all these isoforms were tested for their activity in reducing blood and brain Phe levels in PKU mice and for their ability to reduce clinical manifestations of hyperphenylalaninemia. At the end of the tests, the PEG-PAL double mutant (C503S, C565S) from Anabaena variabilis (Av) was chosen to start the clinical trial with this recombinant protein named pegvaliase (32). Several clinical trials were performed. The clinical trials implemented with pegvaliase began with a phase 1 trial, in which treated subjects received a single dose of the drug by subcutaneous injection and were monitored for the next 42 days. On day 6, from the dose of 0.1 mg/kg of pegvaliase, there was a significant reduction in plasma L-Phe concentrations (48.3%). Phase 2 of Biomarine experimentation continued with two studies: PAL-002 (NCT00925054) and PAL-004 (NCT01212744). PAH-002 was an open-label, multi-center study involving 40

adults with PKU. Patients entered an 8-week induction phase in which they were given various doses of pegvaliase, either fixed or based on their body weight. PAH-004 was an "open label" and multicenter study involving 16 adults with PKU who were administered doses of pegvaliase for 5 days/week in a range of 0.06-0.8 mg/kg, these underwent hypersensitivity reactions.
Phase 3 of the clinical trial, PRISM-1 (NCT01819727), involved patients who had never taken pegvaliase and who were given increasing doses of the drug. On May 24, 2018, the FDA approved the use of pegvaliase as an enzyme replacement therapy in PAH deficiency under the trade name of Palynziq® (https://www.fda.gov/newsevents /newsroom/pressannouncements/ucm608835.htm). The risk of adverse effects remains a problem in the use of this therapy and for this reason Palynziq® is to date only available within a very restrictive program called REMS (Risk Evaluation and Mitigation Strategies) that requires the drug to be prescribed only in case of certificated need and only after a course of education mandatory for the patient and patient family. Also, due to the anti-PEG IgM and IgG antibodies that develop in the subject after treatment, it is not possible to use other drugs conjugated with PEG. Finally, this therapy is only permitted in adults, with circulating L-Phe levels > 600 µmol/L. Further studies should be undertaken to evaluate the safety and efficacy of this treatment in younger patients and in ones with milder forms of PKU. Due to the adverse effects that the administration of Palynziq® can elicit, a new route of administration of the PAL enzyme free of PEG, which is primarily responsible for adverse reactions to this treatment, is under investigation. In order to overcome this problem, we hypothesized that the PAL enzyme could be loaded inside red blood cells so as to protect it from the action of the immune system and, at the same time, allow it to carry out its catalytic activity on circulating L- Phe.

2. Aim of the work

In this work we aimed to demonstrate the ability of recombinant *Anabaena variabilis* PAL (rAvPAL) enzyme-loaded RBCs to act as an effective bioreactor in vitro and in vivo capable of reducing PHE levels and safety values. To this purpose, the wild type form of rAVPAL enzyme was produced by a production process that encompasses the following steps: cloning, production, optimization, scaling up and characterization. Once the final product was obtained, the work focused on the entrapment of the PAL into murine red blood cells for preclinical studies was conducted in a murine model of PKU.

3. Materials and methods

3.1 Generation of pET45b/His-UB-PAL construct

The chosen cloning and purification strategy are shown in Figure 9:

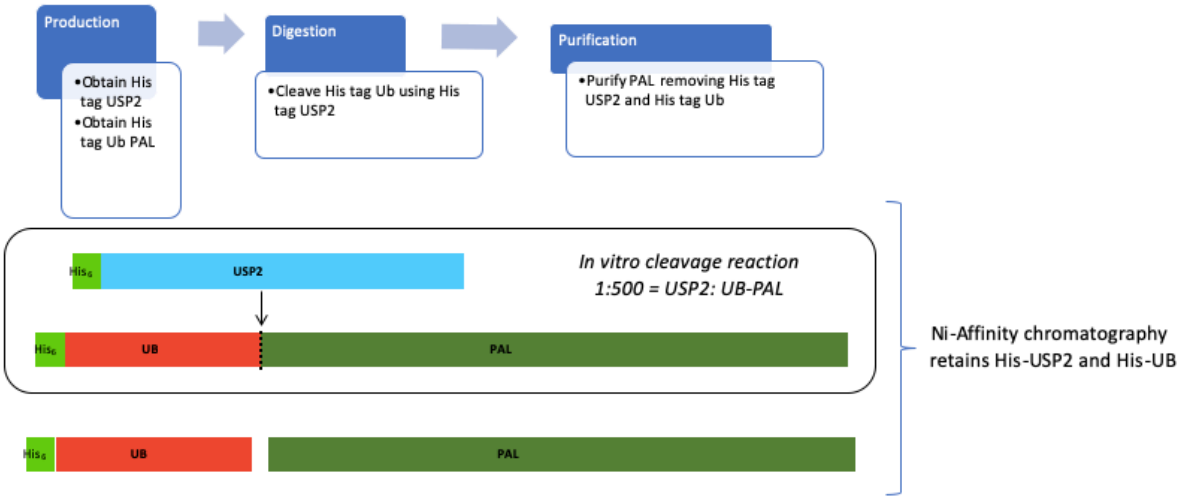

Figure 9 Expression strategy to obtain NO-tag PAL from the pET45b/His-UB-PAL construct.

The coding sequence for the wild type rAvPAL protein was synthesized in vitro and purchased from GenScript. The sub-cloning was performed using specific degenerate primers designed to amplify the PAL coding sequence.

Primer sequences are reported below:

Cloning primers	
NAME	**SEQUENCES (5' to 3')**
PAL Forward	CGTCTCCGCGGTGGAATGAAGACCCTGAGCCAGGC
PAL Reverse	CGTCTGCGGCCGCTTAATGCAGGCACGGCAGGA

The PCR product coding for rAvPAL was cloned into the pET45b-UB expression vector downstream of the $(His)_6$-ubiquitin coding sequence. The ligase reaction was used to transform Novablue E. coli strain following a standard protocol: incubation 30 min on ice; heat pulse for 90 s at +42°C and then 5 min on ice; addition of 200 µl SOC medium, followed by 1 h incubation at +37°C, before plating the transformation reaction on LB agar plates containing 100 µg/ml ampicillin. Positive colonies were screened by colony PCR and confirmed by sequencing. A positive clone was chosen and the recombinant plasmid was purified with the "QIAprep Spin Miniprep Kit" (Qiagen).

3.2 Establishment BL21(DE3) E. coli strain expressing PAL

BL21(DE3) competent cells (50 µl) were transformed by 2ng of pET45b-UB_PAL construct, according to the transformation protocol abovementioned for Novablue. A few clones of BL21(DE3) bearing the pET45b-UB_PAL construct was tested for PAL expression.

3.3 Establishment of rAvPAL Research Cell banks

For both Novablue and BL21(DE3) transformed strains, a single colony was chosen from the agar plate and inoculated in LB + ampicillin 100 µg/ml. The bacterial culture was incubated at +37°C under shaking at 250 rpm until optical density at 600 nm ($O.D._{600}$) reached approximately 0.7-0.8 (~ 4-6 h required). Then, 900 µl of the bacterial culture were added to 600 µl of glycerol, previously dispensed in suitable cryovials. Twenty glycerol stock tubes of *E. coli* cells (Novablue and BL21(DE3)) transformed with pET45b-UB_PAL construct was prepared and immediately frozen at -80°C.

3.4 Lab scale induction of recombinant PAL

The "small-scale" induction protocol is following described (any eventual variation in induction parameters is reported in the "Results" section).

Starting culture: an isolated colony was picked from a freshly streaked plate and grown overnight (ON) at +37°C in 10 ml of vegetable pepton + ampicillin (100 µg/ml) in a 50 ml tube on a benchtop orbital shaker. A sample of the ON culture was withdrawn and diluted 1:10 before reading $O.D._{600}$. The ON inoculum was then diluted into 2000 ml of synthetic media+ ampicillin (100 µg/ml) and put in a bioreactor in order to reach an $O.D._{600}$ of about 0.1. The culture was then incubated at +37°C under aeration and shaking at 250 rpm. Bacterial growth was constantly monitored until culture density reached an $O.D._{600}$ of about 0.5-0.6. 10 ml of culture were then removed, transferred to a labeled 50 ml tube and let grow at +37°C (Not Induced control, NI). To induce protein production, IPTG at 1 mM final concentration was added into the bioreactor (Induced sample, I). At 1 h-intervals, 10 ml of induced bacterial culture were withdrawn, transferred into a 15 ml-tube and put on ice. Total induction time was 3 h. At the end of the induction, cells were collected by centrifugation at 2750 g for 20 min at +4°C, the supernatant was then removed and the pellet frozen at -20°C for later processing.

3.5 Preparation of bacterial extracts and SDS-PAGE analysis

Cell lysis was obtained by resuspension of the cell pellets (from both NI and I samples) in 0.05 ml culture volume of ice cold Lysis Buffer (25mM Tris-HCl, 150mM NaCl, 10mM L-Phe, 3mM B-MSH and 10% Glycerol, pH 7.4), followed by four cycles (30 s on, 30 s off at 50% amplitude capacity) of sonication at 75 watt, while keeping the sample on ice. Samples were centrifuged 10 min at 9600 g and +4°C: the supernatant (S), corresponding to the soluble cytoplasmic fraction, was transferred into a new microcentrifuge tube, while the residual pellet was resuspended in Lysis Buffer and sonicated as above; this further sample has been referred to as the Pellet (P) sample.

The protein concentration in both S and P samples was determined by the Bradford assay (60), to normalize the samples for loading.

For SDS-PAGE, an aliquot corresponding to 10 µg of proteins (for P loaded 3µl), was diluted with an equal volume of 2X Sample Buffer (2X SB = 2% SDS, 100 mM Tris-HCl, pH 6.8, 20% glycerol, 0.0025% bromophenol blue,) and boiled for 1 min at +100°C to denature proteins. Proteins were resolved by a 10% (w/v) polyacrylamide gel electrophoresis, in parallel with the Low Molecular Weight standard (LMW) as size reference.

3.6 Immobilized metal ion affinity chromatography (IMAC)

The recombinant His-tagged UB-PAL in the supernatant fraction was purified by the immobilized metal ion affinity chromatography (IMAC), exploiting the interaction between chelated transition metal ions (Ni^{2+}) and side-chains of histidines on proteins, essentially according to the manufacturer's instructions. Briefly, the column was equilibrated with the Binding buffer which corresponds to the Lysis Buffer in which the sample has been resuspended. The lysis/storage buffer has been optimized. After sample loading, washings were initially performed with the same Binding buffer, and then with Binding Buffer + 20 mM imidazole. Elution of the His-tagged recombinant protein was obtained by Binding buffer + 300 mM imidazole.

3.7 USP2 digestion of rHis-UB-PAL

rHis-UB-PAL obtained upon Ni-Sepharose affinity chromatography was digested with the recombinant His-tagged deubiquitinating enzyme USP2 (rHis-USP2) to remove the His-UB partner fused at the N-terminus of PAL. For optimal digestion, His-UB-PAL and rHis-USP2 were combined allowing a mass ratio of 20:1 and incubated at least 3 h at +37°C, in the same PAL buffer. After cutting reaction, the protein was purified by Diethylaminoethyl (DEAE) Chromatography.

3.8 DEAE Chromatography

NO-tag Pal was purified from all the His-tag byproducts generated during the digestion and His-USP2 itself, by DEAE chromatography. Briefly, the column was equilibrated with the Binding buffer (25mM Tris-HCl, 10mM L-Phe, 3mM B-MSH and 10% Glycerol, pH 7.4). After sample loading, washings were initially performed with the same Binding buffer, and then with Binding Buffer + 50 mM NaCl. Elution of the recombinant protein was obtained by Binding buffer + 300 mM NaCl.
Recovery yield was calculated upon the protein concentration assay with Bradford (60) while the purity of the enzyme was assessed by SDS-PAGE. rhPAL was finally stored at -80°C.

3.9 Scaling-up

Once the effectiveness of the recombinant PAL induction was ascertained, an induction in a 7 L fermenter was carried out. The pre-inoculation of a pET45b-Ub-PAL clone in BL21 (DE3) was carried out in 300 mL of vegetable peptone (pH 7.5) added, at the moment of use, with ampicillin 100 µg/mL and prepared according to the following indications:

- Vegetable peptone 18 g/L

- Dextrose 2.5 g/L

- Dibasic potassium phosphate 2.5 g/L

- Yeast extract 3 g/L

- NaCl 5 g/L

Growth took place overnight in a shaker (200 RPM) at 37 ° C.

The following day the fermenter was set up with 5 L of synthetic medium (standard conditions), suitable for the production of drugs as it is free of animal proteins, and produced under controlled conditions. After calculating the overnight growth OD of pET45b-Ub-PAL in BL21 (DE3), a dilution of the OD was performed by adding an adequate volume of the ON growth product to the fermenter containing 5 L of synthetic medium in order to obtain OD equal to 0.1. Once an OD of 0.5 was reached, a 10 mL sample of growth medium was

taken as an “uninduced” (NI) sample, then 1 mM IPTG was added to induce the production of PAL. The subsequent steps were similar to those described in paragraph 3.2 until the cell pellet was obtained.

3.10 Animals

Adult homozygous Pahenu2-/- (ENU2), heterozygous Pahenu2+/- (HT)and Pahenu2+/+ (Wild Type; WT) male mice of the BTBR background strain, employed in this study, were issued from heterozygous mating Pahenu2+/-. The presence of the enu2 mutation was determined by PCR amplification of exon 7 of the PAH gene on DNA obtained from tail tissue, according to bibliography (33). The genetic enu2 modification is chemically induced after treatment of BTBR wild type mice with ethylnitrosurea (hence the name). The treatment causes an A>T835C missense mutation in exon 7 of the PAH gene, resulting in a phenylalanine-to-serine amino acid substitution in position 263 of the protein chain (F263S). These mice present a biochemical and neurological phenotype strictly resembling the human PKU disease, with serum L-Phe 10- to 20-fold higher on a normal diet, increased L-Phe concentration in the cerebral cortex with a concomitant 70% reduction in brain serotonin levels, microcephaly at birth and hypopigmentation (Figure 10) (34) (35). Three groups of adult ENU2 male mice (ENU2-rAvPAL loaded RBC treated mice, n=6; ENU2-free rAvPAL treated mice, n=6; ENU2-control, n=6), one group of heterozygous genetic background mice (HT-control, n=6), and one group of healthy genetic background mice (WT-control, n=6) were used for biochemical analyses as described below.

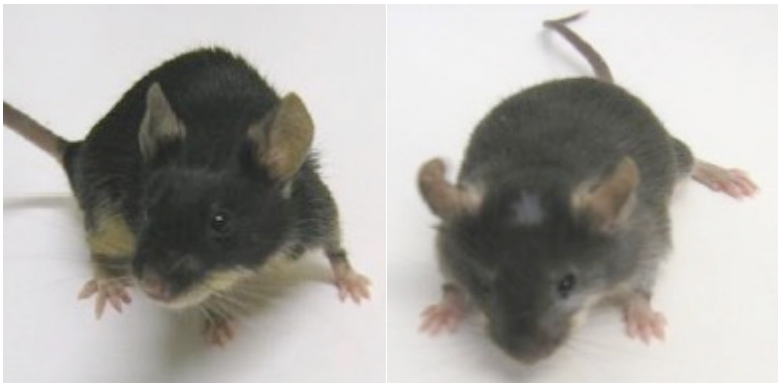

Figure 10 BTBR wild type (left) and Pahenu2 (right) mice. The lighter fur of the mutated mouse is particularly evident from the picture

Animals were housed in standard cages, 3 to 6 mice per cage, on a 12 h light:dark cycle and in controlled conditions (temperature 22 ± 1°C, humidity 60%, air change every 12 hours). All mice were fed on Teklad global 18% protein rodent diet (Harlan Laboratories Inc., Madison, WI) and water ad libitum. BTBR-WT and HT mice were used as blood donors for the loading procedure, while BTBR-Pahenu2 mice received rAvPAL-RBCs. The experiments were carried out in accordance with European legislation (2010/63/UE), with Italian national legislation (DL26/2014) governing the use of animals for research and with the guidelines of the National Institute of Health on the use and the care of laboratory animals (Authorization n° 486/2017-PR).

3.11 Loading procedure and in vivo efficacy of single infusion of rAvPAL-RBCs

Blood was collected from anesthetized control BTBR-WT and BTBR-HT mice by puncture of the retro-orbital sinus in heparinized tubes. rAvPAL (SA 1.6 IU/mg) was loaded into mouse RBCs by means of a procedure of hypotonic dialysis, isotonic resealing and "reannealing", essentially according to bibliography (36). Whole blood was centrifuged to remove plasma and washed twice by 10 min centrifugations at + 4°C, at 900 g and 1500 g respectively, in a physiological saline solution with 10 mM 2-[4-(2-hydroxyethyl)piperazin-1-yl]-ethanesulfonic acid (HEPES, pH 7.4), 154 mM NaCl and 5 mM glucose (henceforth named Hepes solution). The procedure was carried out with 30 IU rAv-PAL (corresponding to 300 µl of enzyme solution with SA 1.6 IU/mg) being added to 700 µl packed RBC suspension to reach 1 ml final volume at 50% Ht inside the dialysis membrane. This condition (1 ml final volume) was dialyzed 1 h at + 4°C in a cellulose tube (14 kDa MWCO, Roth, Karlsruhe, Germany) vs 50 ml of hypotonic dialysis buffer optimized for murine RBC loading, containing 15 mM NaH_2PO_4, 15 mM $NaHCO_3$ (pH 7.4), 20 mM glucose, 4 mM $MgCl_2$, 3 mM glutathione, and 2 mM ATP. The final osmolality of the hypotonic solution was 85 mOsm, measured by Osmometer Fiske Associates, Model 210 (Norwood, MA, USA). This procedure was carried out for 10 separate tubes; at the end, all RBC suspensions were pooled and, at this stage, the cells reached 120 mOsm (the opening of membrane pores in murine RBCs starts at values ≤ 150 mOsm). Subsequent resealing and reannealing steps were carried out by incubating the dialyzed RBC suspension to equilibrate 5 min at + 37°C; after that PIGPA solution (10% v/v) was added to the RBCs to restore isotonicity (300 mOsm) and the suspension was incubated another 25 min at + 37°C under gentle stirring, to allow pore closure. Final washing steps were performed by 10 min centrifugation at 300 g and + 4°C twice to avoid cell lysis and to remove the unentrapped enzyme, while the amount of encapsulated enzyme was determined according to bibliography (37) and briefly summarized later on. Hematological parameters were measured by an automatic ABX Micros® 60 cell counter (Horiba Medical, Irvine, CA) and percent RBC recovery was calculated from the number of RBCs submitted to the dialysis step and those recovered at the end of the loading procedure.

Loaded erythrocytes were then resuspended to 40% Ht and the amount of entrapped enzyme was assayed before infusion into BTBR-Pahenu2 mice (mean body weight 31.3 ± 4.6 g). rAvPAL-RBCs were prepared at 35% Ht (corresponding to approx. 2.275 rAvPAL/ml) in Hepes solution, in order to administer the scheduled dose in the volume of 400 µl.

The dose of rAvPAL-RBCs was administered to a cohort of BTBR-Pahenu2 mice by intravenous infusion, so as mice of the cohort received (0.9 IU/0.6mg/mouse). Treatment efficacy was evaluated by biochemical monitoring of blood L-Phe, sampling blood at time 0, and then 1, 4 and 7 days after a single injection. For the experiment, untreated ENU2 mice (ENU2-veh) (n=6), untreated heterozygous mice (HT-veh) (n=6) and untreated healthy mice (WT-veh) (n=6) underwent the same manipulations and received an i.v. injection of native RBC solution (at the same Ht) following the same schedule as the ENU2 mice treated with loaded RBCs (ENU2-rAvPAL-RBC mice (n=6)).

Whole blood (40 µl) was collected from the submandibular vein by special animal lancets (Goldenrod 5.5 mm, Braintree Scientific Inc., Braintree, MA) after 2 h of food deprivation, spotted on filter papers and analyzed by MS/MS for amino acid levels.

3.12 Tandem mass spectrometry

RBC suspensions from the in vivo study and mouse whole blood were collected on Schleicher&Schuell 903 grade filter paper, dried at room temperature and stored at + 4°C in plastic bags until use. L-Phe analysis in dried blood spots (DBS) was performed in the Department of Experimental Medicine of the "Sapienza" University of Rome, essentially according to a previous method proposed by bibliography (38) with some modifications. Three millimeter diameter dots were punched out from DBS and eluted in 100 µl of methanol/water (80:20) solution spiked with labeled amino acid internal standards (CIL, Andover, MA, USA). The samples were shaken 30 min at + 30°C, then 65 µl of supernatant was dried under nitrogen flow at + 45°C. The residues were derivatized by treatment with 50 µl of 3 M HCl in n-butanol solution at + 60°C for 30 min. After derivatization, the samples were dried under nitrogen flow at + 45°C and recovered in 70 µl of acetonitrile/water (80:20) containing 0.1% formic acid. A 20 µl volume was injected into a LC-MS/MS system (API 2000, Sciex, Toronto, Canada) equipped with a Series 200 micro pump (Perkin Elmer, Norwalk, CT, USA) and a Series 200 autosampler (Perkin Elmer) for solvent delivery and automated sample loading. The mobile phase was acetonitrile/water (80:20) pumped at a flow rate of 50 µl/min. Neutral loss scan of 102 Da fragment and a total acquisition time of 2 minutes were used to detect L-Phe.

4. Results

4.1. PAL cloning

The PAL CDS (NCBI Reference Sequence: CP000117.1:4958808-4960511) was successfully cloned (with NotI and SacII restriction enzymes) into the pET45b-UB, an expression vector engineered to produce the recombinant enzyme directly fused to the C-terminus of the ubiquitin partner. PAL was cloned downstream of the vector encoded His-tag to improve the yield and provide an easy purification of the authentic protein (39). The recombinant PAL precursor has been referred to as His-UB-PAL from which the NO-tag enzyme was obtained by digestion with the rHis-USP2. By this strategy, rAvPAL has been expressed and purified. Moreover, most of the recombinant product was partitioned in the insoluble fraction (referred to as Pellet sample) but the protein was obtained from the soluble part.

4.2. Optimization of PAL expression in BL21(DE3) E. coli strain

Expression studies were performed at lab scale to optimize PAL product yield. Scaling-up production was first performed in Synthetic media. In this section the results obtained in the different fermentation processes are reported.

Experiment N. 1: <u>SCALING-UP (5.5 liters synthetic, in Bioreactor)</u>

EXPERIMENTAL CONDITIONS:

Stage 1: 0.5 L Flask	
Working Volume:	500 ml
Starting material:	Research Cell Bank (Not qualified)
Medium:	Vegetable pepton + Ampicillin (100 µg/ml)
Incubation condition:	T: +33°C
Stage 2: 5 L (n. 2)	
Working volume	5,5 L
Starting material:	Culture broth from Stage 1, start O.D. = 0.1
Medium:	Synthetic medium supplemented with Glucose-$MgSO_4$-Thiamine-Ampicillin
Incubation condition:	T: +37°C
Induction with 1mM IPTG at:	0.49 $O.D._{600nm}$ (1:30 h)
Feed	None (antifoam twice)

RESULTS:

Stage 1	
final O.D.$_{600nm}$:	4.740 after 16 h
Stage 2	
final O.D.$_{600nm}$:	1.630 after 3 h
Proteins in the soluble bacterial extract	2000mg
His-UB-PAL after the 1st Ni-affinity chromatography	173.5 mg (total amount)
urbPAL after USP2 cleavage and DEAE chromatography	50,4 mg (total amount); recovery= 28,8%
Specific activity	1.2 U/mg
Stability data	

Experiment N. 2: <u>SCALING-UP (12 liters synthetic, in Bioreactor at Diatheva srl)</u>

EXPERIMENTAL CONDITIONS:

Stage 1: 5L	
Working Volume:	5L
Starting material:	Research Cell Bank (Not qualified)
Medium:	Vegetable pepton + Ampicillin (100 µg/ml)
Incubation condition:	T: 37°C
Stage 2: 12L (n. 2)	
Working volume	12L (high density)
Starting material:	Culture broth from Stage 1, start O.D. = 5.17
Medium:	Synthetic medium supplemented with Glucose-$MgSO_4$-Thiamine-Ampicillin
Incubation condition:	T: +37°C
Induction with 1mM IPTG at:	10.0 O.D.$_{600nm}$ (:7 h)
Feed	None (antifoam twice)

RESULTS: (see also Figure 11);

Stage 1	
final O.D.$_{600nm}$:	5,17 after 16 h
Stage 2	
final O.D.$_{600nm}$:	19.3 after 3 h of induction (high density)
Proteins in the soluble bacterial extract	4g
His-UB-PAL after the 1st Ni-affinity chromatography	2 g (total amount)
urbPAL after USP2 cleavage and DEAE chromatography	500mg (total amount); recovery= 25%
Specific activity	1,2 U/mg
Stability data	

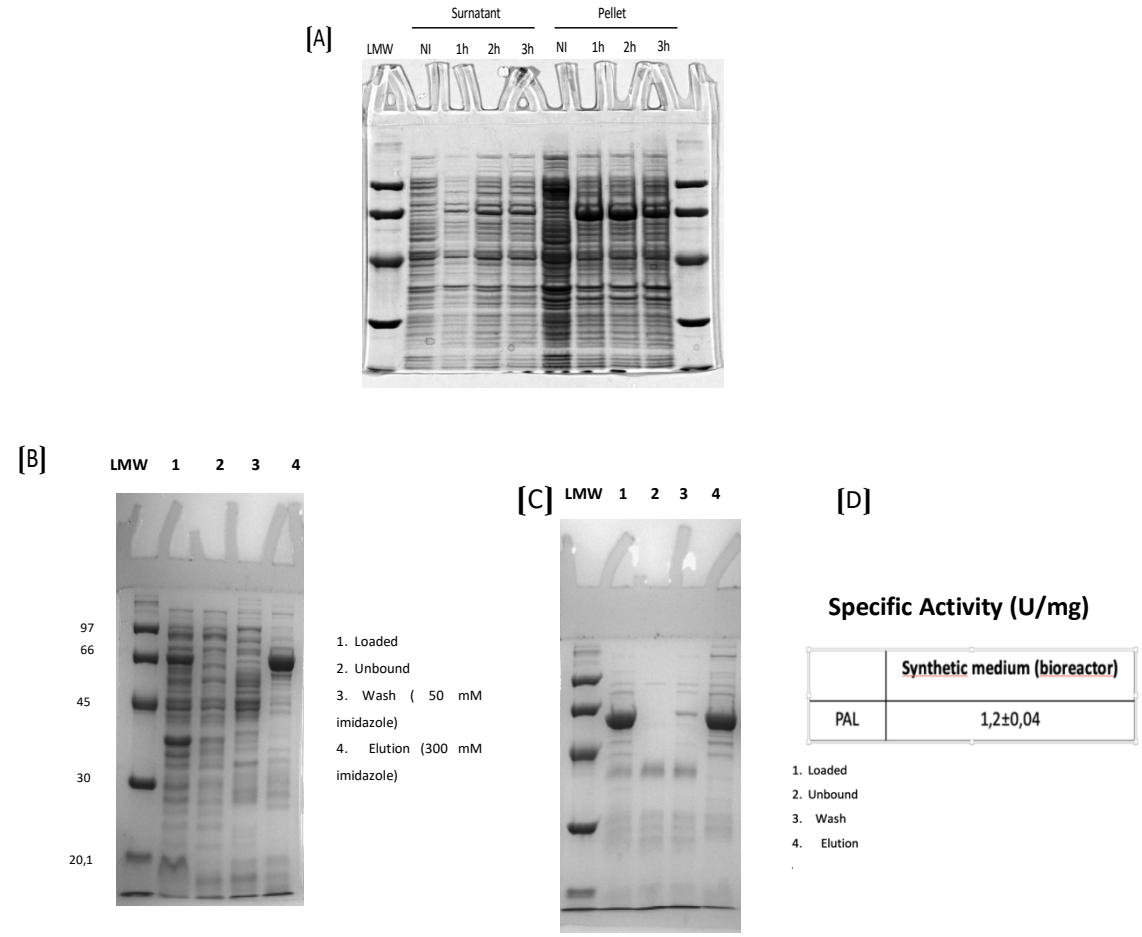

Figure 11 Scaling-up induction and purification of PAL. [A] Time-course induction of the pET45b-UB_PAL construct (in 5.5 liters Synthetic medium, using the Bioreactor). Supernatant and Pellet fractions are resolved by SDS-PAGE; NI is the not-induced sample. [B] Purification of r-His-UB-PAL by immobilized metal ion affinity chromatography (IMAC), with the Akta Purifier. LMW, low molecular weight protein standard. [C] Purification of PAL by Diethylaminoethyl chromatography (DEAE), with the Akta Purifier Specific. [D] activity of the final product (PAL NO-tag).

4.3 Preclinical study: efficacy of rAvPAL-RBC treatment

A bulk loading procedure was used, obtaining at the end 3.25 ml of RBCs at 40% Ht loaded with 21.125 IU rAvPAL (corresponding to 6.5 IU rAvPAL/ml RBCs 100% Ht). Table 5 summarizes the results and RBC parameters of the loading procedure.

Loaded RBCs had a final Ht value of 40%. The suspension was diluted in Hepes solution to 35% final Ht, corresponding to 2.275 IU rAvPAL/ml, in order to administer the scheduled dose in the volume of 400 µl. Mean basal L-Phe values before treatment (± standard deviation, SD) were 1.523 ± 348 µM, in group that received 0.9 IU/mouse and were not significantly different ($p > 0.05$ by ANOVA). The treatment with selected dose of rAvPAL-RBCs yielded the results shown below.

The dose was successful in causing blood L-Phe to decrease steeply in the first hours after treatment, with low peak values reached 24 h from rAvPAL-RBC injection. In fact, after one day, injection of RBCs with 0.9 IU enzyme/mouse produced L-Phe values of 14 ± 19 µM. The tested dose was able to maintain the reduced amino acid levels beyond the first day. In fact, as shown in Figure 12, L-Phe slowly grew to higher levels,

reaching on day 4 after rAvPAL-RBC administration roughly 15% of the pre-treatment values (222 ± 127 µM), and raising up to 40% (570 ± 138 µM) on day 7.
Thus, the results obtained from the evaluation of blood L-Phe over time suggest the treatment was significantly effective until 7 days after treatment (ANOVA, $p < 0.05$ vs pre-treatment).

Table 5. Loading results and RBC parameters of the procedure performed for the preclinical study.

RBC dialysis Ht	Added rAvPAL (IU)	Loaded rAvPAL (IU/ml RBCs 100% Ht)	RBC recovery (%)	rAvPAL entrapment* (%)	MCV (μm^3)	MCH (pg)	MCHC (g/dl)	RDW (%)
50%	30	6.5	25	3	44	14	31.7	17.9
Control native RBC**					49	19.5	39.6	14.1

*rAvPAL entrapment was calculated in respect to the actual total initial amount of enzyme IU measured after dialysis.
**Reference values belong to RBCs prior to be submitted to the procedure.

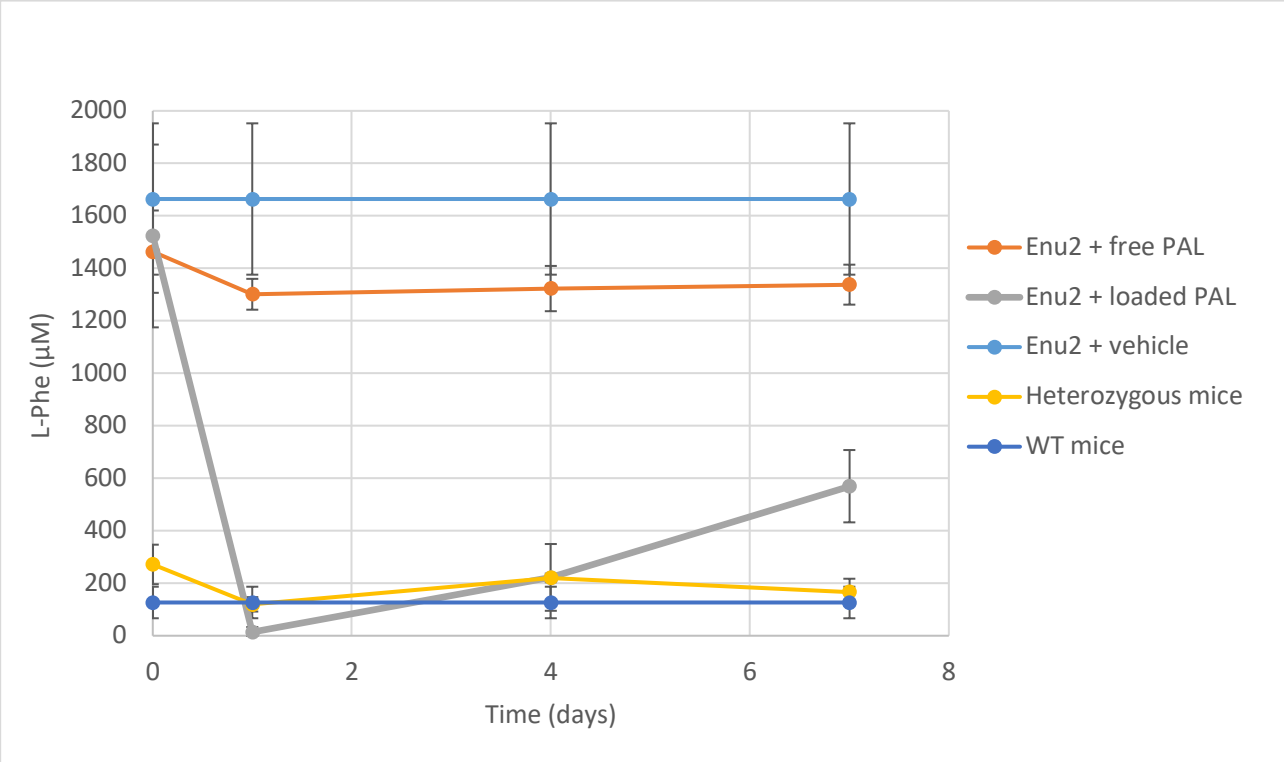

Figure 12 Blood L-Phe concentrations (mean ± SD) before and after rAvPAL-RBC injection.

5. Discussion

A recombinant AvPAL enzyme has been produced and its activity has been characterized (1.2 ± 0.04 U/mg). The production scaling up returned a good production of protein, managing to obtain up to 500mg of protein. We performed the preclinical study exploring and demonstrating that murine RBCs Loaded with AvPAL are able to act as bioreactors to decrease blood Phe in BTBR-Pah mice.

Our future goal is to perform repeated infusions of RBC loaded with AvPAL to demonstrate the stabilization of the biochemical controls of the disease. In addition, this allows us to assess the safety of the treatment and its effectiveness by examining behavioral parameters.

On the whole, these data demonstrate that blood L-Phe levels can effectively be modulated in vivo by injection of rAvPAL-RBCs: in fact, the amino acid levels of treated mice stayed significantly below those of control Pah-deficient mice receiving vehicle solution or free eAvPAL.

Once verified the in vivo validity and viability of this enzyme substitution therapy approach, it would be possible to move on to the development and optimization of a protocol of loading of human erythrocytes, with the perspective of a future clinical application. To this purpose, we could exploit the technology owned by the company EryDel S.p.A. (Italy), namely the Red Cell Drug Loading system, consisting of a proprietary combination of an electromedical device, the Red Cell Loader® (RCL), and a disposable sterile kit, EryKit_01, projected to work together under the control of an opportune software (latest version 3.2.0) to obtain erythrocytes loaded with different therapeutic agents suitable for clinical use.

The successful development and optimization of a loading protocol performed by the RCL system opportunely modified to fit to protein loading would therefore facilitate the transition of the enzyme replacement therapeutic approach from the lab to the clinics of PKU patients.

In conclusion, we demonstrated the great potential of rAvPAL-RBCs as enzyme replacement therapy for the treatment of phenylketonuria, thus opening new perspectives for the development of enzyme replacement therapies for other disorders involving enzyme deficiencies.

APPLICATION OF MAT2A/GAMT-LOADED RBCs IN THE TREATMENT OF GAMT DEFICIENCY

1. Introduction

1.1 Creatine

Creatine (Cr, Figure 13) is a non-protein nitrogen metabolite that plays an extremely important role in energy metabolism. In mammals, most of the daily Cr requirement is provided by the diet but can also be synthesized endogenously.

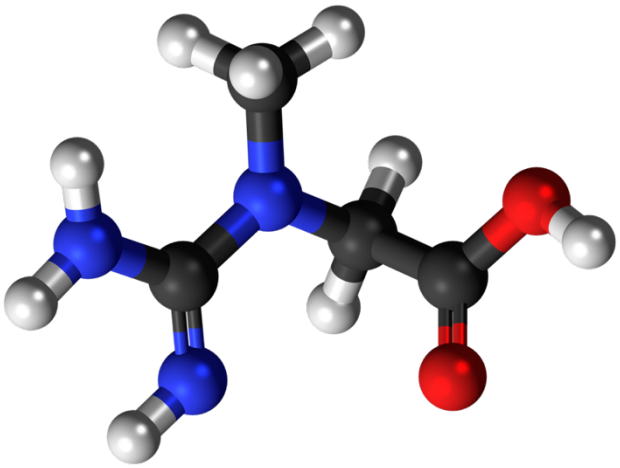

Figure 13 Structure of creatine. Creatine is formed from a guanidine group, an acetic group and a methyl group.

Physiologically, creatine is supplied in equal measure by the diet and by the endogenous synthesis of arginine and glycine, with subsequent involvement of the enzymes arginine glycine amidinotransferase [AGAT] and guanidinoacetate methyltransferase [GAMT] (Figure 14).

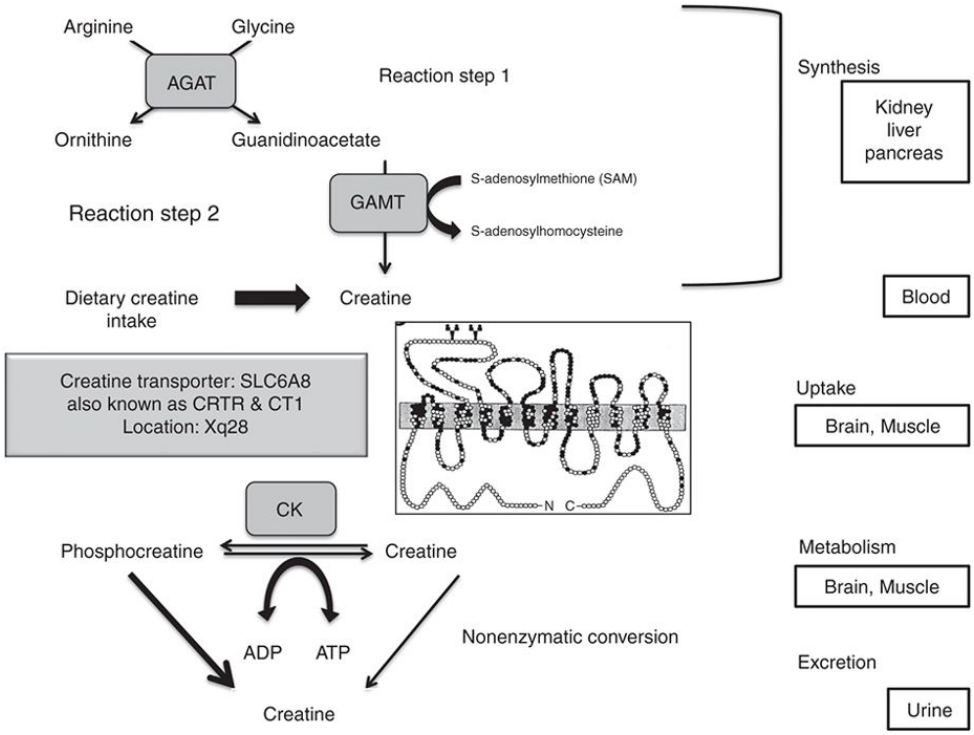

Figure 14 Synthesis of creatine. A schematic summary of the reactions required for the synthesis, absorption, metabolism and excretion of creatine (text and image taken from Clark JF & Cecil Km 2015).

The first reaction takes place at the renal level in the intramembrane space of the mitochondrion, where AGAT catalyzes the transfer of the amino group from arginine to glycine, obtaining Ornithine and Guanidinoacetate (GAA). The neo synthetized GAA leaves the kidney through the SLC6A8 transporter and is internalized by the liver, where it is transformed into creatine by the cytoplasmic enzyme GAMT.
The GAMT enzyme transfers a methyl group from S-adenosylmethionine (SAM) to GAA thus producing creatine.

Most of the biosynthesized creatine is produced by the liver, in quantities of about 1-2 grams/day but its production also occurs in the brain, skeletal muscle, pancreas and testicles. The concentration of creatine in the bloodstream is generally around 50 µmol/L (40).
Creatine is an important resource for those cells subjected to large variations in energy demand such as the cells of the myocardium, skeletal muscle and neurons; in these tissues it is transformed into phosphocreatine, which represents an immediate source of energy. These tissues have a high energy expenditure and require constant levels of ATP, maintained by phosphocreatine which is able to transfer a phosphate group to ADP in order to synthesize ATP (41).
Intracellular creatine is spontaneously cyclized to form creatinine. Creatinine is a non-metabolically active catabolite that is excreted in the urine following filtration by the renal glomeruli. Under normal conditions, the levels of creatine and phosphocreatine are directly proportional to the concentration of creatinine and its excretion. The determination of creatinine in the urine of 24 hours, known as clearance, constitutes a good index of renal function (42).

1.2 Cerebral Creatine Deficiency Sindromes

Cerebral creatine deficiency syndromes (CCDSs) are a group of inborn errors of creatine metabolism comprising two autosomal recessive disorders that affect the biosynthesis of creatine and one X-linked:

- Arginine Glycine Amidinotransferase deficiency (AGAT; MIM 602360)
- Guanidinoacetate *N*-Methyltransferase deficiency (GAMT; MIM 601240)
- Creatine transporter SLC6A8 deficiency (SLC6A8; MIM 300036)

Individuals with CCDS, if untreated, are generally unable to care for themselves at any age. CCDS typically present with developmental delay, intellectual deficiency and severe speech deficits. Developmental delay is often observed prior to 1 year of age with many developmental milestones (43).

Previously, the group of creatine biosynthesis defects and the creatine transporter defect were referred to as creatine deficiency syndromes (CDSs). However, in body fluids, no creatine deficiency exists in creatine transporter deficient patients; thus, this term may be misleading. Therefore, it may be more appropriate to use the term CCDSs, which correlates better to the main clinical hallmarks that are related to CNS involvement. The discovery of CCDSs has brought new diagnostic options in patients with unexplained mental retardation, speech and language disorders, autism and epilepsy. Moreover, these defects are important for unravelling of the physiologic functions and pharmacologic potential of creatine, as well as of intermediates of creatine (44).

The frequency of CCDS is unknown and probably underestimated. But in one study, lead over a period of 18 months, 188 children (referred to the Department of Pediatric Neurology with unexplained mild to severe mental retardation, normal karyotype, and absence of fragile X syndrome) were retroprospectively screened for CCDS providing the following results: the prevalence of CCDS was 2.7% (5/188, CI: 0.36 to 4.96) in the whole population and 4.4% (5/114, CI: 0.63 to 8.15) in boys. None of the 74 girls had a CCDS. Family history revealed 151 sporadic cases, with a prevalence of CDDS was 1.9% (3/151, CI: 0 to 4.21), and 37 familial cases, in which the prevalence was 5.4% (2/37, CI: 0 to 12.7) (45). In particular, deficiency of GAMT is the first described creatine biosynthesis defect, which leads to depletion of creatine and phosphocreatine, and accumulation of guanidinoacetate in brain.

1.3 Guanidinoacetate N-Methiltransferase and GAMT deficiency

Guanidinoacetate methyltransferase (GAMT, EC 2.1.1.2) is the enzyme that catalyzes the last step of creatine synthesis, facilitating the transfer of a single methyl group from S-adenosylmethionine (SAM) to guanidinoacetic acid (GAA).

The gene encoding for GAMT maps to chromosome 19p13.3 and contains 6 introns (46). In the literature there are 2 transcript variants, called variant 1 (NM_000156.5) and variant 2 (NM_138924.2). The two variants differ for a different splice site and consequently for the length: variant 1 is 711bp (236 aa) long, while variant 2 is 810bp (269 aa) (47). The proteins have a weight of 26.3 KDa (variant 1) (EC 2.1.1.2) and 29.4 KDa (variant 2), respectively. These enzymes are found in monomeric form and are present in the cytoplasm (48). The Km of this enzyme for its substrates depends on the tissue in which GAMT is expressed (49). GAMT has an α/ß open-sandwich structure, and the N-terminal section (residues 1-42) covers the active site entrance so that the active site is not available.

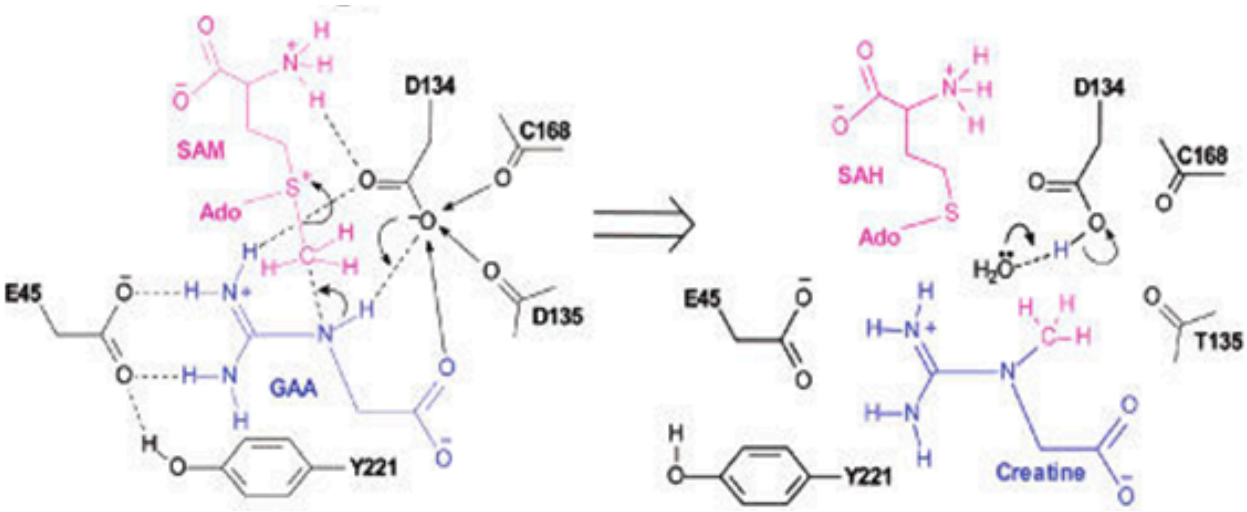

Figure 15 Proposed mechanism of the methyl transfer reaction of GAMT. (A) Transition stage in which NE of GAA has sp3 hybridization. The three slightly negatively charged carbonyl oxygens (O of T135, O of C168, and OB of GAA) increase the pKa value.

SAM has extensive interactions with GAMT through H-bonds and hydrophobic interactions. The guanidino groups of GAA form two pairs of H-bonds with E45 and D134, respectively (50).

Deficiency of guanidinoacetate methyltransferase (GAMT) is the first described creatine biosynthesis defect, which leads to depletion of creatine and phosphocreatine, and accumulation of guanidinoacetate in brain (51).

In particular, GAMT deficiency is a rare autosomal recessive disorder. The estimated incidence of GAMT deficiency is 1:250,000 newborns (0.0004% calculated through direct sequencing of the GAMT gene) (52) whereas the carrier frequency of GAMT deficiency is 0.123% in the general population (53).

1.4 Characteristics of the disease

The deficiency of the GAMT enzyme causes a strong lowering of creatine levels resulting in its deficit and serious damage, especially in the CNS.

The clinical presentation of GAMT-deficient patients is extremely heterogeneous but mental retardation is without doubt the most common clinical manifestation, given that it is present in all patients, albeit with varying degrees of severity.

GAMT-deficient patients may also present the following characteristics: delayed psychomotor development, which can stop abruptly or even there may be a strong regression, epilepsy (unresponsive to the treatment with antiepileptic drugs), mental retardation, language difficulties, muscle hypotonia, presence of involuntary movements (dyskinesia), behavioral disturbances (autistic signs with self-mutilating syndrome and signs of hyperactivity) and epilepsy (48) (51) (52).

High concentrations of GAA are believed to be responsible for the neurological dysfunctions and epileptic syndromes that are often found in patients; furthermore, GAA has been shown to have the ability to bind and activate $GABA_A$ receptors, thus acting as a direct agonist of the neurotransmitter GABA (γ-aminobutyric acid) (54). It has been hypothesized that the high concentration of the GAA may alter the activity of $GABA_A$ receptors, which could undergo first desensitization and ultimately reduction of their expression.

The circulating concentration of GAA in patients with GAMT deficiency is around 10-30 µM; at these concentrations there is the passage of GAA from the periphery to the SNC crossing the blood brain barrier. The GAA values in healthy subjects are in the order of nM (55).

1.5 Diagnosis of GAMT deficiency

In Italy, metabolic screening for GAMT deficiency occurs at birth. High levels are characteristic of GAMT deficiency, as very little GAA is taken with the diet and there are not causes of GAA accumulation in the blood other than GAMT-deficiency.

The genetic test allows to diagnosize most of the congenital errors of GAMT-deficiency; the diagnosis is made by sequencing the mRNAs, exons or entire genes coding for GAMT, with new mutations being identified regularly. These include missense mutations, abnormal splicing, small deletions and insertions. The search for GAMT gene mutations, carried out on patients, has reported 45-50 mutations within the entire gene (56).

1.6 Current treatments

In GAMT-deficient patients, all the available therapies have the objective of eliminating the accumulated and toxic GAA and to restore normal creatine reserves. Current treatments are thus aimed at controlling metabolites rather than curing the disease (Fig 15).

Treatment for GAMT-deficiency includes:

1. The restriction of arginine intake within 15-25 mg/ kg/day, which corresponds to a protein intake of only 0.4-0.7 g/kg /day. To avoid protein malnutrition, supplementation with a mix of essential amino acids in the patients' diet is recommended.
2. The oral administration of creatine monohydrate in high doses, between 350 mg and 2 g per day per kg of body weight, generally distributed between 3-6 doses.
3. The intake of ornithine, at doses between 400 and 800 mg per day per kg of body weight, distributed between 3-6 doses.
4. The administration of sodium benzoate, which is able to strongly bind amino acids, including glycine. This aptitude is exploited in the therapy against GAMT-deficiency, as glycine is one of the substrates of the AGAT enzyme; by sequestering it, sodium benzoate would therefore reduce GAA production.

These kinds of therapeutic regimens are able to improve the degree of psychomotor retardation and in some cases to make the epileptic symptoms and movement disorders of patients disappear. It is noteworthy that these treatments must be started as soon as possible and must be continued for long periods of time without interruption (47).

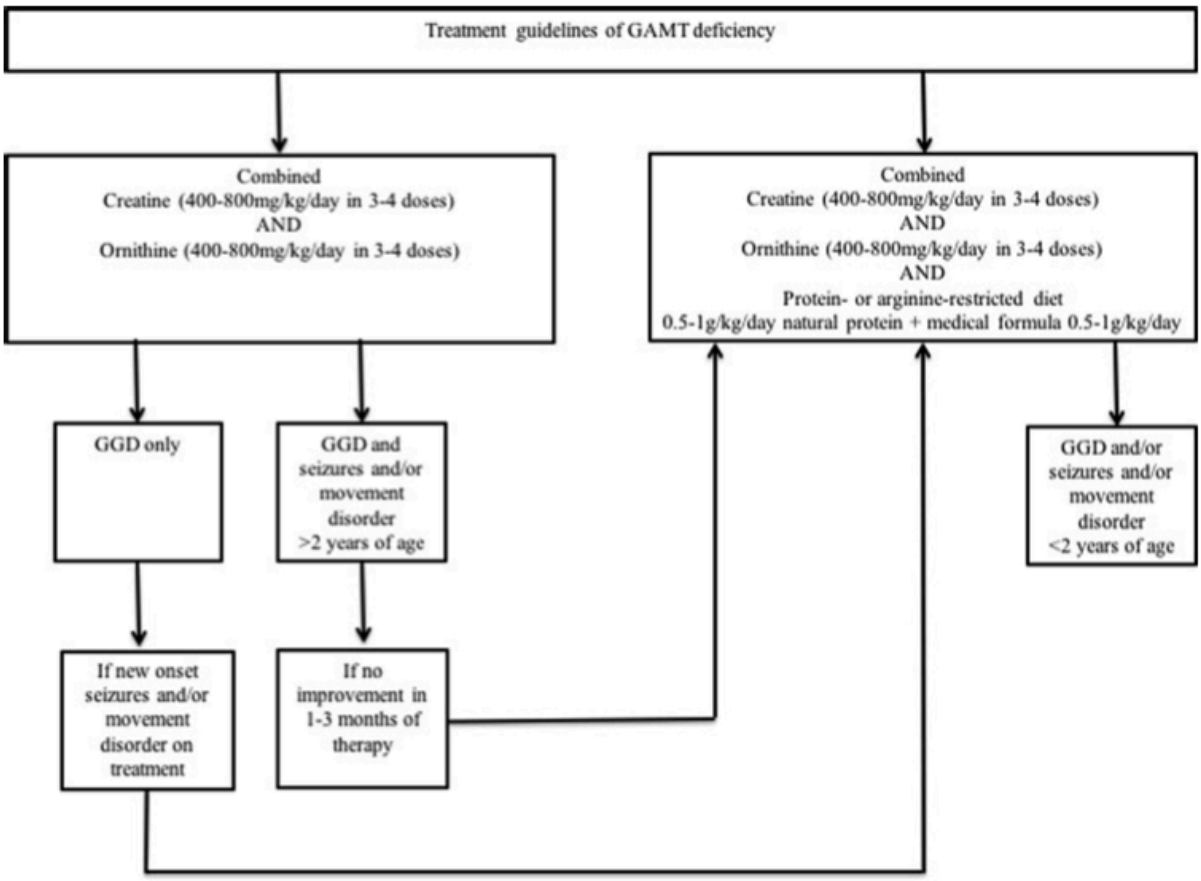

Figure 16 Treatment guidelines of GAMT deficiency are depicted based on the symptoms of the patients with GAMT deficiency

1.7 Methionine adenosyltransferase

Methionine adenosyltransferase (MAT) (EC 2.5.1.6) (also known as S-adenosylmethionine synthetase) is an enzyme that creates S-adenosylmethionine (SAM) starting from methionine (a non-polar amino acid) and ATP (the basic currency of energy). SAM is a methyl donor for transmethylation.

The reaction catalyzed by MAT combines methionine, ATP and water to produce SAM, pyrophosphate and inorganic phosphate; the enzyme requires both Mg^{2+} and K^{+} ions for its maximal activity (57).

Mammalian isoenzymes are encoded by three genes: MAT1A, MAT2A and MAT2B (58). The catalytic subunits (MAT1A and MAT2A) are 85% identical at the amino acid level, and derive from the MAT1A and MAT2A genes and codes for proteins of 396 (MATα1) and 395 (MATα2) residues, respectively. While the regulatory β subunit is coded by the MAT2B gene that includes an ORF for a 335 amino acid protein (59).

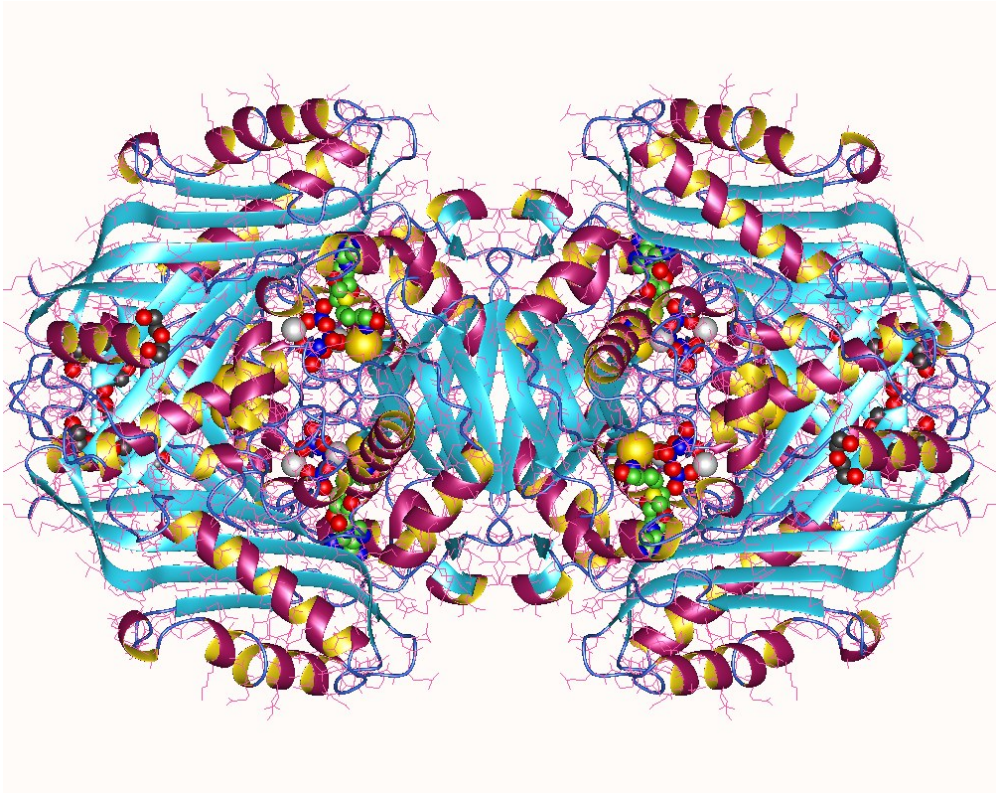

Figure 17 The Figure show S-adenosylmethionine synthase 2, tetramer, Human

The SAM produced by the enzymes of the MAT family is essential for GAMT activity and for the production of creatine.

2 Aim of the work

In this work we aimed to demonstrate the ability of the engineered red blood cells loaded with both rGAMT and rMAT2A enzymes to act as effective bioreactors in vitro and in vivo capable of reducing GAA levels, increasing Cr and safety values.

For this purpose, we employed a best performing variant of rGAMT enzyme, developed in our laboratory by site-directed mutagenesis. This new variant has been first tested at small scale production. So, we kept on with performing the scaling up and the characterization. In parallel, rMAT2A (hereinafter referred as MAT) was produced by means of a process that included: cloning, production, process optimization, scaling up and characterization. Once the final products have been obtained, the work focused on the co-entrapment of the two recombinant proteins (rGAMT and rMAT) into human red blood cells for in vitro studies. Finally, a preclinical study was performed in a murine model of GAMT deficiency.

3 Materials and methods

3.1 Establishment of BL21(DE3) E. coli strain expressing the newly synthesized rGAMT

BL21(DE3) competent cells (50 µl) were transformed with 1 µl of a 2ng/µl dilution of the GAMT expression vectors, following the transformation protocol already detailed for Novablue. A few clones of BL21(DE3), bearing the different pET45b/His-UB-GAMT expression constructs were tested for GAMT expression.

3.2 Establishment of rGAMT Research Cell Banks

A single colony from the agar plate was inoculated in LB + ampicillin 100 µg/ml. The bacterial culture was incubated at +37°C shaking at 250 rpm, until optical density at 600 nm (O.D.600) reached approximately 0.7-0.8 (4-6 h required). Then, 900 µl of the bacterial culture were added to 600 µl of glycerol, previously dispensed in the cryovials. Twenty glycerol stock tubes of E. coli cells (Novablue and BL21(DE3), transformed with each GAMT construct, identified as Research Cell Bank (RCB) were prepared and immediately frozen at -80°C.

3.3 Induction of rGAMT at lab scale level

The standard "small-scale" induction protocol is described below (any variation of induction parameters is reported in the "Results" section).

Starting culture: an isolated colony was picked from a freshly streaked plate and grown overnight (ON) at +37°C in 10 ml LB + ampicillin (100 µg/ml) in a 50 ml tube on a benchtop orbital shaker. A sample of the overnight culture was withdrawn and diluted 1:10 before reading O.D.600, in a spectrophotometer. The ON inoculum was then diluted into 100 ml LB + ampicillin (100 µg/ml), put in a 0.5 l flask, in order to reach an O.D.600 of about 0.1. The culture was then incubated at +37°C with aeration and shaking at 250 rpm. Bacterial growth was monitored, at regular intervals, until culture density reached an O.D.600 of about 0.5-0.6. 10 ml of culture were then removed and transferred to a labeled 50 ml tube and let grow at +37°C (this is the Not Induced control, NI). To induce the protein expression, IPTG at 1 mM final concentration was added into the flask (this is the Induced sample, I). At 1 h-intervals, 10 ml of induced bacterial culture were withdrawn, transferred into a 15 ml-tube and put on ice. Total induction time was 4 h. At the end of the induction step, cells were collected by centrifugation at 2750 g for 20 min at +4°C: the supernatant was removed and the pellet frozen at -20°C for later processing.

3.4 Preparation of bacterial extracts and SDS-PAGE analysis

Cell lysis was obtained by resuspension of the cell pellets (from both NI and I samples) in 0.05 culture volume of ice cold Lysis Buffer (20 mM Na/K Phosphate buffer pH 7.5, 15 mM β-Mercaptoethanol, 15% (v/v) glycerol, 500 mM NaCl), followed by three cycles (30 s each) of sonication at 75 watt; during sonication the sample has been kept on ice. Samples were centrifuged 10 min at 9600 g and +4°C: the supernatant (S), corresponding to the soluble cytoplasmic fraction, was transferred into a new microcentrifuge tube; while the residual pellet was resuspended in Lysis Buffer and sonicated as above; this sample has been referred to as the Pellet (P) sample.

The protein concentration in both S and P samples was determined by the Bradford assay (60), to normalize the samples for loading.

For SDS-PAGE, an aliquot corresponding to 20 µg of proteins (for P loaded 10µl), was diluted in an equal volume of 2X Sample Buffer (2X SB = 2% SDS, 100 mM Tris-HCl, pH 6.8, 20% glycerol, 0.0025% bromophenol blue,) and boiled for 1 min at +100°C to denature proteins. Proteins were resolved by a 12% (w/v)

polyacrylamide gel electrophoresis, in parallel with the Low Molecular Weight standard (LMW) as a size reference.

3.5 Immobilized metal ion affinity chromatography (IMAC)

The recombinant His-tagged UB-GAMT in the supernatant fraction, was purified by the immobilized metal ion affinity chromatography (IMAC), exploiting the interaction between chelated transition metal ions (Ni2+) and side-chains of histidines (His) on proteins, essentially according to the manufacturer's instructions. Briefly, the column was equilibrated with the Binding buffer (that corresponds to the Lysis Buffer: 20 mM Na/K Phosphate buffer pH 7.5, 15 mM β-Mercaptoethanol, 15% (v/v) glycerol, 500 mM NaCl, in which the sample was resuspended. After sample loading, washings were initially performed with the same Binding buffer, and then with Binding Buffer + 40 mM imidazole. Elution of the His-tagged recombinant protein was obtained by Binding buffer + 150 mM imidazole.

3.6 USP2 digestion of His-UB-GAMT

His-UB-GAMT obtained upon Ni-Sepharose affinity chromatography was digested with the recombinant His-tagged deubiquitinating enzyme USP2 (rHis-USP2) to remove the His-UB partner fused at the N-terminus of GAMT. For optimal digestion, His-UB-GAMT and rHis-USP2 were combined allowing a mass ratio of 20:1 (other conditions tested were 200:1 and 100:1 ratio) and incubated at least 3 h at +37°C, in the same GAMT Elution buffer, suitably diluted by loading buffer in order to keep the imidazole concentration ≤ 50 mM.
rhGAMT NO-tag was purified from all the His-tag byproducts generated during digestion, not-digested His-UB-GAMT and His-USP2, by Nickel affinity chromatography. Recovery yield was calculated upon the protein concentration assay with Bradford (60), while the purity of the enzyme was assessed by SDS-PAGE. rhGAMT was stored at -80°C.

3.7 Determination of GAMT activity

The evaluation of enzyme activity was performed by a method based on the quantification of creatine. The dosage method was performed according to the bibliography (61) with some minor modifications. Briefly, in a final volume of 250 µl, the reaction mixture contained 50 mM Tris-HCl (pH 7.5), 2 mM DTT, 0.25 mM SAM, 1 mM GAA, and GAMT (in our experiments it has been standardized on amount of 10 µg). The incubation was carried out at +37°C for 15 min and at different incubation times (0-5-10-15 min) the reaction was stopped by the addition of 250 µl of 1 N PCA. The reaction mixture was then centrifuged at 18500 g for 15 min at +4°C and 50 µl of the clear supernatant was injected into the HPLC after filtration with 0.2 µm filter into special vials. Blanks, containing the reaction mixture without enzyme, were analyzed as well.
The analysis was performed by the method of reverse phase chromatography at +30°C and using a gradient elution system as reported below:

CHROMATOGRAPHIC METHOD

Time (min)	% buffer A	% buffer B
0-2	100%	0%
2-20	100% to 0%	0% to 100%
20-22	0%	100%
22-25	0% to 100%	100% to 0%
25-30	100%	0%

The mobile phase consisted of buffer A: Na_2HPO_4 (7.1 g), SDS (2 g), distilled water (750 ml) and buffer B: Na_2HPO_4 (7.1 g), SDS (2 g), distilled water (500 ml), acetonitrile (250 ml). Both buffers reached a final pH 3 by H_3PO_4. Before used the buffers were filtered by Polypro filters.

The increase of creatine levels after different analysis times (0-15 min) has been observed.

3.8 Stability tests

We checked the stability of the different enzyme productions over time at +37°C. The test has been performed after 24, 48 and 72 h. At each time point, a 10 µg-aliquot was analyzed using the same dosage protocol applied for the determination of enzyme activity. In some experiments the stability of the rGAMT, at the protein level, was also verified by SDS-PAGE analysis.

3.9 Evaluation of SAM levels in loaded RBCs

SAM was extracted as reported in literature (64). Briefly, frozen packed RBCs were added with an equal volume of 0.1 M sodium acetate, pH 6 (ice-cold) and vortex-mixed. The protein was precipitated by adding 40% (w/v) TCA equal to one-fifth of the original volume of the RBC solution and placed on ice for 30 min to complete precipitation. To remove precipitated protein, the tubes were centrifuged at 25000 g for 10 min at +4°C. The supernatant containing SAM was added with an equal volume of ice-cold peroxide-free diethyl ether to extract lipids (ether extraction step). The tubes were vortex-mixed for 20 s and centrifuged to separate the phases. The top layer was drawn off and discarded. The ether extraction step was repeated once. The samples were filtered and injected into HPLC system.

The assay has been performed as reported in bibliography (65). Briefly, the mobile phase consisted of two solvents: Solvent A, 8 mM octanesulfonic acid sodium salt and 50 mM NaH_2PO_4 adjusted to pH 3.0 with H_3PO_4 and Solvent B, 100% methanol. The HPLC column was equilibrated with 80% Solvent A and 20% Solvent B. The sample was injected and separation was obtained using a step gradient. The gradient consisted of 8 min at the equilibration conditions, 30 s to increase Solvent B to 40%, 12.5 min at the new condition, and 30 s to return to the equilibration conditions and a minimum of 10 min before a subsequent injection. The flow-rate was 1 ml/min and detection was monitored at 254 nm. SAM standard was dissolved in water at a concentration of 1 mM and then diluted to 0.05 mM with 0.4 M PCA.

3.10 Determination of the basal activity of MAT into RBCs

RBCs were washed three times with 10 volumes of 5 mM sodium phosphate, 150 mM NaCl, pH 7.4 and centrifuged at 3400 g for 10 min at +4°C. The supernatant was aspirated and final RBC pellet was lysed in 4 volumes of ice-cold deionized water and incubated for 20 min in ice. The membrane fraction was pelleted by

centrifugation at 20000 g for 1 h and cytosolic fraction was recovered from the supernatant. The cytosol was dialyzed overnight against 30 mM KCl, 40 mM Hepes pH 7.4 at +4°C.
MAT activity was assayed by measuring the rate of formation of [3H]SAM from ATP and L-[methyl-3H] methionine as reported in Cheng H et al., 1997 with some modifications. Briefly, the reaction mixture (total volume of 0.1 ml, pH 7.4) contained 50 µl of cell extracts and final concentrations of 30 mM $MgCl_2$, 26 mM KCl, 35 mM Hepes, 10 mM ATP and 20 µM L-[methyl-3H]methionine (12600 cpm/nmol). The samples were incubated at +37°C for 60 min and the reaction was stopped by the addition of 1.0 ml ice-cold 1.6 mM citric acid in 50% ethanol. The time 0 of reaction was used as blank. After adsorption to an ion-exchange resin (column in the NH^{4+} form), S-adenosyl-[methyl-3H]methionine was eluted with 1.0 ml of 3.0 M NH_4OH into a vial containing 5 ml of scintillation fluid. The samples were counted in a Packard scintillation counter. The results of MAT activity were expressed as pmol/mg/min.

3.11 Metabolic modeling of rGAMT-loaded RBCs

In order to define the limiting steps in the biotransformation of GAA and to obtain preliminary information about our experimental setup, we created a Bio-PEPA (62) model of creatine synthesis pathway, based both on experimental and literature data (63) and performed in silico simulations. The simplified pathway modeled is:

(Methionine + ATP) -- MAT -> SAM SAM + GAA_in -- GAMT -> SAH + Cr GAA_out <- uptake -> GAA_in.

By assuming a constant supply of methionine (Met) and ATP and a net influx of GAA, our model represented the behavior of a single bolus (10 ml) of 100% Hct RBCs loaded with 1 mg of GAMT and variable amounts MAT, over 10 hours from injection in a patient with a plasmatic concentration of GAA of 50 µM. We also assume this timescale is small enough for the organism not to replenish the plasmatic levels of GAA.

3.12 Generation of pET45b/His-UB-MAT2A construct

The chosen cloning and purification strategies are shown in Figure 18:

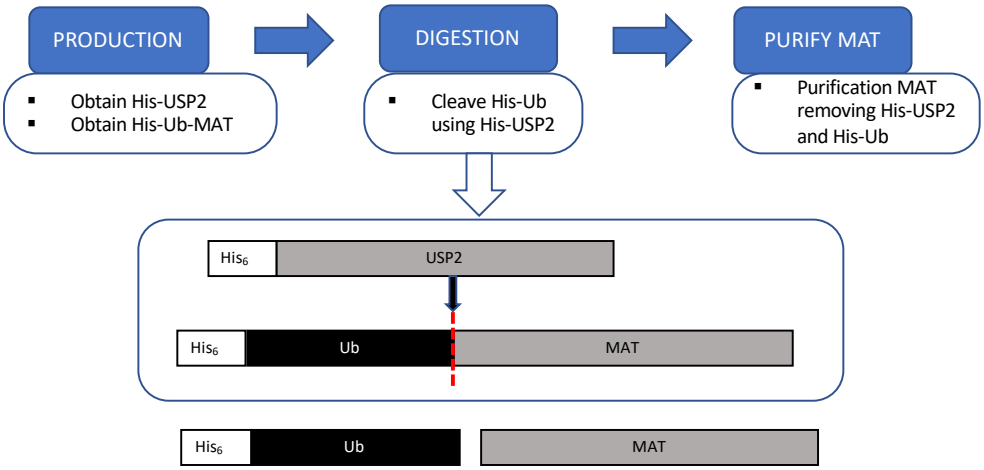

Figure 18 Expression strategy to obtain NO-tag MAT from the pET45b/His-UB-MAT construct.

To this end, total RNA from HeLa cells was extracted by "RNeasy Plus Mini Kit" (Qiagen) and quantified by NanoDrop ND-1000 System. RNA (1 µg) has been retrotranscribed using the "PrimeScript™ RT Master Mix (Perfect Real Time) kit" (Takara, Kusatsu, JPA), with oligo-dT (0.5 µg/reaction) and random hexamers (0.15 µg/reaction) in a final volume of 20 µl.

Specific degenerate primers were designed to amplify the MAT coding sequence of the human mat2a gene (NM_005911.5).

Primer sequences are reported below:

Cloning primers	
NAME	**SEQUENCES (5' to 3')**
NotI Forward	CGTCTCCGCGGTGGAATGAACGGACAGCTCAACGGC
SacII Reverse	CGTCTGCGGCCGCTCAATATTTAAGCTTTTTGGGCACTTCCC

The MAT coding PCR product was cloned downstream of $(His)_6$-ubiquitin coding sequence in to the pET45b-UB expression vector. The PCR conditions were as follows: 200 µM dNTPs, 200 nM primers, 3.5 mM $MgCl_2$, and 0.625 U TaqPlatinum® DNA Polymerase (Invitrogen) per reaction.
The thermic profile was:

Cycle name	**Temperature**	**Time**	
Initial denaturation	+94°C	5 min	
Denaturation	+94°C	15 s	30 cycles
Annealing	+60°C	30 s	
Extension	+68°C	78 s	
Final Extension	+68°C	5 min	
Hold	+4°C	NA	

The PCR products were purified by the "QIAquick PCR Purification Kit" (Qiagen), quantified by NanoDrop and cloned in the pET45b-UB vector by using the NotI/SacII restriction enzymes. The MAT coding PCR product was thus inserted downstream of $(His)_6$-ubiquitin coding sequence into the pET45b-UB expression vector. The ligase reaction was used to transform the Novablue E. coli strain following a standard protocol: incubation 30 min on ice; heat pulse for 90 s at +42°C and then 5 min on ice; addition of 200 µl SOC medium, followed by 1 h incubation at +37°C, before plating the transformation reaction on LB agar plates containing 100 µg/ml ampicillin. Positive colonies were screened by PCR and confirmed by sequencing. Primer sequences are reported in Table 2. A positive clone was chosen, and the plasmid DNA was purified with the "QIAprep Spin Miniprep Kit" (Qiagen).

3.13 Establishment of BL21(DE3) E. coli strain expressing MAT

BL21(DE3) competent cells (50 µl) were transformed by 2ng of pET45b-UB_MAT construct, following the transformation protocol detailed above for Novablue. A few clones of BL21(DE3) bearing the pET45b-UB_MAT construct were tested for MAT expression.

3.14 Establishment of MAT Research Cell Banks

A single colony from the agar plate was inoculated in LB + ampicillin 100 µg/ml. The bacterial culture was incubated at +37°C shaking at 250 rpm , until optical density at 600 nm (O.D.600) reached approximately 0.7-0.8 (~ 4-6 h required). Then, 900 µl of the bacterial culture were added to 600 µl of glycerol, previously dispensed in the cryovials. Twenty glycerol stock tubes of E. coli cells (Novablue and BL21(DE3), transformed with pET45b-UB_MAT construct, identified as Research Cell Bank (RCB) were prepared and immediately frozen at -80°C.

3.15 Induction of recombinant MAT at lab scale

The "standard small-scale" induction protocol is described below (any variation of induction parameters is reported in the "Results" section).

Starting culture: an isolated colony was picked from a freshly streaked plate and grown overnight (ON) at +37°C in 10 ml Vegetable pepton + ampicillin (100 µg/ml) in a 50 ml tube on a benchtop orbital shaker. A sample of the ON culture was withdrawn and diluted 1:10 before reading $O.D._{600}$. The ON inoculum was then diluted into 2000 ml Synthetic media + ampicillin (100 µg/ml) and put in a bioreactor in order to reach an $O.D._{600}$ of about 0.1. The culture was then incubated at +37°C with aeration and shaking at 250 rpm. Bacterial growth was constantly monitored until culture density reached an $O.D._{600}$ of about 0.5-0.6. 10 ml of culture were then removed, transferred to a labeled 50 ml tube and let grow at +37°C (Not Induced control, NI). IPTG at 1 mM final concentration was added into the bioreactor to induce protein production (Induced sample, I). At 1 h-intervals, up to 3 h, 10 ml of induced bacterial culture were withdrawn, transferred into a 15 ml-tube and put on ice. Cells were collected by centrifugation at 2750 g for 20 min at +4°C: the supernatant was removed and the pellet frozen at -20°C for later processing.

3.16 Preparation of bacterial extracts and SDS-PAGE analysis

Cell lysis was obtained by resuspension of the cell pellets (from both NI and I samples) in 0.05 culture volume of ice cold Lysis Buffer (40 mM Tris-HCl, 110 mM NaCl, 2.2 mM KCl, 0.04% Tween and 20% Glycerol, pH 8.0), followed by four cycles (30 s on, 30 s off at 50% amplitude capacity) of sonication at 75 watt, while keeping the sample on ice. Samples were centrifuged 10 min at 9600 g and +4°C: the supernatant (S), corresponding to the soluble cytoplasmic fraction, was transferred into a new microcentrifuge tube, while the residual pellet was resuspended in Lysis Buffer and sonicated as above; this further sample has been referred to as the Pellet (P) sample.

The protein concentration in both S and P samples was determined by the Bradford assay (60), to normalize the samples for loading.

For SDS-PAGE, an aliquot corresponding to 20 µg of proteins (for P loaded 10µl), was combined with an equal volume of 2X Sample Buffer (2X SB = 2% SDS, 100 mM Tris-HCl, pH 6.8, 20% glycerol, 0.0025% bromophenol blue,) and boiled 1 min at +100°C to denature proteins. Proteins were resolved by a 10% (w/v) polyacrylamide gel electrophoresis, in parallel with the Low Molecular Weight standard (LMW) as a size reference.

3.17 Immobilized metal ion affinity chromatography (IMAC)

The recombinant His-tagged UB-MAT in the supernatant fraction was purified by the immobilized metal ion affinity chromatography (IMAC), exploiting the interaction between chelated transition metal ions (Ni^{2+}) and side-chains of histidines on proteins, essentially according to the manufacturer's instructions. Briefly, the column was equilibrated with the Binding buffer which corresponds to the Lysis Buffer in which the sample was resuspended. The lysis/storage buffer has been optimized. After sample loading, washings were initially performed with the same Binding buffer, and then with Binding Buffer + 40 mM imidazole. Elution of the His-tagged recombinant protein was obtained by Binding buffer + 200 mM imidazole.

3.18 USP2 digestion of rHis-UB-MAT

His-UB-MAT obtained upon Ni-Sepharose affinity chromatography was digested with the recombinant His-tagged deubiquitinating enzyme USP2 (rHis-USP2) to remove the His-UB partner fused at the N-terminus of MAT. For optimal digestion, His-UB-MAT and rHis-USP2 were combined allowing a mass ratio of 20:1 (other conditions tested were 200:1 and 100:1 ratio) and incubated at least 3 h at +37°C (other conditions tested were 2-day digestion), in the same MAT buffer. After cut reaction, the protein was pooled and then dialysed ON against MAT buffer at 4 °C.

rhMAT NO-tag was purified from all the His-tag byproducts generated during digestion, not-digested His-UB-MAT and His-USP2, by Nickel affinity chromatography.

Recovery yield was calculated upon the protein concentration assay with Bradford (60) while the purity of the enzyme was assessed by SDS-PAGE. rhMAT was stored at -80°C.

3.19 Determination of MAT activity in loaded RBCs

The evaluation of enzyme activity was performed by a method based on the quantification of S-(5'-Adenosyl)-L-methionine chloride dihydrochloride (SAM). The dosage method was performed according to bibliography (66) with some modifications. Briefly, in a final volume of 250 µl, the reaction mixture contained 100 mM Tris-HCl (pH 7.5), 50 mM $MgCl_2$, 100 mM KCl, 8 mM GSH, 20 mM ATP, 20 mM L-Met and MAT (in our experiment it has been standardized on amount of 10 and 20 µg). The incubation was carried out at +37°C for 10 min and at different incubation times (0-1-2.5-5-10 min) the reaction was stopped by the addition of 250 µl of 2 N PCA. After filtration with 0.2 µm filter, 50 µl of reaction mixture were injected into the HPLC. Blanks, containing the reaction mixture without enzyme, were analyzed as well.

The analysis was performed as reported bibliography (65) with some modifications: the method was a reverse phase chromatography and the detection was monitored at 254 nm, at +25°C and using a gradient elution system at a flow-rate of 1 ml/min as reported in Table 3. The mobile phase consisted of buffer A: 8 mM $C_8H_{17}O_3SNa$ and 50 mM NaH_2PO_4, and buffer B: CH_3OH 100%. Buffer A reached a final pH 3 by H_3PO_4 and it was filtered by Polypro filters before use. Before and after sample analysis, the column was equilibrated and standard solution of 0.05 mM of SAM in 1 N $HClO_4$ was analyzed. SAM peak was identified according to its retention time and co-chromatography with SAM standard. The increase of SAM levels after different analysis times (0-10 min) has been observed. Quantification was based on integration of peak areas and compared to the standard calibration curves of SAM.

3.20 Co-entrapment of GAMT and MAT in human RBCs

Whole blood (WB) was obtained from healthy volunteers included in the Italian blood donor registry (registered A.V.I.S. donors) who signed an informed consent form. Blood was collected in heparinized tubes and provided by the "Santa Maria della Misericordia" Hospital in Urbino. Briefly, GAMT/MAT was loaded into human RBCs by means of hypotonic dialysis, isotonic resealing and re-annealing, according to literature (67) with some modifications.

Whole blood was centrifuged 10 min at +4°C and 1800 g to remove plasma and then washed twice by 10 min centrifugation at +4°C, at 1800 g, in a physiological saline solution containing: 10 mM 2-[4-(2-hydroxyethyl)piperazin-1-yl]-ethanesulfonic acid (HEPES, pH 7.4), 154 mM NaCl and 5 mM glucose. The dialysis procedure was carried out with different concentrations of proteins added to RBCs suspended in Hepes solution at 60% haematocrit (Ht), as follows:

A. 125 µg (0.025 IU) of enzyme GAMT (50 µl protein solution [2.5 mg/ml] with SA 0.2 IU/mg);
B. 125 µg (0.025 IU) of enzyme MAT (125 µl protein solution [1 mg/ml] with SA 0.2 IU/mg);

C. 125 µg (0.025 IU) of enzyme GAMT (50 µl protein solution [2.5 mg/ml] with SA 0.2 IU/mg) and 125 µg (0.025 IU) of enzyme MAT (125 µl protein solution [1 mg/ml] with SA 0.2 IU/mg);
D. 125 µg (0.025 IU) of enzyme GAMT (50 µl protein solution [2.5 mg/ml] with SA 0.2 IU/mg) and 250 µg (0.050 IU) of enzyme MAT (250 µl protein solution [1 mg/ml] with SA 0.2 IU/mg);
E. 250 µg (0.050 IU) of enzyme GAMT (100 µl protein solution [2.5 mg/ml] with SA 0.2 IU/mg) and 125 µg (0.025 IU) of enzyme MAT (125 µl protein solution [1 mg/ml] with SA 0.2 IU/mg).

All the conditions (in 1 ml final volume) were dialyzed for 90 min at +4°C in a cellulose tube (14 kDa MWCO, Roth, Karlsruhe, Germany) placed in a rotating plate vs 50 ml of hypotonic dialysis buffer optimized for human RBC loading, containing 10 mM NaH_2PO_4, 10 mM $NaHCO_3$ (pH 7.4), 20 mM glucose, 3 mM GSH and 2 mM ATP, replacing the buffer with fresh one after 45 min. The final osmolarity of the hypotonic solution was 68±2 mOsm, measured by Osmometer Fiske Associates, Model 210 (Norwood, MA, USA). After dialysis, the cells reached about 90±4 mOsm. Subsequent resealing and re-annealing steps were carried out by incubating the pooled dialyzed RBC suspensions 5 min at +37°C. Then, PIGPA solution (100 mM inosine, 20 mM ATP, 10 mM anhydrous glucose, 100 mM sodium pyruvate, 4 mM $MgCl_2$, 190 mM NaCl, 1666 mM KCl and 33 mM NaH_2PO_4) was added to the RBCs (10% v/v) to restore isotonicity (300 mOsm) and the suspensions were incubated 25 min at +37°C under gentle stirring, to allow pore closure. Final washing phase in physiological saline solution was carried out twice, centrifuging 10 min at 500 g and +4°C. Unloaded RBCs submitted to the same procedure without the addition of the recombinant proteins were used as controls. Final packed loaded RBCs were re-suspended in phosphate buffered saline solution (PBS) pH 7.4, at about 40% Ht in presence of 200 µM $^{13}C_2$ GAA and 200 µM L-Met and incubation of these suspensions (A-E) were performed for 21 hours at +37°C. At the planned time points (0-1-2-3-4-5-21h) 50 µl-aliquot of each suspension was collected on a standardized filter paper and the dried blood spots obtained were submitted to biochemical monitoring of $^{13}C_2$ GAA, $^{13}C_2$ CRE and L-Met by MS/MS analysis by Department of Molecular Medicine, La Sapienza University of Rome (68).

3.21 Animals

Adult homozygous GAMT-deficient mice and wild type (WT) mice were employed in this study. Animals involved were bred in Urbino University. To start the breeding, mice of the C57BL/6J background strain were issued from heterozygous mating GAMT+/- of mice provided by the Hamburg University. The genetic characterization is evaluated through PCR analysis on DNA/RNA obtained from tail tissue.

The knockout mouse model for GAMT deficiency was generated by gene targeting in embryonic stem cells in according to bibliography (69); disruption of the open reading frame of the murine GAMT gene in the first exon resulted in the elimination of 210 of the 237 amino acids present in mGAMT. GAMT knockout mice have markedly increased GAA and reduced Cr and creatinine levels in brain, serum and urine, which are key findings in human GAMT patients. In vivo 31P magnetic resonance spectroscopy showed high levels of PGAA and reduced levels of C phosphate in heart, skeletal muscle and brain. These biochemical alterations were comparable to those found in human GAMT patients and can be attributed to the very similar GAMT expression patterns in human and mouse tissues (70) (71) . It has been highlighted as GAMT deficiency in mice causes biochemical adaptations in brain and skeletal muscle. It is associated with increased neonatal mortality, muscular hypotonia, decreased male fertility and a non-leptin-mediated life-long reduction in body weight due to reduced body fat mass (Figure 19).

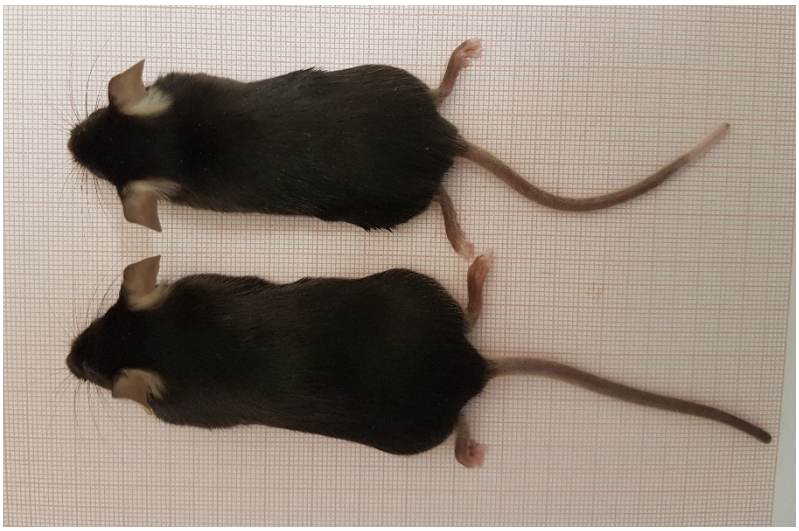

Figure 19 WT and GAMT (-/-) mice. In this picture we can easily notice the different size of the mice which is lower in the diseased mouse (A) than in the healthy mouse (B). (A) GAMT Wild type (+/+) mice. (B) GAMT (-/-) mouse.

Three groups of adult GAMT mice (GAMT-treated mice, n=5; GAMT-control, n=5) and one group of healthy genetic background mice (WT-control, n=5) were used for biochemical analyses as described below. Animals were housed in standard cages, 3 to 6 mice per cage, on a 12 h light: dark cycle and in controlled conditions (temperature +22±1°C, humidity 60%, air change every 12 h); all mice were fed on Teklad global 18% protein rodent diet (Harlan Laboratories Inc., Madison, WI) and water ad libitum.
GAMT-WT and GAMT heterozygous mice were used as blood donors for the loading procedure, while GAMT -/- mice received MAT_GAMT loaded RBCs. The experiments were carried out in accordance with European legislation (2010/63/UE), with Italian national legislation (DL26/2014) governing the use of animals for research and with the guidelines of the National Institute of Health on the use and the care of laboratory animals (Authorization n° 223/2019-PR).

3.22 In vivo study: Loading procedure and in vivo efficacy of MAT_GAMT-RBC treatment

Blood was collected from anesthetized control GAMT-WT mice by puncture of the retro-orbital sinus in heparinized tubes. Both MAT (SA 0.2 IU/mg) and GAMT (SA 0.1 IU/mg) were loaded into mouse RBCs by means of a procedure of hypotonic dialysis, isotonic resealing and "reannealing", essentially according to bibliography (36) and previously explained for the first preclinical study.
In this second preclinical study, the procedure was carried out with 0.2 IU MAT and 0.1 IU GAMT (corresponding to 125 µl of MAT solution with SA 0.2 IU/mg and 125 µl of GAMT solution with SA 0.1 IU/mg, respectively) being added to 750 µl packed RBC suspension to reach 1 ml final volume at 60% Ht inside the dialysis membrane. This condition (1 ml final volume) was dialyzed 1 h at + 4°C in a cellulose tube (14 kDa MWCO, Roth, Karlsruhe, Germany) vs 50 ml of hypotonic dialysis buffer optimized for murine RBC loading, containing 20 mM NaH_2PO_4, 20 mM $NaHCO_3$ (pH 7.4), 20 mM glucose, 4 mM $MgCl_2$, 3 mM glutathione, and 2 mM ATP. The final osmolality of the hypotonic solution was 102±2 mOsm, measured by Osmometer Fiske Associates, Model 210 (Norwood, MA, USA). This procedure was carried out for several separate tubes; at the end, all RBC suspensions were pooled and, at this stage, the cells reached 138±10 mOsm. Subsequent resealing and reannealing steps and final washing steps were carried out as described above, while the amount of encapsulated enzyme was determined and briefly summarized later on. Hematological parameters were measured by an automatic ABX Micros® 60 cell counter (Horiba Medical, Irvine, CA) and percent RBC recovery was calculated from the number of RBCs submitted to the dialysis step and those recovered at the end of the loading procedure.

Final packed MAT_GAMT-loaded RBCs were resuspended in Hepes solution at approximately 35% Ht in order to administer 0.05 ± 0.004 IU MAT/mouse and 0.03 ± 0.004 IU GAMT/mouse in a final volume of 400 ± 40 µl by performing intravenous injections in the retro-orbital sinus of the mice.
A cohort of 6 GAMT -/- mice underwent the following treatment: 3 mice received a single infusion of loaded enzymes, the remaining 3 ones received two more subsequent infusions at a weekly interval for a total of three infusions each. A time lag of 7 days between injections was selected. This part aimed at evaluating the longer-term therapeutic capacity of a higher number of repeated infusions in lowering GAA, increasing Cr and maintaining their levels near the physiologic condition. GAMT-WT (n = 5) and GAMT -/- (n = 5) mice were used as healthy and GAMT deficiency controls respectively, and submitted to the same series of injections as the RBC-treated mice, but they received i.v. infusions of native untreated RBC suspensions at the same Ht.
Blood GAA and Cr concentration was measured by MS/MS on dried blood spots (DBS) collected as previously described from all animals, including control healthy and GAMT -/- mice. GAA and Cr monitoring was performed at time 0 before the first administration and then 2 and 5 days after each infusion.

3.23 Tandem mass spectrometry

RBC suspensions from the *in vitro* study and mouse whole blood were collected on Schleicher&Schuell 903 grade filter paper, dried at room temperature and stored at + 4°C in plastic bags until use. GAA and Cr analysis in DBS was performed in the Department of Experimental Medicine of the "Sapienza" University of Rome, essentially according to a previous method proposed by bibliography (72) with some modifications. Three millimeter diameter dots were punched out from DBS and eluted in 100 µl of methanol/water (90:10) solution spiked with labeled internal standards (CIL, Andover, MA, USA). The samples were shaken 30 min at + 30°C, then 65 µl of supernatant was dried under nitrogen flow at + 45°C. The residues were derivatized by treatment with 50 µl of 3 M HCl in n-butanol solution at + 60°C for 30 min. After derivatization, the samples were dried under nitrogen flow at + 45°C and recovered in 50 µl of methanol/water (80:20) containing 0.1% acetic acid. A 20 µl volume was injected into a LC-MS/MS system (API 2000, Sciex, Toronto, Canada) equipped with a Series 200 micro pump (Perkin Elmer, Norwalk, CT, USA) and a Series 200 autosampler (Perkin Elmer) for solvent delivery and automated sample loading. The mobile phase was methanol/water (80:20) pumped at a flow rate of 80 µl/min. For the detection of the compounds of interest multiple reaction monitoring and a total acquisition time of 1 minute were used.

4 Results

4.1 Expression optimization of GAMT in BL21(DE3)

Expression studies were performed at lab scale to optimize GAMT product yield. Scaling-up production was first performed in LB medium and next in Synthetic media. In this section are reported the results obtained in the different fermentation processes.

Experiment N. 1: LB versus SYNTHETIC MEDIUM (0.5 L, in Flask)

EXPERIMENTAL CONDITIONS:

Stage 1: 0.5 L Flask		
Working Volume:	100 ml	
Starting material:	Research Cell Bank	
Medium:	LB broth + Ampicillin (100 µg/ml)	
Incubation condition:	T: +37°C	
Stage 2: 2 L Flask	**LB**	**Synthetic**
Working volume	0.5 L	0.5 L
Starting material:	Culture broth from Stage 1, start O.D. = 0.100	Culture broth from Stage 1, start O.D. = 0.100
Medium:	LB broth supplemented with Ampicillin (100 µg/ml)	Synthetic medium supplemented with Glucose-MgSO4-Thiamine-Ampicillin (25µg/ml)
Incubation condition:	T: +37°C	T: +37°C
Induction with 1mM IPTG at:	0.534 O.D.600nm (1 h 20 min)	0.498 O.D.600nm (3 h 15 min)
Feed	none	none

RESULTS (see also Figure 20):

Stage 1		
final O.D.$_{600nm}$:	4.925 after 16 h	4.925 after 16 h
Stage 2		
final O.D.$_{600nm}$:	1.630 after 3 h	1.130 after 3 h
Proteins in the soluble bacterial extract	57.02 mg (total amount)	82.17 mg (total amount)
His-UB-GAMT after the 1st Ni-affinity chromatography	10.42 mg (total amount)	2.40 mg (total amount)
GAMT after USP2 cleavage and 2nd Ni-affinity chromatography	2.21 mg (total amount); recovery= 28.9%*	0.20 mg (total amount); recovery= 11.3%*
Specific activity	0.15±0.02 U/mg	0.09±0.005 U/mg
Stability data	/	/

*Dialysis performed before USP2 digestion to dilute imidazole (150 mM in the elution buffer).

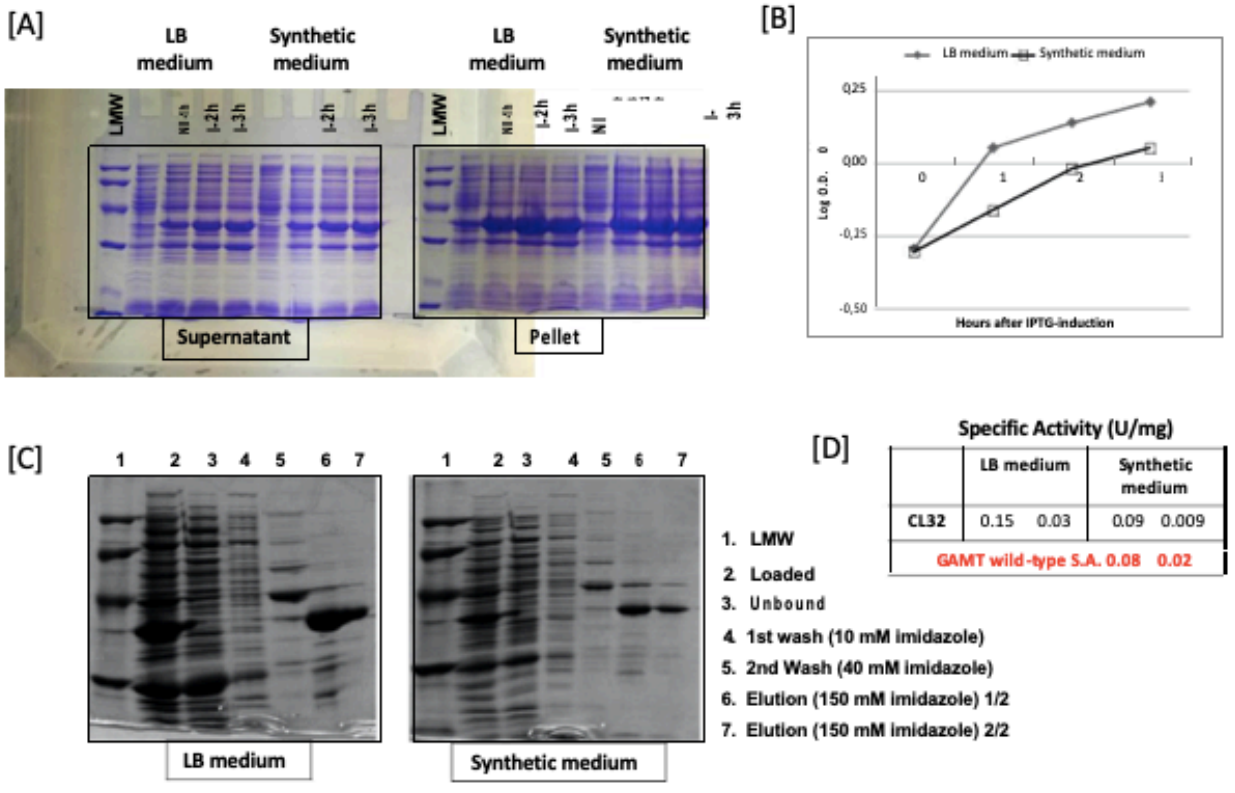

Figure 20 Expression and purification of GAMT CL32, using different culture media. [A] Time-course induction of the mutagenized construct CL32, in two different media: LB broth and Synthetic medium. Supernatant and Pellet fractions are resolved by SDS-PAGE; NI is the not-induced sample. LMW, low molecular weight protein standard. [B] Bacterial growth after IPTG induction, in LB versus synthetic medium. [C] Purification of r -His-UB-GAMT CL32 by immobilized metal ion affinity chromatography (IMAC). [D] Specific activity of GAMT CL32 NO-tag, produced in LB and synthetic medium.

Experiment N. 2: <u>SCALING-UP (3.3 L LB, BIOREACTOR)</u>

EXPERIMENTAL CONDITIONS:

Stage 1: 0.5 L Flask	
Working Volume:	100 ml
Starting material:	Research Cell Bank
Medium:	LB broth + Ampicillin (100 μg/ml)
Incubation condition:	T: +37°C
Stage 2: BIOREACTOR	
Working volume	3.3 L
Starting material:	Culture broth from Stage 1, start O.D. = 0.100
Medium:	LB broth supplemented with Ampicillin (100 μg/ml)
Incubation condition:	T: +37°C
Induction with 1mM IPTG at:	0.536 $O.D._{600nm}$ (1 h 30 min)
Feed	None (antifoam twice)

<u>RESULTS (see also Figure 21):</u>

Stage 1	
final $O.D._{600nm}$:	4.995 after 16 h
Stage 2	
final $O.D._{600nm}$:	3.010 after 4 h
Proteins in the soluble bacterial extract	603 mg (total amount)
His-UB-GAMT after the 1st Ni-affinity chromatography	224.3 mg (total amount) 157.07 mg (after concentration and dialysis to dilute imidazole)
GAMT after USP2 cleavage and 2nd Ni-affinity chromatography	11.02 mg (total amount); recovery= 9.5%*
Specific activity	0.16±0.013 U/mg
Stability data	/

*Dialysis performed before USP2 digestion to dilute imidazole (250 mM in the elution buffer).

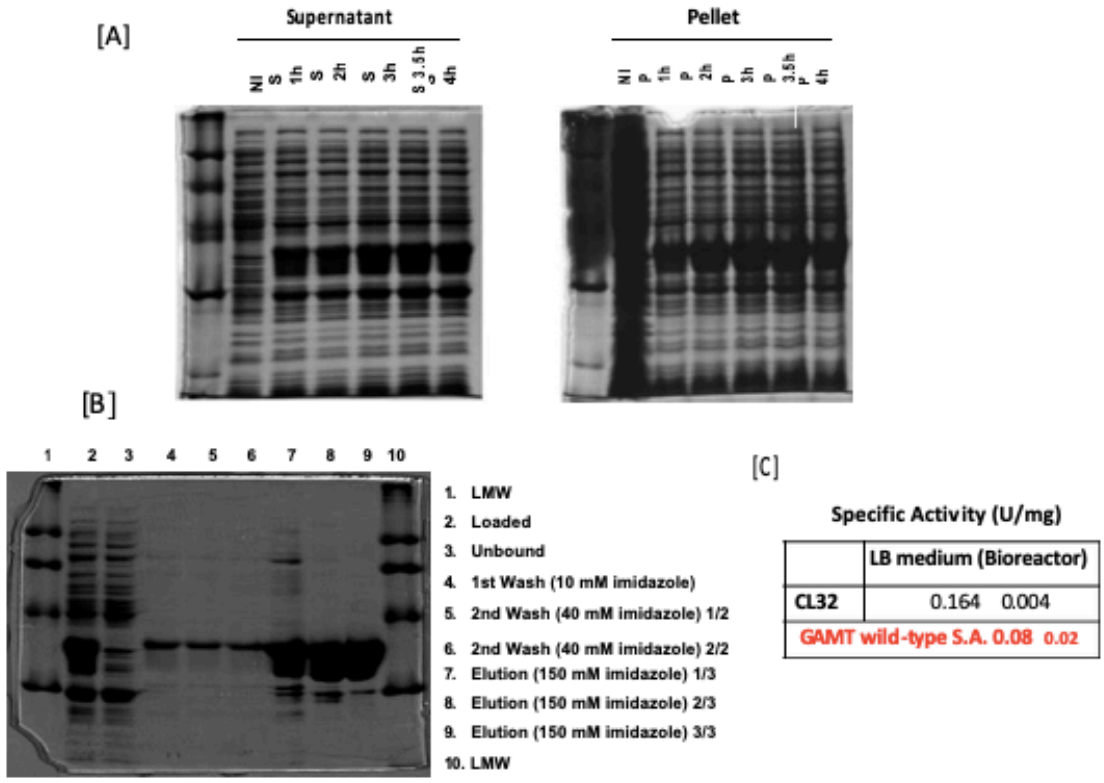

Figure 21 Scaling-up induction and purification of rGAMT CL32. [A] Time-course induction of the mutagenized construct CL32 (in 3.3 L LB, using the Bioreactor). Supernatant and Pellet fractions are resolved by SDS-PAGE; NI is the not-induced sample. [B] Purification of r-His-UB-GAMT CL32 by immobilized metal ion affinity chromatography (IMAC), with the Akta Purifier. LMW, low molecular weight protein standard. [C] Specific activity of GAMT CL32 NO-tag.

4.2 Activity and stability of rGAMT

The activity of CL32 evaluated at the end of purification (time 0), was: 0.13 U/mg. The analysis of rGAMT stability showed that CL32 maintained about 57% of activity after three days at +37°C. The Clone was the selected lead candidate for the successive studies. This enzyme has been produced at lab scale level and its activity, at the end of the purification step (time 0), was shown similar to the previous test production (0.09 vs 0.13 nmol/min/µg). In addition, the analysis of its stability showed that the enzyme activity decreased of about 30% after 24 h and then remained stable until three days at +37°C, as shown in below:

Stability at +37°C (nmol/min/µg)	**0h**	**24h**	**48h**	**72h**
rGAMT CL32	0.09	0.07	0.07	0.06

4.3 Activity of lead candidate (CL32) produced in LB vs Synthetic media

The activity of CL32 produced in 500 ml of LB medium was 0.15 nmol/min/µg, while the activity of the enzyme produced in 500 ml of synthetic medium was 0.09 nmol/min/µg. So, we can observe a 40% reduction of the CL32 activity in synthetic with respect to LB medium.

4.4 Metabolic modeling of GAMT-loaded RBCs

The overall behavior of our model initialized with 1mg of MAT cloned from *E. coli* is shown in Figure 22. From the figure it can be seen that SAM is constantly depleted, therefore MAT kinetic limits the entire pathway. The overall kinetic allows the RBCs to seize GAA from plasma so quickly, it is reduced by 2/3 after 10 h and a great amount of creatine is produced.

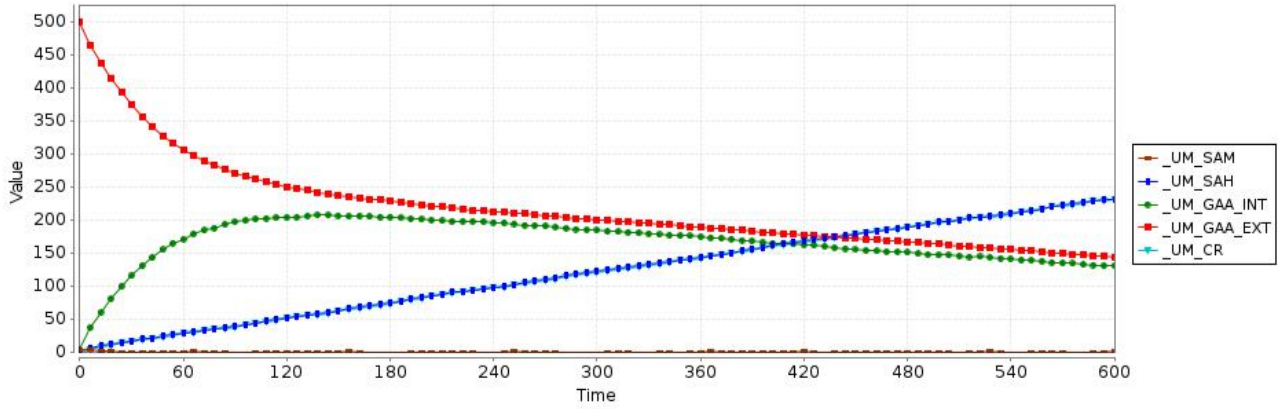

Figure 22 Behavior of RBC modeling engineered with 1 mg of MAT cloned from E. coli Bio-PEPA model of creatine synthesis pathway by engineered RBCs..

At the same time, the amount of creatine produced in simulations with various amounts of MAT, cloned from *E. coli* and the control simulation with endogenous human MAT, is shown in Figure 23.

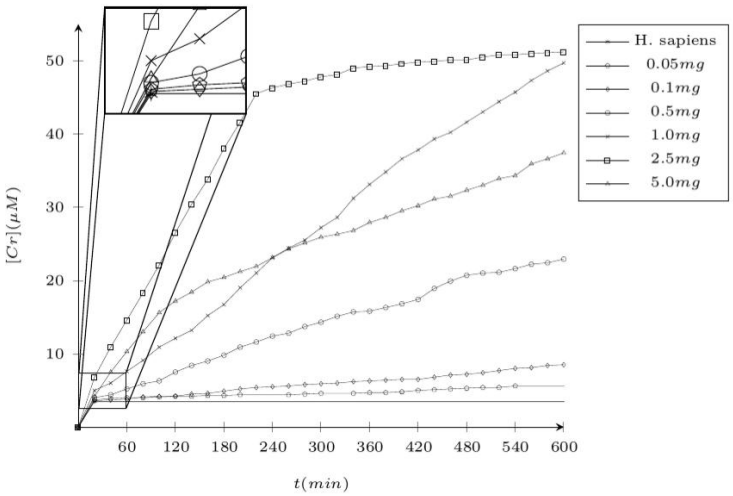

Figure 23 Creatine synthesis in RBCs engineered with different amounts of MAT from E. coli. Bio-PEPA model of creatine synthesis pathway by engineered RBCs.

It can be also noticed that both the control simulation and the one with 0.05 mg of MAT produced negligible amounts of creatine. In general, it can be observed a quick synthesis supported by initial depletion of intracellular SAM (during the first 20 min), followed by a slower synthesis limited by MAT kinetics, until depletion of intracellular GAA occurs (in the simulation using 5 mg of MAT this happens at 3 h); after that point, GAA uptake becomes the limiting factor.

4.5 MAT cloning

Human MAT2A CDS (NCBI Reference Sequence: NM_005911.5) was successfully cloned (with NotI and SacII restriction enzymes) into the pET45b-UB, an expression vector engineered to produce the recombinant enzyme directly fused to the C-terminus of the ubiquitin partner. MAT2 was cloned downstream of the vector encoded His-tag, to improve the yield and provide an easy purification of the authentic protein, without any tag (73).

The recombinant MAT precursor has been referred to as His-UB-MAT from which the NO-tag enzyme was obtained by digestion with the rHis-USP2, a deubiquitylating enzyme which removes the His-UB from the fusion product. By this strategy, rhMAT has been expressed, purified and proved to be active. Moreover, most of the recombinant product was partitioned in the insoluble fraction (referred to as Pellet sample) but the protein is obtained from the soluble part.

4.6 Expression optimization of MAT in BL21(DE3)

Expression studies were performed at lab scale to optimize MAT product yield. Scaling-up production was first performed in Synthetic media. In this section the results obtained in the different fermentation processes are reported.

Experiment N. 1: SCALING-UP (2 liters of synthetic medium, in Bioreactor)

EXPERIMENTAL CONDITIONS:

Stage 1: 0.5 L Flask	
Working Volume:	100 ml
Starting material:	Research Cell Bank (Not qualified)
Medium:	LB + Ampicillin (100 µg/ml)
Incubation condition:	T: +37°C
Stage 2: 2 L	
Working volume	2 L
Starting material:	Culture broth from Stage 1, start O.D. = 0.1
Medium:	Synthetic medium supplemented with Glucose-$MgSO_4$-Thiamine-Ampicillin
Incubation condition:	T: +37°C
Induction with 1mM IPTG at:	0.325 $O.D._{600nm}$ (3 h)
Feed	None (antifoam twice)

RESULTS:

Stage 1	
final $O.D._{600nm}$:	5.23 after 16 h
Stage 2	
final $O.D._{600nm}$:	0.614 after 3 h
Proteins in the soluble bacterial extract	47 mg (total amount)
His-UB-MAT after the 1st Ni-affinity chromatography	9 mg (total amount)
MAT after USP2 cleavage and 2nd Ni-affinity chromatography	2.85 mg (total amount); recovery= 31.7%*
Specific activity	0.04 U/mg

*Dialysis performed before USP2 digestion to dilute imidazole (200 mM in the elution buffer).

Experiment N. 2: <u>SCALING-UP (5.5 liters of synthetic medium, in Bioreactor)</u>

EXPERIMENTAL CONDITIONS:

Stage 1: 0.5 L Flask	
Working Volume:	500 ml
Starting material:	Research Cell Bank (Not qualified)
Medium:	Vegetable pepton + Ampicillin (100 µg/ml)
Incubation condition:	T: +33°C
Stage 2: 5 L (n. 2)	
Working volume	5,5 L
Starting material:	Culture broth from Stage 1, start O.D. = 0.1
Medium:	Synthetic medium supplemented with Glucose-$MgSO_4$-Thiamine-Ampicillin
Incubation condition:	T: +37°C
Induction with 1mM IPTG at:	0.505 $O.D._{600nm}$ (2:30 h)
Feed	None (antifoam twice)

RESULTS: (see also Figure 24);

Stage 1	
final $O.D._{600nm}$:	2.250 after 16 h
Stage 2	
final $O.D._{600nm}$:	1.425 after 3 h
Proteins in the soluble bacterial extract	2000mg (used 1000mg for next steps)
His-UB-MAT after the 1st Ni-affinity chromatography	187.4 mg (total amount)
MAT after USP2 cleavage and 2nd Ni-affinity chromatography	51 mg (total amount); recovery= 27,2%*
Specific activity	0.2±0.04 U/mg
Stability data	

*Dialysis performed before USP2 digestion to dilute imidazole (200 mM in the elution buffer).

[A]

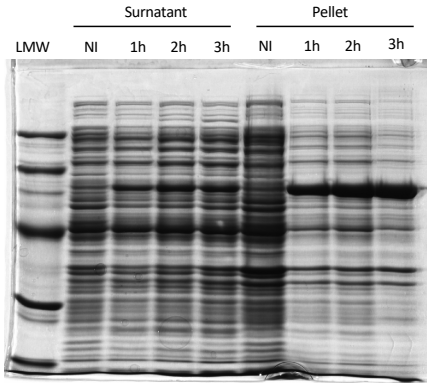

[B]

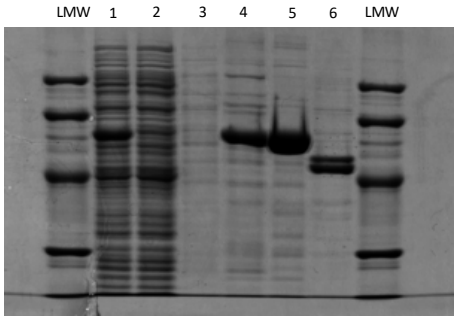

1. Loaded
2. Unbound
3. Wash (10 mM imidazole)
4. Elution (200 mM imidazole)
5. Elution (200 mM imidazole)
6. **MAT**

[C]

Specific Activity (U/mg)

	Synthetic medium (bioreactor)
MAT	0,2±0,04

Figure 24 Scaling-up induction and purification of MAT. [A] Time-course induction of the pET45b-UB_MAT construct (in 5.5 liters Synthetic medium, using the Bioreactor). Supernatant and Pellet fractions are resolved by SDS-PAGE; NI is the not-induced sample. [B] Purification of r-His-UB-MAT by immobilized metal ion affinity chromatography (IMAC), with the Akta Purifier. LMW, low molecular weight protein standard. [C] Specific activity of MAT NO-tag.

4.7 Evaluation of SAM levels into RBC extracts

Intra-erythrocyte SAM content, after the loading procedure, resulted 11.7 nmol/ml of packed RBC (Figure 25) in accord with (Wise CK, 1997) (11.86 nmol/ml packed RBC).

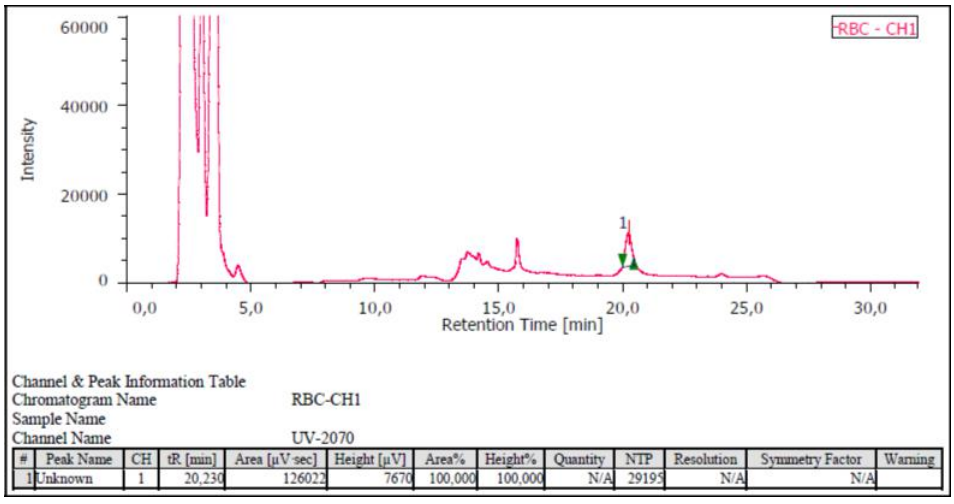

Channel & Peak Information Table
Chromatogram Name RBC-CH1
Sample Name
Channel Name UV-2070

#	Peak Name	CH	tR [min]	Area [µV·sec]	Height [µV]	Area%	Height%	Quantity	NTP	Resolution	Symmetry Factor	Warning
1	Unknown	1	20,230	126022	7670	100,000	100,000	N/A	29195	N/A	N/A	

Figure 25 SAM chromatogram of RBC sample. Representative chromatogram of RBC SAM content of packed RBCs. The retention time for SAM was 20 min.

4.8 Co-entrapment of GAMT and MAT in human RBCs

Human RBCs loaded with both enzymes GAMT and MAT at different entrapped concentrations were able to metabolize from 52 to 58% GAA after 21 h incubation at + 37°C, as reported in Figure 26 (A, B and C) and Table 9.

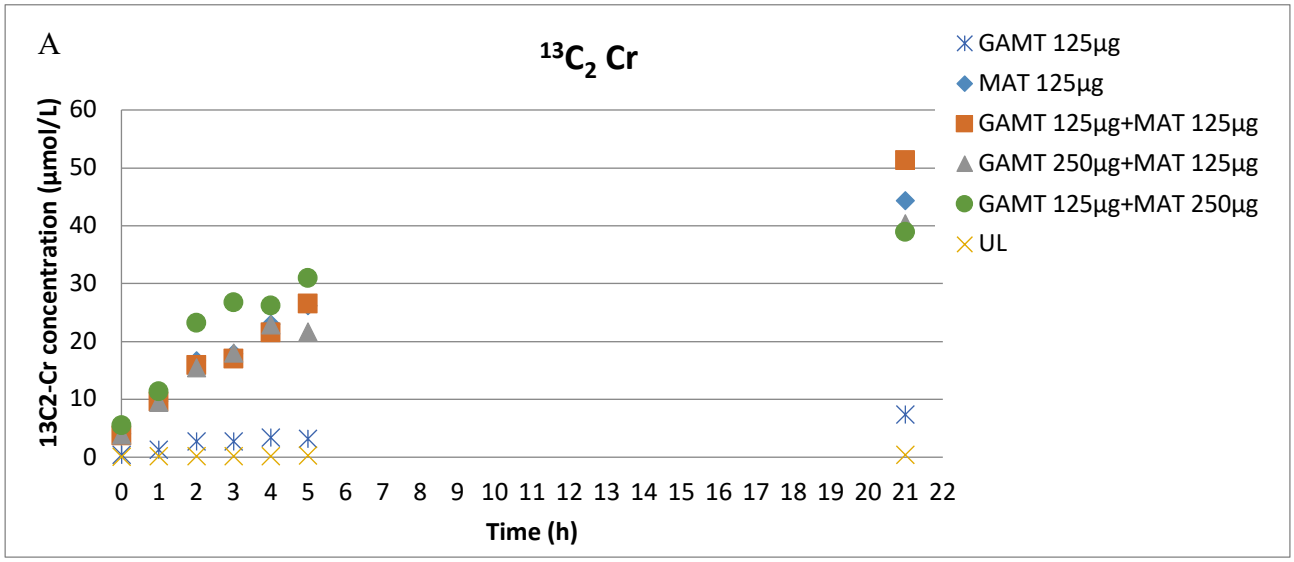

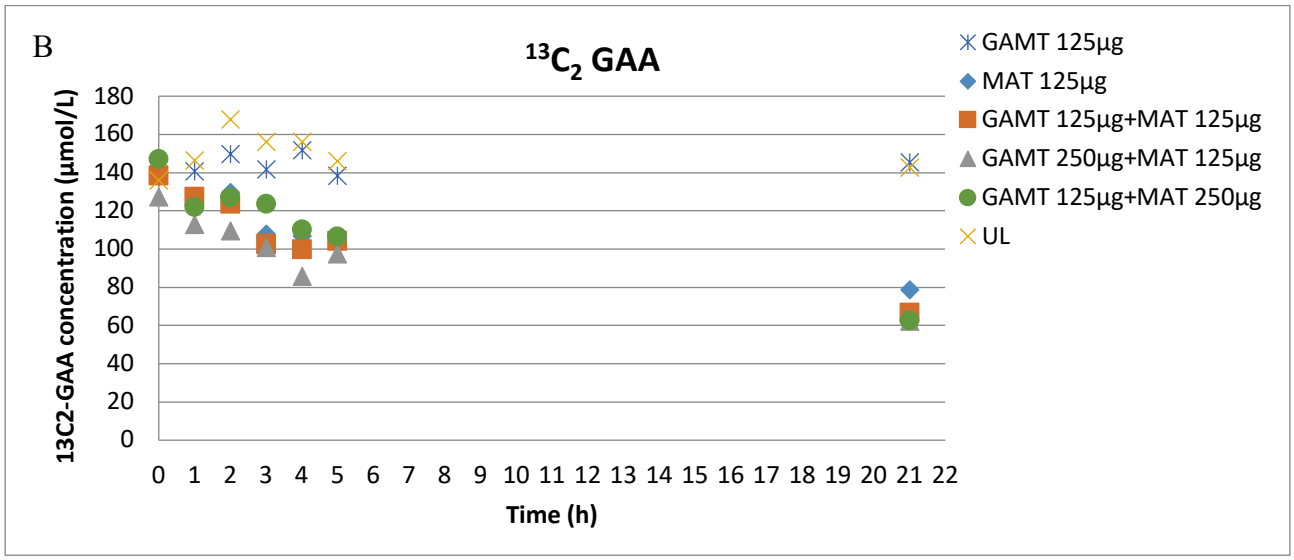

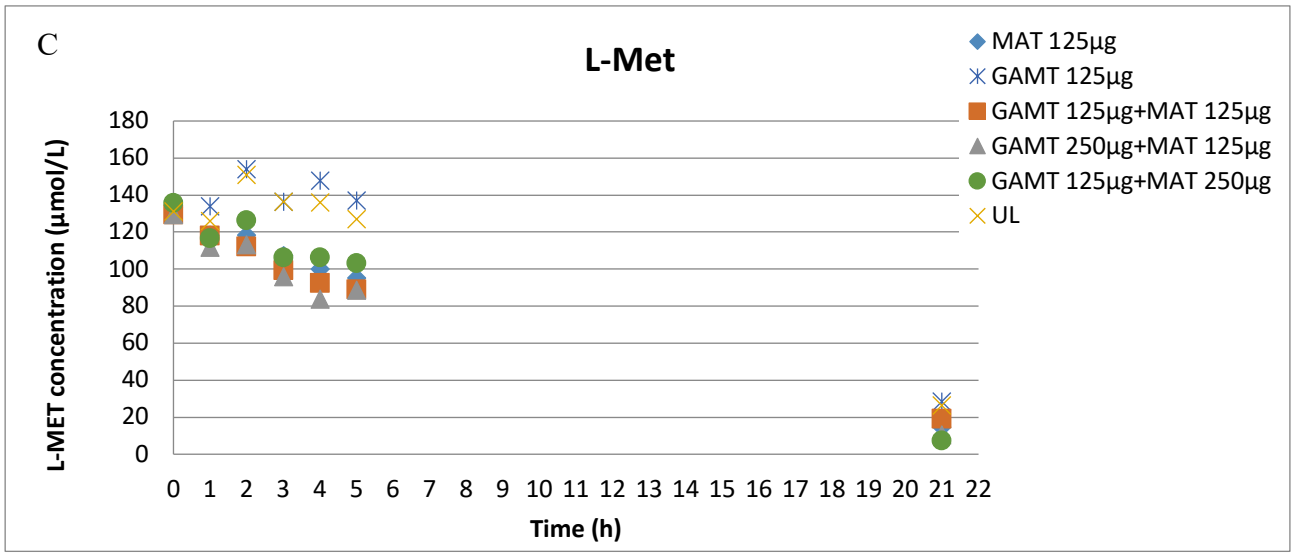

Figure 26 CRE production (A), GAA (B) and L-Met (C) consumption by loaded RBCs.

Sample	Time (h)	13C2 GAA (µmol/L)	13C2 rR (µmol/L)	Reduction of GAA (%)	Met (µmol/L)
Unloaded RBCs	0	135,96	0,08	0,0	131,37
	1	146,19	0,11	-7,5	125,95
	2	167,73	0,14	-23,4	151,08
	3	156,00	0,16	-14,7	136,26
	4	155,97	0,19	-14,7	136,09
	5	145,90	0,28	-7,3	127,25
	21	142,70	0,40	-5,0	26,41
GAMT 125µg-loaded RBCs	0	138,83	0,40	0,0	132,71
	1	140,47	1,29	-1,2	134,03
	2	149,62	2,74	-7,2	154,05
	3	141,57	2,72	-1,9	136,27
	4	151,66	3,42	-8,5	147,67
	5	138,26	3,20	0,4	137,05
	21	145,35	7,39	-4,5	28,33
MAT 125µg-loaded RBCs	0	134,34	0,04	0,0	126,15
	1	121,59	0,06	9,5	111,65
	2	132,74	0,09	1,2	111,30
	3	135,81	0,11	-1,1	107,57
	4	129,99	0,15	3,2	94,63
	5	116,95	0,17	12,9	92,70
	21	130,36	0,71	3,0	40,94
GAMT 125µg and MAT 125µg-loaded RBCs	0	138,31	3,72	0,0	129,63
	1	126,97	9,60	8,2	118,06
	2	123,46	15,92	10,7	112,38
	3	102,44	16,93	25,9	99,31
	4	99,57	21,47	28,0	92,54
	5	103,93	26,49	24,9	89,19
	21	66,54	51,28	51,9	19,20
GAMT 250µg and MAT 125µg-loaded RBCs	0	127,10	3,79	0,0	129,52
	1	112,69	9,45	11,3	111,98
	2	109,48	15,43	13,9	113,31
	3	100,61	17,97	20,8	95,86
	4	85,44	22,80	32,8	83,77
	5	97,48	21,63	23,3	88,63
	21	62,12	40,28	51,1	10,46
GAMT 125µg and MAT 250µg-loaded RBCs	0	146,87	5,49	0,0	135,75
	1	121,73	11,35	17,1	116,62
	2	126,90	23,13	13,6	126,24
	3	123,37	26,71	16,0	106,21
	4	109,99	26,19	25,1	106,23
	5	106,49	30,93	27,5	103,21
	21	62,32	38,89	57,6	7,43

4.9 Preclinical study: efficacy of MAT_GAMT-RBC treatment

Three bulk loading procedures were used, obtaining at the end RBC suspensions at 36 ± 4% Ht loaded with 0.125 ± 0.01 IU/ml of MAT and 0.074 ± 0.009 IU/ml of GAMT, respectively. The results of all series of loading procedures performed are summarized in Table 10. As we can observe, the haematological parameters were evaluated, comparing the mean corpuscular indices of the loaded RBCs with the mean reference characteristic values for volume (MCV), content and concentration of haemoglobin (MCH and MCHC) and the distribution (RDW) of murine red blood cells, in order to assess the degree of alteration they undergo

during the procedure. The comparison of the corpuscular indices showed that there were no significant differences with respect to the reference values. In fact, the MCV index reached a value only lightly lower than the normal range (below 20%); the MCH and MCHC parameters were similar to the normal starting values and the RDW exhibited a slight increase as expected.

The suspension was diluted in Hepes solution to final Ht adjusted in order to administer the same dose of both enzymes for each injection in the same volume of approximatively 400 µl, corresponding to 0.05 ± 0.004 IU MAT/mouse and 0.03 ± 0.004 IU GAMT/mouse. Mean basal values of the compounds before treatment (± standard deviation, SD) were: 40.01 ± 11.25 µM for GAA and 1.21 ± 0.59 µM for Cr in treated group; 40.01 ± 4.23 µM for GAA and 1.10 ± 0.91 µM for Cr in untreated group respectively, and they were not significantly different among them ($p > 0.05$ by ANOVA). The treatment produced the results shown below in Figure 27, where time-dependent GAA and Cr values of the single groups of mice involved in the study are reported.

Some differences in GAA and Cr blood levels were observed between the treated and untreated groups, although the values obtained following the administrations are not comparable with those of the healthy mouse group. The tested dose, in fact, was not effective in lowering GAA, increasing Cr and restoring their levels near the physiologic condition at a stable and safe concentration.

As shown in Figure 27 A, while blood GAA values in treated mice slowly diverge compared to controls and appear significantly reduced after the second infusion reaching a 20% drop from basal values (by ANOVA test, $p < 0.05$ *vs* pre-treatment), blood Cr levels result to be constant and mostly superimposable to those of controls, native untreated RBCs-receiving GAMT -/- mice (Figure 27 B). Indeed, Cr values slightly raise at time 2 days after each infusion, but no significant difference has been statistically revealed between treated and untreated groups ($p > 0.05$ by ANOVA). The results obtained from the blood GAA and Cr assessment over time suggest that the treatment was not successful in causing an effective response in this preliminary preclinical study.

Table 10. Hematological parameters of MAT_GAMT-RBCs of the preclinical study.

	Loaded GAMT-MAT (IU/ml RBCs 100% Ht)	RBC recovery (%)	MCV (µm³)	MCH (pg)	MCHC (g/dl)	RDW (%)
MAT	0.35 ± 0.003	22 ± 5	39 ± 1.83	12.2 ± 1.47	32.88 ± 2.95	17.53 ± 0.47
GAMT	0.2 ± 0.01					
Control erythrocytes (range)*			48–50	16.5–22.2	33.7–45	13.6–15

*Reference ranges are the minimum and maximum values observed in overall murine blood before being submitted to the loading procedure for which the mean ± SD value is reported. Data are means ± SD. n =3 number of independent loading procedures.

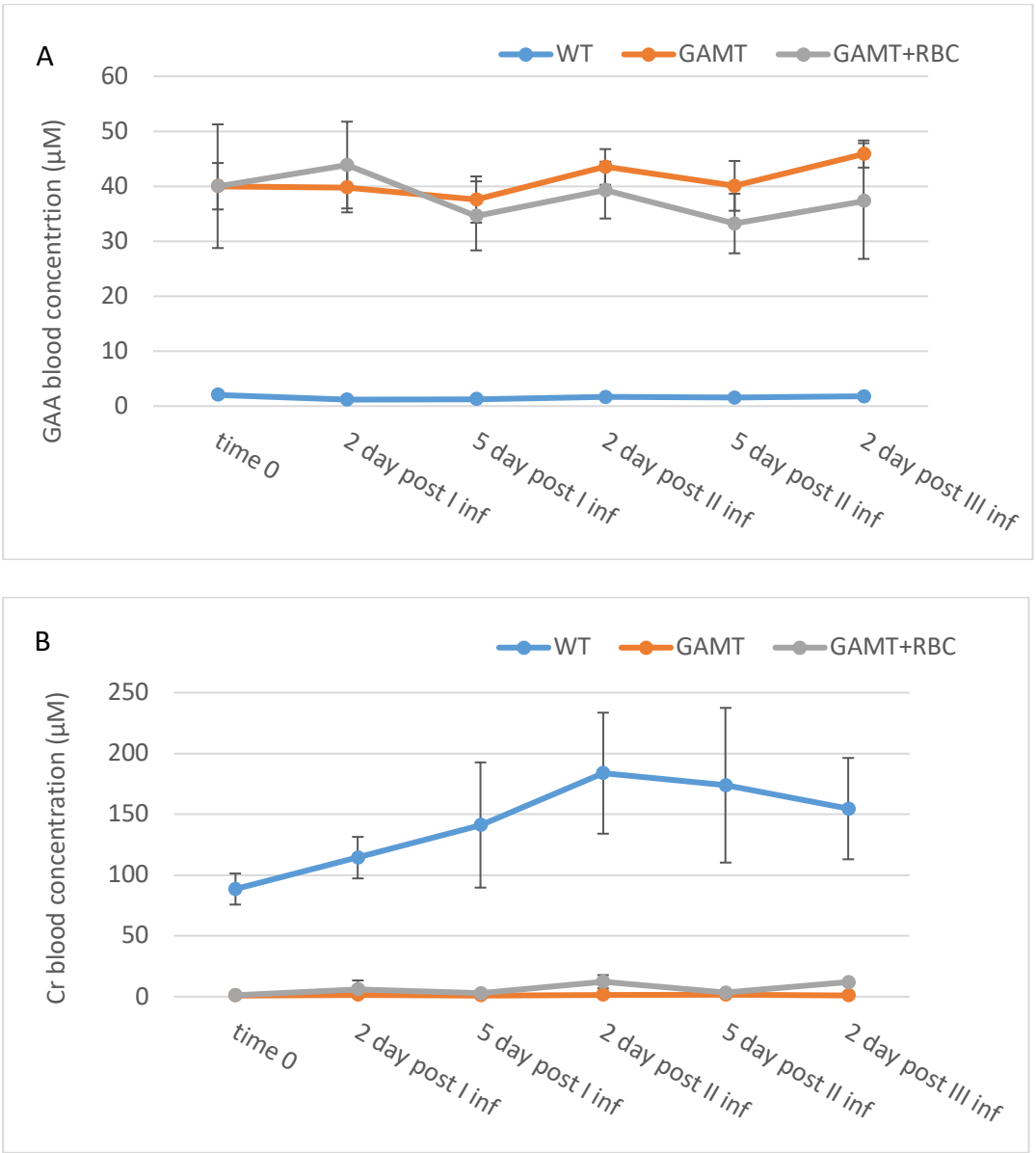

Figure 27 Time course of blood GAA (A) and Cr (B) levels in control and treated mice during enzyme loaded-RBC treatmen

5 Discussion

For the recombinant enzyme GAMT, the production was successfully scaled up, optimizing the conditions and its specific activity (0.164 ± 0.04 U / mg) was characterized.
The recombinant MAT enzyme was cloned, produced and the production increment was performed. Also, for this enzyme an optimization of the conditions (not described in this thesis) was performed and finally it was characterized (0.2 ± 0.04 U / mg).
Co-entrapment with GAMT-MAT was performed in human RBCs and the ability of RBCs loaded with these enzymes to metabolize GAA and form Cr was successfully achieved in vitro.
We performed the preclinical study to demonstrate the efficacy that murine RBCs loaded with GAMT-MAT are able to act as bioreactors to reduce GAA and form creatine in the blood in GAMT deficient mice.
Some differences in blood levels of GAA and Cr were observed between the treated and untreated groups, although the values obtained after administration are not comparable to those of the healthy mouse group. The tested dose, in fact, was not effective in lowering the GAA, increasing the Cr and bringing their levels close to the physiological condition to a stable and safe concentration.
Our future goals will be the production of both enzymes in the most concentration form and the optimization of the loading protocol in murine erythrocytes obtained from wild type GAMT mice, by entrapping the highest concentrations of both proteins and then the performance of two consecutive preclinical studies. At first, a “dose finding study” to evaluate the efficacy of a single infusion of different doses of MAT GAMT-loaded RBCs in order to normalize the biochemical parameters of the disease by reducing blood GAA levels and increasing Cr values in GAMT deficient mice. Secondly, a “repeated administration study” for the preclinical evaluation of the safety and the long-term efficacy of repeated infusions of a selected dose of enzyme (resulting from the dose finding study) in restoring and maintaining the physiological levels of GAA and Cr. On the whole, this project will desirably lead to the optimized production of processed MAT GAMT-loaded erythrocytes with features as similar as possible to those of native untreated RBCs, but with the additional ability to efficiently metabolize GAA for the treatment of GAMT deficient patients, in order to to develop an enzyme substitution therapy for this genetic metabolic disease by means of erythrocytes employed as circulating bioreactors, in order to overcome all the bioavailability and immunogenicity issues risen by administration of the free enzymes.

FINAL CONCLUSIONS

We focused on the use of engineered red blood cells (RBCs) for enzyme replacement therapy as bioreactors for the sustained maintenance in the bloodstream of recombinant enzymes removing circulating noxious metabolites. Thus, we demonstrated that engineered red blood cells loaded with recombinant proteins could be used in the treatment of two genetic metabolic diseases, namely PKU and GAMT deficiency.
To this end, we developed at first the cloning, expression and purification of recombinant enzymes to treat these types of inherited metabolic disorders, then we optimized the enzymes' loading procedure in murine erythrocytes to test the strategy in preclinical studies.
For PKU, the excellent in vivo results obtained, which led to a stable control and normal values of blood L-Phe concentration, lay the basis for the optimization of the production process of the PAL enzyme. It will be necessary, as already discussed, to perform repeated infusions of red blood cells loaded with the PAL enzyme to verify the safety and efficacy of the treatment in the long term.
For the GAMT deficiency, the results obtained in the preclinical study are encouraging. Physiological values have not been reached but the study has made it possible to highlight improvements that are ongoing. The data shown in this thesis will be soon published in scientific peer review journals; the respective manuscripts are in preparation.
Ultimately, there are many bibliographic examples of enzyme replacement therapy but, due to the limitations described in the introductory chapter, we believe that it is possible to overcome several of such limitations by using red blood cells as bioreactors.

REFERENCES

1. Daniela Concolino, Federica Deodato and Rossella Parini. Enzyme replacement therapy: efficacy and limitations. s.l. : Ital J Pediatr., 2018, Vol. 44.

2. Azam Safary, Mostafa Akbarzadeh Khiavi, Rahimeh Mousavi, Jaleh Barar and Mohammad A. Rafi. Enzyme replacement therapies: what is the best option? s.l. : Bioimpacts, 2018, Vol. 8.

3. Savio L. C. Woo, Alan S. Lidsky, Flemming Güttler, Chandra Thirumalachary, Kathryn J. H. Robson. Prenatal Diagnosis of Classical Phenylketonuria by Gene Mapping. s.l. : JAMA, 1984, p. doi:10.1001/jama.1984.03340390052029.

4. Heidi Erlandsen, Angel L. Pey, Alejandra Gámez, Belén Pérez, Lourdes R. Desviat, Cristina Aguado, Richard Koch, Sankar Surendran, Stephen Tyring, Reuben Matalon, Charles R. Scriver, Magdalena Ugarte, Aurora Martínez, and Raymond C. Stevens. Correction of kinetic and stability defects by tetrahydrobiopterin in phenylketonuria patients with certain phenylalanine hydroxylase mutations. s.l. : PNAS, 2004, Vol. 101.

5. Fabrizia Fusetti, Heidi Erlandsen, Torgeir Flatmark, Raymond C. Stevens. Structure of Tetrameric Human Phenylalanine Hydroxylase and Its Implications For Phenylketonuria. 1998.

6. H Erlandsen, R C Stevens. The structural basis of phenylketonuria. s.l. : Genet Metab , 1999.

7. Allosteric mechanisms in ACT domain containing enzymes involved in amino acid metabolism. Amino Acids (. 2005.

8. Werner, Ernst R., Blau, Nenad e Thöny, Beat. Tetrahydrobiopterin: biochemistry and pathophysiology. Biochem J . 2011, Vol. 438.

9. Nenad Blau, Nan Shen, Carla Carducci. Molecular genetics and diagnosis of phenylketonuria: State of the art. Nenad BlauNan ShenNan ShenCarla CarducciCarla Carducci : Expert Review of Molecular Diagnostics, 2014, Vol. 14, p. DOI: 10.1586/14737159.2014.923760.

10. John J Mitchell, Yannis J Trakadis & Charles R Scriver. Phenylalanine hydroxylase deficiency. s.l. : Genetics in Medicine, 2011, Vol. 13.

11. J Pietz, B Fätkenheuer, P Burgard, M Armbruster, G Esser, H Schmidt. Psychiatric disorders in adult patients with early-treated phenylketonuria. Pediatrics. 1997, Vol. 99.

12. Marieke Hoeksma, Dirk-Jan Reijngoud, Jan Pruim, Harold W de Valk, Anne M J Paans, Francjan J van Spronsen. Phenylketonuria: High plasma phenylalanine decreases cerebral protein synthesis. s.l. : Mol Genet Metab ., 2009, Vol. 96.

13. Christian Landvogt, Eugen Mengel, Peter Bartenstein, Hans Georg Buchholz, Mathias Schreckenberger, Thomas Siessmeier, Armin Scheurich, Reinhold Feldmann, Josef Weglage, Paul Cumming, Fred Zepp, Kurt Ullrich. Reduced Cerebral Fluoro-l-Dopamine Uptake in Adult Patients Suffering from Phenylketonuria. s.l. : Journal of Cerebral Blood Flow & Metabolism, 2007.

14. F J van Spronsen, Marieke Hoeksma, Dirk-Jan Reijngoud. Brain dysfunction in phenylketonuria: is phenylalanine toxicity the only possible cause? s.l. : J Inherit Metab Dis ., 2009.

15. Erin L Macleod, Denise M Ney. Nutritional Management of Phenylketonuria. s.l. : Ann Nestle Eng, 2010, Vol. 68.

16. Kirsten Ahring, Amaya Bélanger-Quintana, Katharina Dokoupil, Hulya Gokmen Ozel, Anna Maria Lammardo, Anita MacDonald, Kristina Motzfeldt, Maria Nowacka, Martine Robert, Margreet van Rijn. Dietary management practices in phenylketonuria across European centres. s.l. : Clin Nutr, 2009, Vol. 3.

17. Acosta, P. B. Recommendations for protein and energy intakes by patients with phenyl-ketonuria. s.l. : European Journal Pediatr, 1996, Vol. 155.

18. Daly, Anita MacdonaldHülya Gökmen-OzelAnne. Changing dietary practices in phenylketonuria. s.l. : The Turkish journal of pediatrics, 2009, Vol. 51, p. 409-415.

19. F. J. van Spronsen, P. G. A. Smit & R. Koch. Phenylketonuria: Tyrosine beyond the phenylalanine-restricted diet. s.l. : Journal of Inherited Metabolic Disease volume, 2001, Vol. 24.

20. D M Ney, S T Gleason, S C van Calcar, E L MacLeod, K L Nelson, M R Etzel, G M Rice, J A Wolff. Nutritional management of PKU with glycomacropeptide from cheese whey. s.l. : J Inherit Metab Dis ., 2008, Vol. 32.

21. Søren W.Gersting, Kristina F.Kemter, Michael Staudigl, Dunja D.Messing, Marta K.Danecka, Florian B.Lagler, Christian P.Sommerhoff, Adelbert A.Roscher, Ania C.Muntau. Loss of Function in Phenylketonuria Is Caused by Impaired Molecular Motions and Conformational Instability. s.l. : American Journal of Human Genetics, 2008.

22. Harvey L Levy, Andrzej Milanowski, Anupam Chakrapani, Maureen Cleary, Philip Lee, Friedrich K Trefz, Chester B Whitley, François Feillet, Annette S Feigenbaum, Judith D Bebchuk, Heidi Christ-Schmidt, Alex Dorenbaum, Sapropterin Research Group. Efficacy of sapropterin dihydrochloride (tetrahydrobiopterin, 6R-BH4) for reduction of phenylalanine concentration in patients with phenylketonuria: a phase III randomised placebo-controlled study. s.l. : Lancet, 2007.

23. S Mochizuki, H Mizukami, T Ogura, S Kure, A Ichinohe, K Kojima, Y Matsubara, E Kobayahi, T Okada, A Hoshika, K Ozawa & A Kume. Long-term correction of hyperphenylalaninemia by AAV-mediated gene transfer leads to behavioral recovery in phenylketonuria mice. s.l. : Gene Therapy, 2004, Vol. 11, p. 1081-1086.

24. Hans D Theiss, David M Kofler, Hildegard Büning, Anna-Lena Aldenhoff, Bernhard Kaess, Thomas Decker, Jens Baumert, Michael Hallek, Clemens-Martin Wendtner. Enhancement of gene transfer with recombinant adeno-associated virus (rAAV) vectors into primary B-cell chronic lymphocytic leukemia cells by CpG-oligodeoxynucleotides. s.l. : Experimental Hematology, 2003,
Vol. 31.

25. Christineh N Sarkissian, Alejandra Gámez. Phenylalanine ammonia lyase, enzyme substitution therapy for phenylketonuria, where are we now? s.l. : Mol Genet Metab ., 2005.

26. Keith Moore, P. V. Subba Rao, and G. H. N. Towers. Degradation of phenylalanine and tyrosine by Sporobolomyces roseus. s.l. : Biochem J., 1968, Vol. 106.

27. László Poppe, János Rétey. Friedel-Crafts-type mechanism for the enzymatic elimination of ammonia from histidine and phenylalanine. 2005.

28. T F Schwede, J Rétey, G E Schulz. Crystal structure of histidine ammonia-lyase revealing a novel polypeptide modification as the catalytic electrophile. s.l. : Biochemistry, 1999.

29. Mathias Baedeker, Georg E Schulz. Structures of two histidine ammonia-lyase modifications and implications for the catalytic mechanism. s.l. : European Journal of Biochemestry, 2002.

30. Michelle C. Moffitt, Gordon V. Louie, Marianne E. Bowman, Janelle Pence, Joseph P. Noel and Bradley S. Moore*§¥. Discovery of Two Cyanobacterial Phenylalanine Ammonia Lyases: Kinetic and Structural Characterization. s.l. : Biochemistry, 2007, Vol. 46.

31. Alejandra Gámez, Christineh N Sarkissian, Lin Wang, Woomi Kim, Mary Straub, Marianne G Patch, Lin Chen, Steve Striepeke, Paul Fitzpatrick, Jeffrey F Lemontt, Charles O'Neill, Charles R Scriver, Raymond C Stevens. Development of pegylated forms of recombinant Rhodosporidium toruloides phenylalanine ammonia-lyase for the treatment of classical phenylketonuria. s.l. : Mol Ther, 2005.

32. C N Sarkissian, A Gámez, C R Scriver. What we know that could influence future treatment of phenylketonuria. s.l. : J Inherit Metab Dis , 2008, Vol. 32.

33. Tiziana Pascucci, Diego Andolina, Rossella Ventura, Stefano Puglisi-Allegra, Simona Cabib. Reduced availability of brain amines during critical phases of postnatal development in a genetic mouse model of cognitive delay. s.l. : Brain Res., 2008, Vol. 27.

34. A Shedlovsky, J D McDonald, D Symula, W F Dove. Mouse models of human phenylketonuria. s.l. : Genetics, 1993, Vol. 134, p. 1205-1210.

35. J D McDonald, C K Charlton. Characterization of mutations at the mouse phenylalanine hydroxylase locus. s.l. : Genomics, 1997, Vol. 39, p. 402-405.

36. Mauro Magnani, Luigia Rossia, Marzia Bianchia, Giorgio Fornainia, Umberto Benatti, Lucrezia Guida, Elena Zocchi, Antonio De Flora. Improved metabolic properties of hexokinase-overloaded human erythrocytes. [a cura di] 1-8. s.l. : Biochimica et Biophysica Acta (BBA) - Bioenergetics, 1988, Vol. 972.

37. Lin Wang, Alejandra Gamez, Holly Archer, Enrique E. Abola, Christineh N. Sarkissian, Paul Fitzpatrick, Dan Wendt, Yanhong Zhang, Michel Vellard, Joshua Bliesath, Sean M. Bell, Jeffrey F. Lemontt, Charles R. Scriver, Raymond C. Stevens. Structural and Biochemical Characterization of the Therapeutic Anabaena variabilis Phenylalanine Ammonia Lyase. s.l. : Journal of Molecular Biology, 2008, Vol. 380, p. 623-635.

38. D H Chace, D S Millington, N Terada, S G Kahler, C R Roe, L F Hofman. Rapid diagnosis of phenylketonuria by quantitative analysis for phenylalanine and tyrosine in neonatal blood spots by tandem mass spectrometry. s.l. : Clin Chem, 1993, Vol. 39, p. 66-71.

39. Ann-Maree Catanzariti 1, Tatiana A Soboleva, David A Jans, Philip G Board, Rohan T Baker. An efficient system for high-level expression and easy purification of authentic recombinant proteins. s.l. : Protein Sci, 2004, Vol. 13.

40. Robert H Andres, Angélique D Ducray, Uwe Schlattner, Theo Wallimann, Hans Rudolf Widmer. Functions and effects of creatine in the central nervous system. s.l. : Brain Res Bull, 2008.

41. Fahmi Nasrallah, Moncef Feki, Naziha Kaabachi. Creatine and Creatine Deficiency Syndromes: Biochemical and Clinical Aspects. s.l. : Pediatric Neurology, 2010.

42. Marie Joncquel-Chevalier Curt, Pia-Manuela Voicu, Monique Fontaine, Anne-Frédérique Dessein, Nicole Porchet, Karine Mention-Mulliez, Dries Dobbelaere, Gustavo Soto-Arese David Cheillan, Joseph Vamecq. Creatine biosynthesis and transport in health and disease. s.l. : Biochimie, 2015, Vol. 119.

43. Cecil, Joseph F. Clark and Kim M. Diagnostic methods and recommendations for the cerebral creatine deficiency syndromes. s.l. : Pediatric research, 2015, Vol. 77.

44. Sylvia Stockler, Peter W. Schutz And Gajja S. Salomons. Cerebral creatine deficiency syndromes: clinical aspects, treatment and pathophysiology. s.l. : Springer, 2007, Vol. 46.

45. L. Lion-François, D. Cheillan, G. Pitelet, C. Acquaviva-Bourdain, G. Bussy, F. Cotton, L. Guibaud, D. Gérard, C. Rivier, C. Vianey-Saban, C. Jakobs, G. S. Salomons, V. des Portes. High frequency of creatine deficiency syndromes in patients with unexplained mental retardation. s.l. : Neurology, 2006, Vol. 67.

46. Hang Lee, Jong-Ho Kim, Young-Jin Chae, Hirofumi Ogawa, Mun-Han Lee, George L. Gerton. Creatine Synthesis and Transport Systems in the Male Rat Reproductive Tract. s.l. : Biology of reproduction, 1998, Vol. 58.

47. Caro-Lyne Desroches, Jaina Patel, Peixiang Wang, Berge Minassian, Christian R. Marshall, Gajja S. Salomons & Saadet Mercimek-Mahmutoglu. Carrier frequency of guanidinoacetate methyltransferase deficiency in the general population by functional characterization of missense variants in the GAMT gene. 2015, Vol. Molecular Genetics and Genomics.

48. Josenato Ilas, Adolf Mühl, Sylvia Stöckler-Ipsiroglu. Guanidinoacetate methyltransferase (GAMT) deficiency: non-invasive enzymatic diagnosis of a newly recognized inborn error of metabolism. s.l. : Clinica Chimica Acta, 2000, Vol. 290.

49. Fernando Andrade, Juan Rodriguez-Soriano, Jose Angel Prieto, Javier Elorz, Mireia Aguirre,˝ Gema Ariceta, Sergio Martin, Pablo Sanjurjo, And Luis Aldamiz-Echevarria. The Arginine-Creatine Pathway is Disturbed in Children and Adolescents With Renal Transplants. s.l. : Pediatric research, 2008, Vol. 64.

50. Junichi Komoto, Taro Yamada, Yoshimi Takata, Kiyoshi Konishi, Hirofumi Ogawa, Tomoharu Gomi, Motoji Fujioka and Fusuo Takusagawa. Catalytic mechanism of Guanidinoacetate Methyltransfersare: Crystal structures of Guanidinoacetate Methyltransferase ternary complexes. s.l. : biochemistry, 2004, Vol. 43.

51. R Ensenauer 1, T Thiel, K O Schwab, U Tacke, S Stöckler-Ipsiroglu, A Schulze, J Hennig, W LehnertR Ensenauer , T Thiel, K O Schwab, U Tacke, S Stöckler-Ipsiroglu, A Schulze, J Hennig, W Lehnert. Guanidinoacetate methyltransferase deficiency: differences of creatine uptake in human brain and muscle. s.l. : Mol Genet Metab, 2004.

52. Mercimek-Mahmutoglu S, Pop A, Kanhai W, Fernandez Ojeda M, Holwerda U, Smith D, Loeber JG, Schielen PC, Salomons GS. A pilot study to estimate incidence of guanidinoacetate methyltransferase deficiency in newborns by direct sequencing of the GAMT gene. s.l. : Gene, 2016.

53. Desroches CL, Patel J, Wang P, Minassian B, Marshall CR, Salomons GS, Mercimek- Mahmutoglu S. Carrier frequency of guanidinoacetate methyltransferase deficiency in the general population by functional characterization of missense variants in the GAMT gene. s.l. : Mol Genet Genomics, 2015.

54. Axel Neu, Henrike Neuhoff, Gerhard Trube, Susanne Fehr, Kurt Ullrich, Jochen Roeper, Dirk Isbrandt. Activation of GABA(A) receptors by guanidinoacetate: a novel pathophysiological mechanism. s.l. : Neurobiol dis., 202.

55. V. Leuzzi, M.C. Bianchi, M. Tosetti, C. Carducci, A. Cerquiglini, G. Cioni, I. Antonozzi. Brain creatine depletion: Guanidinoacetate methyltransferase deficiency (improving with creatine supplementation). 2000, Vol. Neurology.

56. Saadet Mercimek-Mahmutoglu, Joseph Ndika, Warsha Kanhai, Thierry Billette de Villemeur, David Cheillan, Ernst Christensen, Nathalie Dorison, Vickie Hannig, Yvonne Hendriks, Floris C. Hofstede,Laurence Lion-Francois, Allan M. Lund, Helen Mundy, et al. Thirteen New Patients with Guanidinoacetate Methyltransferase Deficiency and Functional Characterization of Nineteen Novel Missense Variants in the GAMT Gene. s.l. : Human Mutation, 2014.

57. Pajares, George D. Markham and María A. Structure-function relationships in methionine adenosyltransferases. s.l. : Cell Mol Life Sci, 2010.

58. Kotb M, Mudd SH, Mato JM, Geller AM, Kredich NM, Chou JY, Cantoni GL. Consensus nomenclature for the mammalian methionine adenosyltransferase genes and gene products. s.l. : Trends Genet., 1997.

59. LeGros HL, Jr., Halim AB, Geller AM, Kotb M. Cloning, expression, and functional characterization of the beta regulatory subunit of human methionine adenosyltransferase (MAT II). s.l. : J. Biol. Chem., 2000.

60. M.Bradford, Marion. A rapid and sensitive method for the quantitation of microgram quantities of protein utilizing the principle of protein-dye binding. s.l. : Analytical Biochemistry, 1976, Vol. 72.

61. Maria Grazia Alessandrì, Lisa Celati, Roberta Battini, Fulvia Baldinotti, Chike Item, Vincenzo Leuzzi, and Giovanni Cionie. HPLC assay for guanidinoacetate methyltransferase. s.l. : ANALYTICAL BIOCHEMISTRY, 2004, Vol. 331.

62. J, Bio-PEPA: A framework for the modelling and analysis of biological systems Ciocchetta FHillston. Bio-PEPA: A framework for the modelling and analysis of biological systems. s.l. : Theoretical Computer Science, 2009, Vol. 410.

63. K L Oden, S Clarke. S-adenosyl-L-methionine synthetase from human erythrocytes: role in the regulation of cellular S-adenosylmethionine levels. s.l. : Biochemistry, 1983, Vol. 22.

64. Carolyn K Wise, Craig A Cooney, Syed F Ali, Lionel A Poirier. Measuring S-adenosylmethionine in whole blood, red blood cells and cultured cells using a fast preparation method and high-performance liquid chromatography. s.l. : Journal of Chromatography B: Biomedical Sciences and Applications, 1997, Vol. 696.

65. APereiraLianhuiTao, WeiWangPaula MKramerSimingYangMichael. Reversed-phase high-performance liquid chromatography procedure for the simultaneous determination of S-adenosyl-l-methionine and S-adenosyl-l-homocysteine in mouse liver and the effect of methionine on their concentrations. s.l. : Journal of Chromatography B: Biomedical Sciences and Applications, 2001, Vol. 761.

66. Shozo Shiozaki, Sakayu Shimizu, Hideaki Yamada. Production of S-adenosyl-l-methionine by Saccharomyces sake. s.l. : Journal of Biotechnology, 1986, Vol. 4.

67. Magnani, M, Serafini, G e Stocchi, V. Hexokinase type I multiplicity in human erythrocytes. s.l. : Biochem J, 1988, Vol. 254.

68. Claudia Carduccia, Silvia Santagata, Vincenzo Leuzzi, Carla Carducci, Cristiana Artiola, Teresa Giovanniello, Roberta Battini, Italo Antonozzi. Quantitative determination of guanidinoacetate and creatine in dried blood spot by flow injection analysis-electrospray tandem mass spectrometry. s.l. : Clinica Chimica Acta, 2006, Vol. 364.

69. Andreas Schmidt, Bart Marescau, Ernest A Boehm, W Klaas Jan Renema, Ruben Peco, Anib Das, Robert Steinfeld, Sharon Chan, Julie Wallis, Michail Davidoff, Kurt Ullrich, Ralph Waldschütz, Arend Heerschap,

Peter P De Deyn, Stefan Neubauer, Dirk Isbrandt. Severely altered guanidino compound levels, disturbed body weight homeostasis and impaired fertility in a mouse model of guanidinoacetate N-methyltransferase (GAMT) deficiency. s.l. : Hum Mol Genet, 2004, Vol. 13, p. 905-921.

70. Ankit Sinha 1, Sohail Ahmed 1 , Chris George 1 , Melina Tsagaris 1 , Amriya Naufer 1 , Ingo von Both 1 , Ilona Tkachyova 1 , Matthijs van Eede , Mark Henkelman , Andreas Schulze. Magnetic resonance imaging reveals specific anatomical changes in the brain of Agat- and Gamt-mice attributed to creatine depletion and guanidinoacetate alteration. s.l. : J Inherit Metab Dis, 2020, Vol. 43, p. 827-842.

71. W Klaas Jan Renema, Andreas Schmidt, Jack J A van Asten, Frank Oerlemans, Kurt Ullrich, Bé Wieringa, Dirk Isbrandt, Arend Heerschap. MR spectroscopy of muscle and brain in guanidinoacetate methyltransferase (GAMT)-deficient mice: validation of an animal model to study creatine deficiency. s.l. : Magn Reson Med, 2003, Vol. 50, p. 936.943.

72. Claudia Carducci, Silvia Santagata, Vincenzo Leuzzi, Carla Carducci, Cristiana Artiola, Teresa Giovanniello, Roberta Battini, Italo Antonozzi. Quantitative determination of guanidinoacetate and creatine in dried blood spot by flow injection analysis-electrospray tandem mass spectrometry. s.l. : Clinica Chimica Acta, 2006, Vol. 346.

73. Ann-Maree Catanzariti, Tatiana A. Soboleva, David A. Jans, Philip G. Board, Androhan T. Baker. An efficient system for high-level expression and easy purification of authentic recombinant proteins. s.l. : Protein Science, 2004, Vol. 13.

Tanti sono i ringraziamenti da fare e molte le motivazioni. Ringrazio il Prof Mauro Magnani, la Prof.ssa Luigia Rossi, la Dott.ssa Francesca Pierigè, la Dott.ssa Sara Biagiotti e la Prof.ssa Marzia Bianchi... per questi tre anni e molto altro!